

Kerstin Pock BSc

**Characterisation of weak spots of state of the art Drug  
Eluting Stent Systems regarding their acute performance  
in clinical applications**

**MASTER'S THESIS**

to achieve the university degree of

Master of Science

Master's degree programme: Biomedical Engineering

submitted to

**Graz University of Technology**

Supervisor

Univ.-Prof. Dipl.-Ing. Dr.techn. Christian Baumgartner

Institut für Health Care Engineering mit Europaprüfstelle für Medizinprodukte

Second supervisor

Christian Gimmel BSc

Catheter Development R&D, Biotronik AG, Bülach (CH)

Graz, March 2019



## EIDESSTATTLICHE ERKLÄRUNG

### **AFFIDAVIT**

Ich erkläre an Eides statt, dass ich die vorliegende Arbeit selbstständig verfasst, andere als die angegebenen Quellen/Hilfsmittel nicht benutzt, und die den benutzten Quellen wörtlich und inhaltlich entnommenen Stellen als solche kenntlich gemacht habe. Das in TUGRAZonline hochgeladene Textdokument ist mit der vorliegenden Masterarbeit/Diplomarbeit/Dissertation identisch.

*I declare that I have authored this thesis independently, that I have not used other than the declared sources/resources, and that I have explicitly indicated all material which has been quoted either literally or by content from the sources used. The text document uploaded to TUGRAZonline is identical to the present master's thesis/diploma thesis/doctoral dissertation.*

---

Datum / Date

---

Unterschrift / Signature

*Die Technische Universität Graz übernimmt mit der Betreuung und Bewertung einer Masterarbeit keine Haftung für die erarbeiteten Ergebnisse: Eine positive Bewertung und Anerkennung (Approbation) einer Arbeit bescheinigt nicht notwendigerweise die vollständige Richtigkeit der Ergebnisse.*



## **Acknowledgements**

First of all, I would like to express my thanks to Univ.-Prof. Dipl.-Ing. Dr. techn. Christian Baumgartner, who was willing to accept this thesis in collaboration with Biotronik AG and who was always willing to answer my questions.

I must express my greatest thanks to my supervisor Christian Gimmel. His expertise and support made it possible to successfully accomplish this work.

I would also like to thank Dr.-Ing. Sebastian Klaus, who gave me the opportunity to write this master thesis and always supported me during the whole period.

Special thanks also go to Carina Haber, who supported me during the entire production of the silicone vessels.

Additionally, I would like to thank my internship colleagues Roberto Munger, Aurelia Bucciarelli and Natalia Jelic, because I was always able to obtain their opinion during different tasks and have contributed to many moments of success.

I would also like to thank Dragana Simic, Rebecca Huber, Gion Etterlin and David Wiedmer, who I could always approach during my work if there were any questions.

Finally, I would like to thank especially my family and friends who have always believed in me over the years of my studies and have supported me in every phase of my life. I am really grateful to have so many people in my life who have always given me courage even during difficult times and who have contributed towards me being where I am today.



## **Zusammenfassung**

In dieser Arbeit wurde eine Schwachstellenanalyse marktgängiger Drug Eluting Stent Systeme hinsichtlich ihrer Akuteigenschaften bei der klinischen Anwendung durchgeführt. Nach der Auswertung der gesammelten Schwachstellen wurde eine neue Testmethode für die Schwachstellen ‚Stentstrebe Malappositionsverhalten‘ und ‚Stentverhalten im überdilatierten Zustand‘ entwickelt. Zu diesem Zweck wurden künstliche Gefäßmodelle entwickelt, die einen Teil der linken Koronararterie nachstellen. Mittels 3D-gedruckten Gussformen wurden dabei 9 Gefäßmodelle hergestellt. Die Verifizierung der Gefäßmodelle auf geometrische und mechanische Eigenschaften ergab, dass ihre Dimensionen teilweise leicht unter den initial definierten Werten lagen. Darüber hinaus lag die radiale Nachgiebigkeit der Modelle leicht unter der von biologischen Arterien. Die ersten Untersuchungen der Stents auf Appositions- und Überdilationsverhalten zeigten, dass Metallartefakte in den Scans unter Verwendung der Mikro-CT Technik sichtbar waren. Das Appositions- und Überdilationsverhalten konnte daher nur eingeschränkt untersucht werden.

Schlüsselwörter: DES, Stent, PCI, Malapposition, Überdilatation

## **Abstract**

In this thesis, a weak spot analysis of state of the art drug eluting stent systems regarding their acute performance in clinical applications was performed. After evaluation of the collected weak spots a new test method was developed for the weak spots 'Stent strut malapposition behaviour' and 'Stent performance in overdilatated condition'. For this purpose, artificial vessel models were developed that imitate a part of the left coronary artery. With 3D-printed casting moulds 9 vessel models were produced. The verification of these vessel models for geometric and mechanical properties revealed that their dimensions were, in some cases, slightly below the initially defined values. In addition, the radial compliance of the models was slightly lower than that of biological arteries. The first investigation of the stents on apposition and overdilatation behaviour showed that metal artefacts were visible in the scans by using the Micro-CT technique. The apposition and overdilatation behaviour could therefore only be examined to a limited extent.

Keywords: DES, stent, PCI, malapposition, overdilatation





# Table of Contents

Acknowledgements .....	I
Zusammenfassung .....	II
Abstract .....	II
Table of Contents .....	III
List of Abbreviations .....	VI
List of Tables .....	VII
List of Figures .....	VIII
1 Introduction .....	1
1.1 Structure of the cardiovascular system .....	2
1.2 Atherosclerosis .....	4
1.3 Percutaneous Coronary Intervention (PCI) .....	6
1.4 Coronary stent system .....	8
1.4.1 Delivery system .....	8
1.4.2 Stent .....	9
1.4.3 Drug eluting coating of stents .....	11
2 Objectives .....	12
<b>Part I. Identification of distinctive weak spots .....</b>	<b>13</b>
3 Methods and materials .....	13
3.1 Pre-selection .....	14
3.1.1 Internal technical reports .....	14
3.1.2 Selected DES systems for test method development .....	14
3.2 Definition and evaluation of weak spots .....	16
3.2.1 First interim rating .....	16
3.2.2 External literature analysis .....	20
3.2.3 Interview analysis .....	22
3.2.4 Overall evaluation matrix .....	24
4 Results .....	26
4.1 Identified weak spots .....	26
4.2 Evaluation of weak spots .....	26
4.2.1 First interim rating .....	26
4.2.2 External literature analysis .....	27
4.2.3 Interview analysis .....	28
4.2.4 Overall evaluation .....	29
5 Discussion .....	31
5.1 First interim rating .....	31
5.2 External literature analysis .....	32
5.3 KOL interview analysis .....	34

5.4	Overall evaluation .....	35
6	Conclusion .....	37
<b>Part II. Development of a new test method .....</b>		<b>38</b>
7	Introduction .....	38
7.1	Malapposition behaviour .....	38
7.2	Overdilatation behaviour .....	38
8	Methods and materials .....	40
8.1	Definition of a selective test program .....	40
8.1.1	Imitation area of mock vessels .....	41
8.1.2	Establishment of customized mock vessels .....	41
8.1.3	Test program for investigating weak spots .....	44
8.2	Design of mock vessels .....	46
8.2.1	Bifurcation geometry .....	46
8.2.2	Stenosis anatomy .....	48
8.2.3	Wall thickness dimensions .....	49
8.3	Manufacture of mock vessels .....	52
8.3.1	Mock vessel rig design and functionality .....	52
8.3.2	Silicone mock vessel production .....	56
8.4	Mock vessel design and process verification .....	59
8.4.1	Visual inspection for air bubbles .....	61
8.4.2	Verification of relevant lengths, diameters and bifurcation angle .....	62
8.4.3	Evaluation of reproducibility of stenosis placement and lumen reduction .....	67
8.4.4	Determination of radial compliance .....	68
8.4.5	Measurement of wall thickness .....	70
8.5	Implantation of stents in mock vessels .....	72
8.5.1	Test setup and implantation procedure .....	72
8.5.2	Measurement of elastic recoil of stent .....	76
8.6	Micro-CT scanning of mock vessel .....	78
8.6.1	X-ray microtomography procedure and used scanner settings .....	78
8.6.2	Evaluation of apposition and overdilatation behaviour .....	79
9	Results .....	82
9.1	Verification of manufactured mock vessels .....	82
9.1.1	Air bubbles and overall dimensions .....	82
9.1.2	Stenosis placement and lumen reduction .....	85
9.1.3	Radial compliance and wall thickness .....	86
9.2	Elastic recoil of stent .....	91
9.3	Apposition and overdilatation behaviour .....	91
9.3.1	Strut malapposition .....	91
9.3.2	Residual stenosis .....	92
9.3.3	Preliminary results of stent strut behaviour after overexpansion .....	93

10	Discussion .....	95
10.1	Verification of mock vessels .....	95
10.1.1	Air bubbles and overall dimensions .....	95
10.1.2	Stenosis placement and lumen reduction .....	99
10.1.3	Radial compliance and wall thickness .....	99
10.2	Elastic recoil of stent .....	101
10.3	Apposition and overdilatation behaviour .....	102
11	Conclusion and Outlook .....	105
12	References .....	107
13	Appendix .....	110
13.1	Internal test methods .....	110
13.2	Identified weak spots .....	113
13.3	Explanation of the seven 'high'-rated weak spots .....	114
13.4	Evaluation of 'medium'-rated weak spots .....	115
13.5	Evaluation of 'low'-rated weak spots .....	116
13.6	Questionnaire for physician interviews .....	118
13.7	CAD drawings .....	119
13.8	Test instruction – Implantation of stent in mock vessel .....	127



## List of Abbreviations

BMS	Bare metal stents
CoCr	Cobalt-chromium
CoNi	Cobalt-nickel
DES	Drug-eluting stent
KOL	Key Opinion Leaders
LAD	Left anterior descendens
LCA	Left coronary artery
LCX	Left circumflex artery
MB	Main branch
MLD	Minimal lumen diameter
MV	Main vessel
ND	Nominal diameter
NP	Nominal pressure
OCT	Optical coherence tomography
OExD	Overexpansion diameter
PCI	Percutaneous coronary intervention
PDA	Posterior descending artery
PLV	Posterolateral ventricular branch
POBA	Plain old balloon angioplasty
PTCA	Percutaneous transluminal coronary angioplasty
PtPr	Platinum-chromium
RAD	Ramus anterior descendens
RBP	Rated burst pressure
RCA	Right coronary artery
RCX	Ramus circumflexus
RD	Ramus diagonalis
RD1	Ramus diagonalis first branch
RIVA	Ramus interventricularis anterior
RV	Right ventricular branches
RS	Ramus septales
SB	Side branch
TZ	Transition zone



## List of Tables

Table 1: Selected competitor products including their design features [20, 23–29].....	15
Table 2: Evaluation matrix of the first interim rating .....	17
Table 3: Classification of the results of the interim rating into low, medium and high.....	17
Table 4: Evaluation <i>Potential of market differentiation</i> .....	18
Table 5: Evaluation <i>Expert feedback</i> .....	18
Table 6: Evaluation <i>Realizability in project</i> .....	19
Table 7: Evaluation <i>Internal test methods &amp; results available</i> .....	19
Table 8: Evaluation <i>Competitor comparison</i> .....	20
Table 9: Evaluation matrix of the external literature analysis .....	21
Table 10: Evaluation of <i>Occurrence, Severity and Quality</i> .....	21
Table 11: Evaluation matrix of the interviews .....	23
Table 12: Evaluation of <i>Known/possible problem, Occurrence and Severity</i> .....	23
Table 13: Overall evaluation matrix for determining final weak spots .....	25
Table 14: Results of the first interim rating including all seven weak spots that have reached a 'high' (high = 10 - 14) .....	27
Table 15: Results of the external literature analysis on the seven weak spots.....	28
Table 16: Results of the overall interview analysis with the KOL on the respective weak spots .....	28
Table 17: Overall evaluation of the seven weak spots .....	29
Table 18: Labelled limitation sizes for 3.00 mm stents of the seven competitor products .....	42
Table 19: Selected proximal inner diameters of the three mock vessels to be developed .....	43
Table 20: Diameters of the distal (D2) and proximal (D1) MB used to calculate the expected SB diameter (D3).....	48
Table 21: Dimensions of the three mock vessel designs that differ .....	53
Table 22: Developed test matrix for testing the manufactured mock vessels for geometric and mechanical properties .....	60
Table 23: Randomized assignment of the nine manufactured mock vessels to the two defined test categories .....	61
Table 24: Results of all air bubbles found in the nine mock vessels manufactured including the location of their occurrence .....	82
Table 25: Measured and calculated length and angle values of the developed mock vessels as well as their deviation from the IDV .....	83
Table 26: Mean values and standard deviations of the $D_o$ of the individual measuring points as well as the deviations from the ID.....	84
Table 27: Stenosis distance measurements as well as its calculated $x$ and $s$ and the deviation to the IDV .....	85
Table 28: Mean values and standard deviations of outer and inner diameters as well as of the radial compliances at the measuring point "MP OExD".....	87
Table 29: Mean values and standard deviations of outer and inner diameters as well as of the radial compliances at the measuring point "MP OExD+7" .....	87
Table 30: Mean values and standard deviations of outer and inner diameters as well as of the radial compliances at the measuring point "MP OExD+14" .....	88
Table 31: Total radial compliance per mock vessel as well as the overall radial compliance of all mock vessels manufactured.....	89
Table 32: Minimum and maximum wall thicknesses determined as well as calculated concentricity of the respective measuring points of the mock vessel and their deviations from the IDV .....	90
Table 33: Mean values and standard deviations of the measured outer diameters as well as indication of the determined $D_{p1}$ and the calculated recoils.....	91
Table 34: Number of malapposed struts as well as total number of struts in cross section per measuring point and the resulting % strut malapposition .....	92





## List of Figures

Figure 1: Overview of the human cardiovascular system [7].....	3
Figure 2: Anatomy of the coronary arteries [9]. .....	4
Figure 3: Progression stages of atherosclerosis [13] .....	6
Figure 4: Stent implantation according to PCI [16].....	7
Figure 5: Delivery system components [20].....	9
Figure 6: Simulation of the mock vessel to be developed .....	44
Figure 7: Simulation of the evaluation of the mock vessels to be developed.....	45
Figure 8: Different scaling laws for determining bifurcation diameters [33].....	47
Figure 9: Medina's classification of coronary bifurcation lesions [46] .....	49
Figure 10: Dimensions of the mock vessel design 1 .....	53
Figure 11: Construction rig for the manufacturing of mock vessel design 1 .....	54
Figure 12: Device for enabling stenosis fixation in the silicone mock vessels .....	55
Figure 13: Design of the defined stenosis.....	55
Figure 14: Assembly of rig.....	57
Figure 15: Placement of the mock vessels on the microscope stage for inspection for air bubbles .....	62
Figure 16: Measurement of the length of RIVA using ruler .....	63
Figure 17: Measurement of the length of the stenosis fixation at 3 measuring points .....	64
Figure 18: Measurement of the bifurcation angle.....	65
Figure 19: Illustration of measuring points at which the outer diameters were determined....	65
Figure 20: Measurement of the outer diameter at measuring point "MP ND" and illustration of the scar .....	66
Figure 21: Measurement of the distance of the stenosis to the distal measuring point "MP ND" .....	68
Figure 22: Measuring points at which diameter changes during dynamic pressure release were recorded .....	69
Figure 23: Measurement of wall thicknesses from cross sections at two measuring points in x-direction and at two in y-direction .....	71
Figure 24: Illustration of the track model of the IIB testing institute for testing trackability of stents .....	73
Figure 25: Modified track model for performing stent implantations in the developed mock vessels .....	73
Figure 26: Optimal placement of the delivery system at the distal and proximal vessel ends	74
Figure 27: Placement of the non-compliant balloon Pantera LEO at the proximal measuring points "MP OExD+10%" and "MP OExD" for performing an optimal overdilatation.....	75
Figure 28: Test setup for performing stent implantations .....	76
Figure 29: Measurement points for determining the outer diameters $D_{p0}$ after stent expansion .....	77
Figure 30: Micro-CT procedure for generating cross section image [60] .....	79
Figure 31: Predefined measuring points and areas in which the stent should be examined for apposition and overdilatation behaviour .....	80
Figure 32: Projection image including marking of the cross section position.....	81
Figure 33: Air bubble in mock vessel no. 3 in the proximal holder .....	83
Figure 34: Measured outer diameters per measuring point and its initially defined diameter value .....	85
Figure 35: Radial compliance at the measuring points "MP OExD", "MP OExD+7" and "MP OExD+14" .....	89
Figure 36: Malapposed struts in cross section of measuring point 1 .....	92
Figure 37: Measurement of the MLD at the maximum point of the stenosis.....	93
Figure 38: Projection image of the proximal section of the mock vessel for examination of overdilatation behaviour .....	94
Figure 39: Minimum gap resulting after assembly of the rig.....	96



# 1 Introduction

Cardiovascular diseases are one of the most frequent causes of death in adulthood worldwide. Every year, according to the World Health Organization (WHO), 17 million people die of cardiovascular disease, mainly caused by heart attacks or strokes as a result of atherosclerotic plaque accumulation on the inner walls of the vessels. This accumulation of plaque leads to a narrowing of the lumen of the arteries and thus prevents the correct supply of blood to the heart muscle. Factors such as stress, smoking, an unhealthy diet and lack of exercise contribute significantly to this high mortality rate. [1]

Percutaneous coronary intervention (PCI) represents one of the most frequently used and efficient therapies for the revascularization of narrowed coronary arteries. The use of drug eluting stents (DES) has become established as the primary treatment option for PCI compared to bare metal stents due to the reduced incidence of in-stent restenosis. The rapid evolution in the field of PCI has contributed to the fact that 40 years after the start of catheter based coronary intervention a multitude of products and manufacturers exists on the market. [2]

Although the current generation of DES systems perform at a very high level in providing excellent safety and efficiency, there are still differences in acute product characteristics regarding to the direct intervention. Each manufacturer has its individual stent design, uses different stent platform materials and different drugs in order to ensure the blood flow through arteries and to reduce the incidence of restenosis. However, individual stent designs correlate with different performances in the clinical intervention. [2, 3]

In the context of this master thesis, the effects of the stent system of different competitors on the performance in acute clinical application will be investigated and a weak spot analysis will be performed. On the basis of the results of this analysis, an appropriate test method is developed as basis for acquiring performance profiles of competitor devices with emphasis on the distinctive weak spots.

## 1.1 Structure of the cardiovascular system

The cardiovascular system consists of the heart, the blood vessels of the body and the blood itself. The heart, which is located obliquely in the mediastinum, represents the system's pump and is responsible for the circulation of the blood through all parts of the body. Blood carries nutrients, oxygen, hormones and other functional cells in order to maintain homeostasis and also transports cellular wastes to elimination sites. The heart is a cone-shaped muscular organ containing four chambers: the left and right atria located in the upper part of the heart, and the left and right ventricles in the lower part. The two atria enable the entering of the blood into the heart, while the more muscular ventricles are responsible for pumping the blood into the body. [4–6]

The cardiovascular system, also known as the circulatory system, is composed of two separate circuits; the pulmonary circuit, which originates in the right side of the heart and pumps the blood into the lungs for gas exchange, and the systemic circuit, which originates in the left side of the heart and supplies the entire body with oxygenated blood [7]. The pulmonary circuit begins when deoxygenated blood enters the right atrium through the superior vena cava, the inferior vena cava and the coronary sinus. This blood then passes through the tricuspid valve to the right ventricle which pumps the blood to the pulmonary trunk, where the pulmonary arteries transport it to the lungs. In the lungs, the deoxygenated or venous blood releases carbon dioxide and picks up oxygen during respiration. Once the gas exchange occurs, the oxygenated blood is returned to the left atrium via the pulmonary veins, where the systemic circuit begins. From the left atrium the oxygenated blood is pumped into the left ventricle through the mitral valve. The left ventricle then pumps the blood out into the aorta via the aortic valve where it gets distributed to all parts of the body, thus completing the systemic circuit. As soon as the blood returns back to heart through the veins, the pulmonary circuit starts again and the entire cycle repeats itself. [6, 7]

Figure 1 illustrates an overview of the human cardiovascular system, with the blue coloured vessel representing the pulmonary circuit transporting the deoxygenated blood, and the red vessel representing the systemic circuit supplying the entire body with oxygenated blood [7].

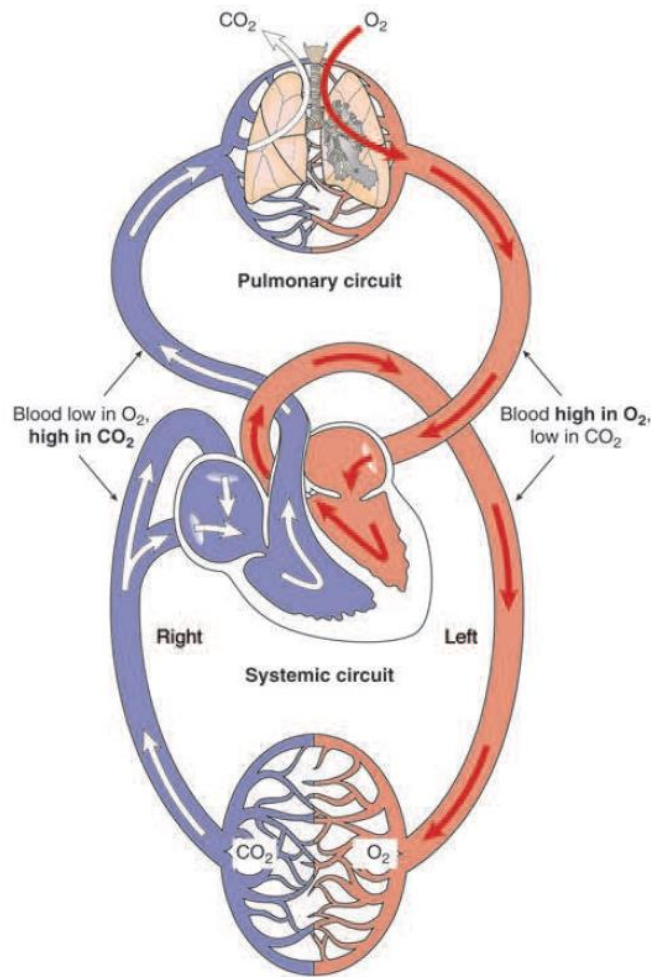


Figure 1: Overview of the human cardiovascular system [7]

Since the heart is a hardworking muscle that constantly pumps blood to all vital organs in the human body, it needs its own oxygen and fuel supply [7]. The coronary arterial system provides this function by supplying the heart muscle with oxygenated blood through the coronary arteries. There are two major coronary arteries responsible for the supply, the right and the left. Both vessels originate from the aortic sinuses of Valsalva which are located slightly above the aortic valve. The right coronary artery (RCA) that arises from the right aortic sinus of Valsalva, branches into the posterior descending artery (PDA) and into the posterolateral ventricular branch (PLV). Further branches like the sinus node artery, the right ventricular branches (RV) and the acute marginal branch (AM) take off from the RCA supplying the right side of the heart with essential oxygen. [6, 8]

The left coronary artery (LCA) divides soon after its origin from the left aortic sinus into the two main branches, the left anterior descendens (LAD), also called Ramus

interventricularis anterior (RIVA) or Ramus anterior descendens (RAD), and the left circumflex artery (LCX) or Ramus circumflexus (RCX) [9]. The LAD as well as the LCX consists of several branches where each of them supplies an individual part of the left side of the heart. The RIVA or LAD runs in the septal branches, the so-called Ramus septales (RS), and the diagonal branches also known as Ramus diagonales (RD). The LCX originates from the left main coronary artery and gives rise to several atrial and marginal branches, which supplies the left ventricular wall. [8, 9]

Figure 2 shows an overview of the anatomy of the coronary arteries.

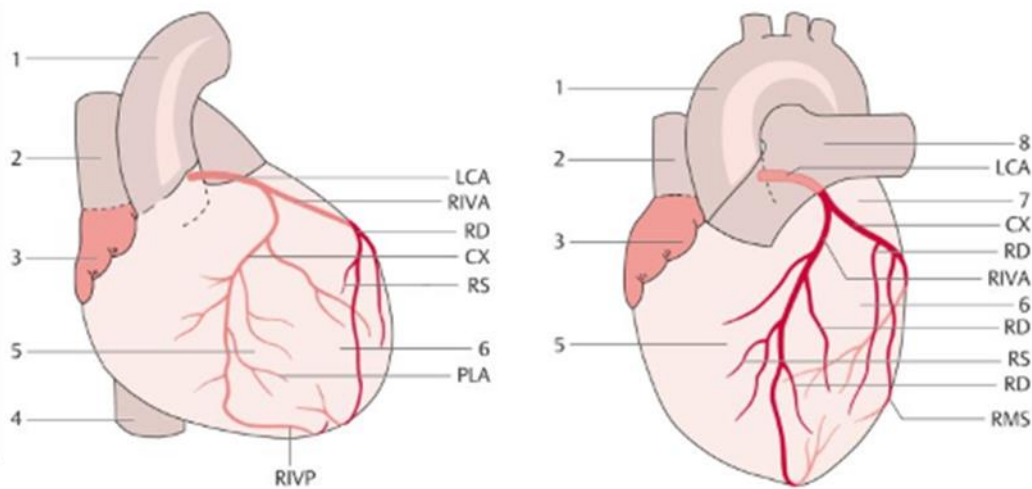


Figure 2: Anatomy of the coronary arteries [9]. 1 = Aorta; 2 = V. cava superior; 3 = right atrium; 4 = V. cava inferior; 5 = right ventricle; 6 = left ventricle; 7 = left atrium; 8 = A. pulmonalis; LCA = left coronary artery; RIVA = Ramus interventricularis anterior; RD = Ramus diagonalis; CX = A. circumflexa; RS = Ramus septalis; PLA = posterolateral branch; RIVP = Ramus interventricularis posterior; RMS = Ramus marginalis sinister

The anatomy of the coronary arteries is highly variable and differs in each person. The differences include individual sizes in the arteries, alternatives in the branch morphologies and individual anatomic courses of the vessels. [8]

Nevertheless, Rogers et al. have reported that despite the individual sizes of the arteries, the typical lumen diameter of the left coronary artery can be up to 4.5 mm compared to the right coronary artery of about 2.5 mm [9].

## 1.2 Atherosclerosis

Cardiovascular diseases are the most common cause of death worldwide every year. According to the latest publications of the World Health Organization (WHO), more

than 30% of all deaths in 2016 were caused by cardiovascular diseases. Over 80% of these deaths are triggered by heart attacks and strokes. Heart attacks and strokes are caused by a blockage in the blood vessel that leads to important parts of the heart or brain no longer being supplied with blood and oxygen. The main reason for this is the building of atherosclerosis plaque on the inner walls of the arteries. Due to this build-up of plaque around the vessel walls, the arteries become narrowed and hardened and thus disrupt the blood flow. The thickening of the arterial wall caused by the development of lesions is called atherosclerosis. [1, 10]

Atherosclerosis plaque is made up of immune cells, lipids, smooth muscle cells, calcium and other substances that accumulate in the arterial wall. According to pathological-anatomical investigations by Rebel et al., the plaque composition is made up of 70% fibrous, 10% calcified, 10% lipid-rich and 10% necrotic parts. The accumulation of plaque typically appears at complex points in the vessel geometry such as vessel curvatures, branching points and bifurcations, and is also referred to as stenosis. [10–12]

The process of atherosclerosis depends on various genetic and environmental factors that influence the pathogenesis individually and over several stages. Atherosclerosis typically starts in childhood and advances with age. The disease occurs in relapses and can subsequently affect multiple sites of the coronary arteries. The progression of atherosclerosis begins with the accumulation of fatty streaks that cannot be reflected in any symptoms. This stage represents the beginning of atheroma. As soon as further fat layers are deposited in the inner channel of the vessel wall, the 'early atheroma' phase is reached and the risk of coronary artery disease increases. The onset of fibre formation in the fat layers of the atheroma leads to the blockage hardening into plaque, which can reduce up to 50% or more of the vascular lumen and thus considerably restricts the natural blood flow through the coronary vessel. An increased blood pressure as well as an accelerated heart rate are the results. Thrombosis and the associated interruption of blood flow occur when the plaque causes a rupture, stimulating the formation of blood clots. The formation of blood clots causes the artery canal to clog further and the patient to experience symptoms such as severe chest pain. This phase of plaque rupture is known as unstable angina. Figure 3 represent the stages of atherosclerosis and gives an overview of the development and changes of the arterial vascular wall. [13]

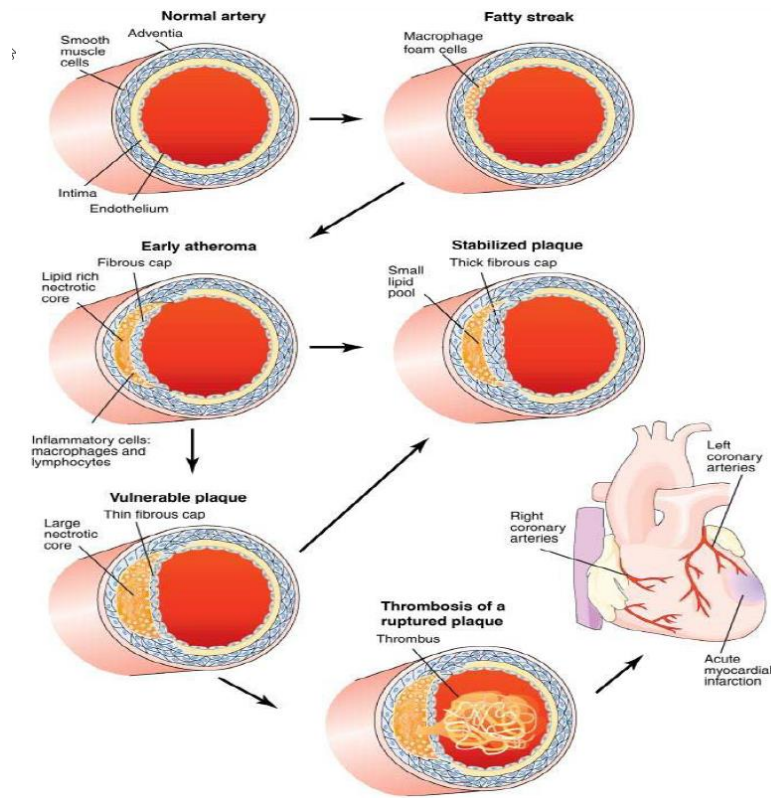


Figure 3: Progression stages of atherosclerosis [13]

### 1.3 Percutaneous Coronary Intervention (PCI)

The Percutaneous Coronary Intervention (PCI) or also called Percutaneous Transluminal Coronary Angioplasty (PTCA) is a minimally invasive procedure to expand plaque-covered areas in the coronary arteries using an inserted balloon catheter that is placed under radiological control. Revascularization with PCI reopens narrowed or blocked coronary arteries found in coronary diseases such as atherosclerosis and thus ensures the blood supply to the heart muscle again. [14]

In 1964 Charles Dotter, a radiologist at Oregon University, was the first to perform a vascular dilatation after studying dilatation techniques for peripheral arteries and developing a catheter/stent guided system. After many scientists and physicians tried to incorporate the technique of Dotter into coronary intervention, Andreas Grüntzig, a physician from Germany, was the first to develop a successful coronary balloon. The first coronary angioplasty was performed in Zurich by Grüntzig on September 1977. The development and successful implementation of his coronary balloon system formed the structural basis for almost all later developed catheter-based technologies related to coronary dilatation. [15]



A PCI starts by inserting an introducer sheath to the artery in order to allow the entering of the catheter system. Typical insertion sites are the femoral artery or the radial artery. To bring the balloon/stent system to the constricted vessel, a guidewire must first be passed through the introducer sheath to the target site in the artery. During the entire procedure, the patient is given the blood thinner heparin to prevent blood clots. Using angiography or other visual techniques, the diameter of the constriction and the surrounding artery is determined in order to select the appropriate balloon/stent sizes. The selected balloon catheter system is then advanced to the stenosis via the guidewire and can be optimally positioned by x-ray markers located at the distal and proximal ends of the balloon system. Once the system is correctly positioned at the restriction, the folded balloon can be dilated using a mixture of contrast agent and saline solution. Depending on the degree and hardness of the calcification, the balloon is inflated with different pressures to push the stenosis into the vessel wall. After balloon dilatation, the blood flow is examined in angiography using x-ray contrast media. If the blood flow is still disturbed, the procedure is repeated with higher pressures or a post-dilatation balloon system. [14]

In addition to balloon angioplasty, in which an inflated balloon relieves the narrowed vessel, nowadays a metal mesh tube called stent is usually implanted in order to protect the vessel permanently against a new constriction [10]. The stent is a thin wire mesh which is placed on the folded balloon and is pressed against the vessel wall after dilatation of the balloon. The process of stent expansion is schematically illustrated in Figure 4. PCI with subsequent stent implantation reduces the risk of the vessel narrowing again and the associated risk of thrombosis. [14]

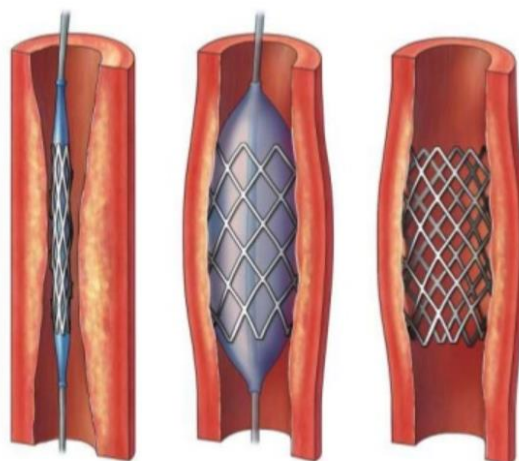


Figure 4: Stent implantation according to PCI [16]

## 1.4 Coronary stent system

In addition to the balloon/stent system, better known as delivery system, a number of important aids are required to enable a successful procedure when performing a PCI. The guiding catheter and guidewire are central instruments for the procedure in order to be able to transport the system to the calcified area in the vessel.

The guiding catheter serves as a guiding path through which the delivery system can be brought into the artery and to the desired location. The use of a guiding catheter is intended to stabilize the vessel in order to facilitate the procedure during a PCI. Typical sizes of guiding catheters vary between 1.7 - 2.7 mm (5 - 8 F). [17]

The primary purpose of the guidewire is to allow access to the narrowed area in the vessel and the passage through the stenosis. Once the guidewire has been placed, the delivery system can be guided over to the target lesion. The guidewire is essentially made of metal and is coated with a hydrophilic layer to facilitate insertion. The properties of the guidewire tip contribute significantly to the passage of the lesion. For stenoses that are difficult to pass, guidewires with a less flexible tip are recommended, while standard guidewires are available that have a very soft spiral tip. [17, 18]

### 1.4.1 Delivery system

The delivery system can be roughly divided into a distal and a proximal part. The distal part starts with the tip of the catheter system and ends up with the guidewire exit point. The proximal part contains the hypotube and the hub which ends with the catheter or luer port. The dilatation system can be attached via the luer port to expand the balloon and the stent placed on it. The so-called hypotube, which is distal to the luer, has increased stiffness and thus enables a better pushability of the catheter system through the arteries. The hypotube connects to the distal part of the system which consists of an inner and outer tube. While the inner tube serves as a shaft for the guidewire, the inflation medium is transported towards the balloon in the outer tube. This type of construction is called Rapid-Exchange-System (RX-System), which represents one of the most frequently used catheter systems. [19]

Figure 5 illustrates the delivery system of Biotronik's DES Orsiro. The outer tube consists of a hydrophilic coating in order to ensure a facilitate insertion. The basic structure of such a delivery system is basically the same for all competitors. Only the de-

sign of the hypotube, the design of the tip or the hub can vary.

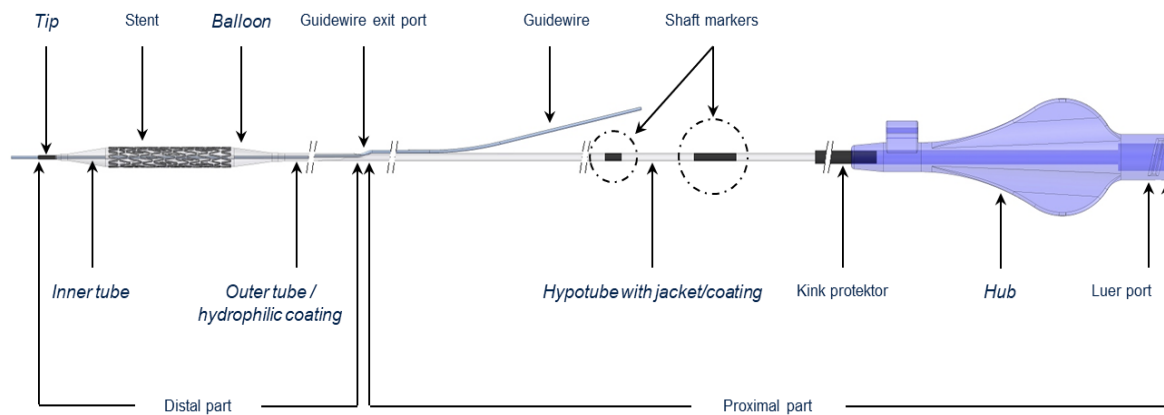


Figure 5: Delivery system components [20]

The balloon which is fixed to the outer shaft of the catheter system is available in different materials depending on the desired compliance. A distinction is made between non-compliant and semi-compliant balloons. Non-compliant balloons have the advantage that they change their diameter only slightly even with increasing pressure and thus minimise the risk of vascular damage during PCI. This type of balloon is preferred for hard and strongly calcified lesions. If the first dilatation with the original catheter system is not sufficient to ensure a complete stent apposition to the vessel wall, such balloons are also used for post-dilatation. Compared to non-compliant balloons, the material of semi-compliant balloons is much softer and can therefore be positioned more easily in bends and angled vessels. The disadvantage of semi-compliant balloons, however, is that the balloons expand strongly with pressure changes and therefore the vessel diameter cannot be determined reliably, which increases the risk of vessel damage. [19]

### 1.4.2 Stent

A stent is a thin, flexible metal scaffold that remains in the vessel after a PCI has been performed in order to ensure permanent vessel opening and correct blood flow. The development of stents was crucial as the dilatation of focal stenoses by balloon angioplasty, known as plain old balloon angioplasty (POBA), led early to new vessel occlusions and thus restenoses. [21]

In order to treat complex lesions while ensuring that the vessel is not damaged, stents must possess a number of general characteristics. One of the most important characteristics of an ideal stent is its radial strength. High radial strength is essential to keep the lumen diameter of the vessel open and therefore ensure that the plaque does not recoil. Furthermore, the stent must be flexible in order to conform to the anatomy of the vessels and thus ensure optimal apposition. Since the stent remains in the vessels after implantation, it has to be biocompatible and thrombo-resistant. Radiographic visibility, better known as radiopaque, as well as deliverability of the stent through the vascular vessel system are also crucial for an ideal PCI. [8]

Different stent model designs provided by the manufacturers have a critical impact on the stent characteristics and thus on the clinical performance. Stent geometry has a major influence on properties such as radial strength, deliverability or conformability. This geometry is dictated by the number of crowns, rings and connectors. [21] A crown, also called peak, is defined as the connection of two adjacent struts through which an angle is formed, the so-called crown angle. A series of crowns attached to each other forms a ring. Rings, in turn, are connected longitudinally by connectors called bridges. The area between a pair of connectors and crowns is called a stent cell. An increased number of connectors initially lead to higher radial strength. This greater number, however, results in a decreased flexibility and conformability of the scaffold. On the other hand, a stent with increased number of struts leads to a drop in radial strength. This indicates that the smaller the crown angle, the lower the radial strength of a stent. The cross-section profile of the stent strut also plays an important role when evaluating the performance of stents. While a round profile causes less flow disturbances and thus decreases the risk of thrombosis, square profiles adapt better to the vessel wall and thus increase the radial strength. Another design feature that has a considerable influence on longitudinal flexibility is the open or closed cell design. In closed cell designs all sides of a sequential ring are connected to each other, while in open cell designs rings are connected only by a few points. While a closed cell design correlates with increased radial strength and reduced risk of plaque prolapse, open cell design provides better flexibility, conformability and access to side branches. Due to the better properties of open cell designs, almost all stents are now manufactured according to this design. [2, 8, 21]

### 1.4.3 Drug eluting coating of stents

The first bare metal stents (BMS) were made up of stainless steel that has good mechanical properties in order to scaffold the vessel and prevent recoil. Due to the predominant proportion of iron in the alloy, the radiopacity was very low, which led to an increase in strut thickness. This increase in strut thickness in turn impaired deliverability to the target lesion and also increased the risk of restenosis. Late complications such as in-stent restenosis led to the fact that after PCI with BMS the procedure of revascularization had to be repeated in the area of the previously implanted stent. With the launch of stronger alloys such as cobalt-chromium (CoCr) and platinum-chromium (PtPr), these limitations and risks associated with stainless steel stents have been overcome. Better properties such as higher elastic modulus and better x-ray densities result in these stents having higher radial strength and better radiopacity than stainless steel stents. Due to these properties, it was possible to reduce the strut thickness and the associated risk of restenosis while maintaining the required radial strength. Further benefits such as better flexibility and trackability were also achieved by reducing the strut profile. In addition to the changes in the metallic composition the development of DES has played an essential part in reducing the rates of restenosis. The release of a drug ensures that the inflammatory and healing process that occurs as a consequence of PCI is reduced, thereby inhibiting cell proliferation. To provide a controlled drug release, the drug is embedded in a bioabsorbable PLLA (Poly-L-Lactid) polymer matrix. Frequently used drugs for the coating of stents are, for example, the immunosuppressive agent Sirolimus and the cancer therapeutic agent Paclitaxel. Both have the effect to block cell progression and enhance re-endothelialization in order to avoid late clinical consequences such as in-stent restenosis. Compared to BMS, the use of DES has reduced the rate of restenosis by about 60%. Thus, the risk of restenosis after PCI is < 10%. As a result of this major advantage, today DES is mainly used in PCI. [8, 21]



## 2 Objectives

The aim of this thesis is to characterize weak spots of state of the art drug eluting stent systems with regard to their acute performance in clinical applications and thus to develop a suitable test program. This test program should serve as a basis for the acquisition of performance profiles of competitor products.

The identification and characterisation of weak spots should be carried out by means of literary research, interviews with medical as well as company-internal professionals and by using internal technical competitor comparisons. The focus thereby should be on the acute product characteristics with direct link to the intervention and not on the clinical long-term behaviour. The collected weak spots will then be evaluated using a specifically developed evaluation matrix, which includes all results of the research and interviews with the experts.

In the practical part of the work, a test method will be developed for the identified weak spots that have achieved the highest result in the evaluation matrix. The test method is developed in such a way that both weak spots can be investigated simultaneously under clinically relevant conditions. The developed test method will then be verified for geometrical and mechanical properties. First investigations with Biotronik's DES on these two weak spots are to be accomplished in order to be able to receive statement about the reproducibility as well as function of the new test method. On the basis of these investigations it should be possible in the future to examine state of the art DES in the developed test method for the identified weak spots in order to be able to acquiring their performance profiles.





## **Part I. Identification of distinctive weak spots**

### **3 Methods and materials**

The identification of distinctive weak spots can be roughly divided into three main steps: the pre-selection, the definition and the evaluation. In the pre-selection phase an analysis of existing internal technical competitor comparison reports is carried out in order to get an overview of which test methods already exist to test product performance of DES and which competing products are compared. In evaluating the internal reports and discussing the outcome with marketing and other internal experts, it was decided which competitor products for comparison are selected. The pre-selection phase concludes with a list of the competitors' product design features and constructions.

The definition and evaluation phase are performed using various methods. In the definition phase, weak spots of state of the art DES systems are collected and listed according to various interviews with internal experts, who have experience with DES systems and their performance. The focus when defining weak spots was on topics that had neither been discussed in the previously reviewed internal technical reports, nor officially tested in any test method.

In order to filter the collected weak spots according to topics such as importance and severity an evaluation matrix is created. The weak spots are first evaluated in cooperation with internal experts in order to include only those which received the highest values in the interim rating, in a more detailed external literary research and in the interview phase with selected physicians, the so-called Key Opinion Leaders (KOL). During the interview phase, selected physicians are asked about the weak spots collected using a precisely defined questionnaire. The results are also included in the evaluation matrix. At the end of the interview phase and after all the mentioned parameters have been integrated into the overall evaluation matrix, a new test method will be developed in Part II for up to three weak spots that have received the highest values in the evaluation.

## **3.1 Pre-selection**

Since there are already a multitude of internal test methods in which acute product characteristics of DES systems from different manufacturers are investigated, it was important to understand these methods and the topics investigated in them in order to enable an identification of weak spots. On the basis of the competitor products already examined in the internal technical reports and from discussions with internal experts, a decision is made for which DES systems a new test method will be developed with regard to the identified weak spots.

### **3.1.1 Internal technical reports**

The internal technical competitor comparisons are performed at the Institute for Implant Technology and Biomaterials IIB e.V. in Rostock-Warnemünde. The institute is an independent and instruction-free testing laboratory with a focus on physical tests on balloon catheters and stent systems [22]. On behalf of Biotronik, different product characteristics of internal and competitor products are investigated and evaluated there. On the one hand, the investigations are of great importance for market studies whereas on the other hand, they serve to scientifically present and verify the performance of the products and can thus be used for design verification.

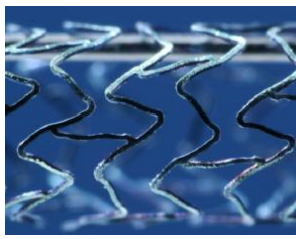

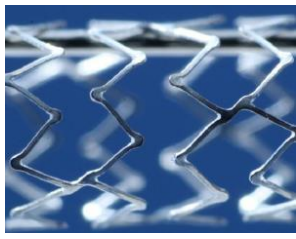

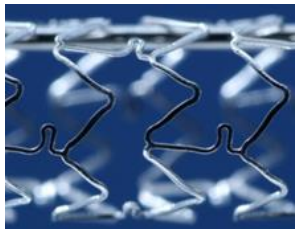

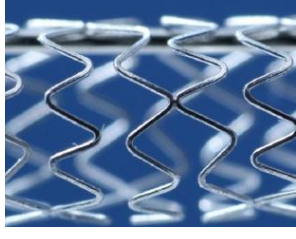



All reports and results of the tests at the IIB testing institute are archived in an internal folder and stored in a directory so as to be accessible to internal experts. By filtering the directory on DES systems, only reports in which coronary DES were examined remained. In order to understand which topics are already being tested using precisely defined test methods, all reports were examined and summarized. The table with the investigated topics and the test methods used can be found in appendix 13.1.

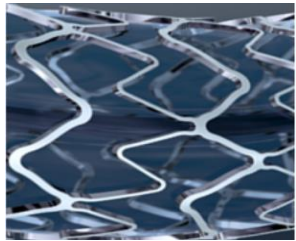

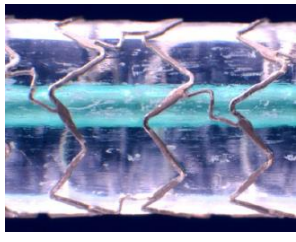

### **3.1.2 Selected DES systems for test method development**

In order to determine the competitor products for which a new defined test method regarding the identified weak spot will be developed, meetings with various experts in the company were arranged. Based on inputs from marketing, research and development experts and taking into account the competitor products already compared in the IIB reports, the following seven state of the art DES listed in Table 1 were cho-

sen. In addition to the company and product name, the respective stent geometry with sizes covered for the stent design as well as strut dimension, material and type of active ingredient are listed in Table 1.

Table 1: Selected competitor products including their design features [20, 23–29]

<b>Company &amp; product name</b>	<b>Stent geometry</b>	<b>Number of crowns/ connectors</b>	<b>Strut design/ thickness</b>	<b>Material/ active ingredient type</b>
Biotronik Orsiro		6 crowns/ 3 connectors	 60 $\mu\text{m}$	CoCr/ Sirolimus
Boston Scientific Synergy		8 crowns/ 2-4 connectors	 74 $\mu\text{m}$	PtCr/ Everolimus
Abbott Xience Sierra		n/a*	 81 $\mu\text{m}$	CoCr/ Sirolimus
Medtronic Resolute Onyx		8.5 crowns/ 2 connectors	 81 $\mu\text{m}$	CoNi/ Zotarolimus
Terumo Ultimaster		8 crowns/ 2 connectors	 80 $\mu\text{m}$	CoCr/ Sirolimus

Cordis Elunir		n/a*	 90 µm	CoCr/ Ridaforolimus
B.Braun Cor- oflex ISAR NEO		n/a*	 55 µm	CoCr/ Sirolimus

\* Information on number of crowns/ connectors are not provided by manufacturers

### 3.2 Definition and evaluation of weak spots

From meetings with internal marketing, research and development experts, potential weak spots were identified ranging from stent and catheter to packaging. During the identification and characterization of weak spots, the main focus was on the acute characteristics with direct link to the intervention and not on the clinical long-term behaviour.

For the evaluation of the collected weak spots an evaluation matrix was developed, which consists of the results of a first interim rating, the results of an external literary research as well as the results of the conducted interviews with selected physicians. In the following chapter, the individual evaluation methodologies are explained in detail.

#### 3.2.1 First interim rating

As not every collected weak spot represents a potential topic for the development of a new test method within the scope of this work, a first interim evaluation was carried out. For this purpose, an evaluation matrix was created with the spreadsheet program Excel (Microsoft Excel, Microsoft Corporation, Washington, USA) which was divided into the following categories:

- Potential of market differentiation

- Expert feedback
- Realizability in project
- Internal test methods & results available
- Competitor comparison

The evaluation of the individual categories in relation to the weak spots varies between low, medium and high as well as yes and no. The interim rating is composed of the ratings of the individual categories and is calculated as shown in Table 2.

Table 2: Evaluation matrix of the first interim rating

<b>First interim rating</b>					
Potential of market differentiation	Expert feedback	Realizability in project	Internal test methods & results available	Competitor comparison	<b>Total</b>
(a)	(b)	(c)	(d)	(e)	
low = 1 medium = 2 high = 3	No = 1 Yes = 2	No = 0 Yes = 1	Yes = 1 No = 2	Yes = 1 No = 2	<b>(a + d + e) · b · c</b>

The results of the interim rating of the individual weak spots can range between 0 and 14 and are divided into low, medium and high depending on the value range as listed in Table 3. For all weak spots that have reached a 'high' in the interim rating, a more detailed literary research is carried out and they are also to be included in the interview phase with the physicians.

Table 3: Classification of the results of the interim rating into low, medium and high

<b><u>Interim rating</u></b>
low = 0 - 4
medium = 5 - 9
<b>high = 10 - 14</b>

The following points explain the criteria on the basis of which the individual evaluations of the five categories are based.

## Potential of market differentiation

Since the investigation of the competitor products regarding the weak spots should enable a market differentiation in addition to the receipt of a detailed performance analysis of the competitor devices, the collected weak spots are first examined for the potential of a market differentiation. This evaluation considers the known product characteristics from existing internal tests as well as internal expert experience and is performed as mentioned in Table 4.

Table 4: Evaluation *Potential of market differentiation*

<b>Potential of market differentiation</b>	
Evaluation	Explanation
low = 1	Based on the results of existing tests and experiences with different DES, this is a potential weak spot of Biotroniks' DES Orsiro and therefore market differentiation is not possible
medium = 2	Orsiro can be classified as good due to its design (related to the weak spot) - market differentiation possible
high = 3	Due to already existing results or because of the design, Orsiro can be classified as very good and potential of market differentiation exist

## Expert feedback

The aspect 'Expert feedback' determines how much internal interest there is in investigating the defined weak spot in more detail. Based on the feedback from internal DES experts the evaluation, presented in Table 5, was performed. The degree of impact of the weak spot on the overall performance of the product as well as the complexity of the weak spot has an influence on the evaluation.

Table 5: Evaluation *Expert feedback*

<b>Expert feedback</b>	
Evaluation	Explanation
No = 1	A more detailed consideration of the weak spot is not recommended as the impact of this issue on the performance of the

	products is low
Yes = 2	Due to the experts feedback a closer investigation of the weak spot is recommended

### Realizability in project

To evaluate whether the development of a new test method related to the defined weak spot within the work is feasible, the aspect 'Realizability in project' is included in the evaluation matrix and is carried out as shown in Table 6.

Table 6: Evaluation *Realizability in project*

<b>Realizability in project</b>	
Evaluation	Explanation
No = 0	The development of a new defined test method regarding the weak spot would exceed the duration of the project (e.g. long-term fatigue tests)
Yes = 1	The development of a new defined test method regarding the weak spot is possible during the time of the project

### Internal test methods & results available and Competitor comparison

Although the focus in identifying distinctive weak spots is limited to topics for which no precisely defined internal test method currently exists and which are not yet examined as standard in competitor product comparisons, some already known topics accumulated during the internal expert interviews. In order to assess these well-known topics in the evaluation matrix, the aspects 'Internal test methods & results available', as listed in Table 7, as well as the evaluation 'Competitor comparison' shown in Table 8, are included in the evaluation matrix.

Table 7: Evaluation *Internal test methods & results available*

<b>Internal test methods &amp; results available</b>	
Evaluation	Explanation
Yes = 1	There are already internal technical test methods in which the defined weak spot is investigated

No = 2	No internal technical test methods and results regarding the weak spot are available
--------	--

Table 8: Evaluation *Competitor comparison*

<b>Competitor comparison</b>	
Evaluation	Explanation
Yes = 1	Competitor products are already being compared in a test method regarding the defined weak spot
No = 2	No competitor products comparison to this weak spot exist

For each defined weak spot, the evaluations of the individual categories were carried out in order to then obtain the overall interim rating of the weak spot using the formula given in Table 2.

### **3.2.2 External literature analysis**

In order to reduce the number of weak spots even further, a more detailed literary research in various medical and medical-technical journals such as the Journal of Interventional Cardiology, EuroIntervention, ResearchGate and many more, regarding the respective weak spots was carried out. During the research, the weak spot itself was searched for by itself and in combination with keywords such as "DES", "Stent", "PCI" or "cardiology intervention". The literature used was limited to articles published in the last five to ten years. The collected literature provides information about the topics of the weak spots that were searched for. The unused articles from the literary research partly contained only short general information about the weak spots or the keywords entered and were therefore not relevant for this part of the work.

The evaluation of the collected literature on the weak spots and the results from the interviews with the physicians can be compared with the evaluation scheme of FMEA (Failure Mode and Effects Analysis) method. Within the context of this work, however, the evaluation was adapted to the literature and interview analysis. Thus, the classical evaluation scheme of FMEA, SOD (*Severity S, Occurrence O, Detection D*



[30]) deviates from 'Occurrence', 'Severity' and 'Quality' in the literature evaluation and from 'Known/possible problem', 'Occurrence' and 'Severity' in the interview analysis.

When evaluating the literature found on the weak spots, it was decisive how often the topic/weak spot appears in the literature, what severity the weak spot has on the performance of the products and how high the quality of the literature is. The evaluation matrix developed for this purpose is shown in Table 9.

Table 9: Evaluation matrix of the external literature analysis

<b>External literature analysis</b>			
Occurrence (O)	Severity (S)	Quality (Q)	<b><u>Total</u></b>
high = 1	low = 1	high = 1	<b>O + S + Q</b>
medium = 2	medium = 2	medium = 2	
low = 3	high = 3	low = 3	

The evaluation of the individual categories is described in Table 10.

Table 10: Evaluation of *Occurrence*, *Severity* and *Quality*

<b>Occurrence</b>	
Evaluation	Explanation
high = 1	The weak spot has already often been dealt with in the literature (> 5 times)
medium = 2	The weak spot was found in the literature (< 5 times)
low = 3	Nothing was found about the weak spot
<b>Severity</b>	
Evaluation	Explanation
low = 1	No correlation was found between the weak spot and impact on product performance
medium = 2	The weak spot may have an impact on product performance
high = 3	The weak spot is directly related to negative impacts on

	the product performance
<b>Quality</b>	
<b>Evaluation</b>	<b>Explanation</b>
high = 1	The weak spot is already being investigated in detail (results are meaningful, competitor products are already being compared)
medium = 2	The weak spot is already investigated in the literature, but the results obtained differ from those defined for the weak spot
low = 3	The weak spot is not addressed in the literature or at least only mentioned in a report (no concrete investigation and no results available)

The evaluation using the matrix given in Table 9 was carried out for each of the 'high'-rated weak spots after the literary research had been carried out.

**3.2.3 Interview analysis**

The last parameter that is included in the final overall evaluation matrix and thus also determines for which weak spots a new test method is developed in order to acquiring performance profiles of competitor devices, is represented by the results from the physician interviews.

Due to good cooperation with the marketing department and sales managers of the Biotronik AG, interviews with eight interventional cardiologists from six different nations could be arranged. The interviews were conducted during direct visits to the physicians' catheter laboratories and during a visit to an internal company medical event. The aim of the interviews was to ask the physicians about the weak spots and to incorporate their answers into the evaluation. In order to be able to include all 'high'-rated weak spots in the interviews, a defined questionnaire (see appendix 13.6) was compiled in advance.

For a uniform evaluation of the interviews, the evaluation matrix listed in Table 11

was developed.

Table 11: Evaluation matrix of the interviews

<b>Interview analysis</b>			
Known/possible problem (P)	Occurrence (O)	Severity (S)	<b><u>Total</u></b>
No = 1	n/a = 0	n/a = 0	<b>P + O + S</b>
Yes = 2	low = 1	low = 1	
	medium = 2	medium = 2	
	high = 3	high = 3	

Table 12 shows how the categories ‘Known/possible problem’, ‘Occurrence’ and ‘Severity’ are assessed.

Table 12: Evaluation of *Known/possible problem*, *Occurrence* and *Severity*

<b>Known/possible problem</b>	
Evaluation	Explanation
No = 1	The defined weak spot is not a known problem
Yes = 2	The weak spot is a known problem or may present a problem during the intervention
<b>Occurrence</b>	
Evaluation	Explanation
n/a = 0	The weak spot is not known and never occurred during intervention
low = 1	The weak spot is known or could be a potential vulnerability, but did not occur during intervention
medium = 2	The weak spot is a known problem and has already occurred during intervention
high = 3	The weak spot is one of the most common problems during intervention

<b>Severity</b>	
Evaluation	Explanation
n/a= 0	The weak spot is not a known problem and therefore no severity of its vulnerability is known
low = 1	The weak spot did not occur during intervention and therefore did not lead to acute problems
medium = 2	The weak spot already occurred during intervention and had a negative impact on the procedure (e.g. prolongation of the intervention, use of a new system or follow-up treatment)
high = 3	The weak spot is a problem that occurs frequently and has serious negative effects on the procedure (emergency surgery, bypass, etc.)

After each interview, the answers to the respective weak spot were evaluated using the matrix shown in Table 11. The answers of all interviewed physicians to the respective weak spots were then summed up.

### **3.2.4 Overall evaluation matrix**

The final overall evaluation of each weak spot is made up of the result of the first interim rating, the result of the external literary research and the result of the interviews conducted.

The overall evaluation matrix that is used to characterize the final weak spots is shown in Table 13.

Table 13: Overall evaluation matrix for determining final weak spots

<b>Overall evaluation matrix</b>			
First interim rating	External literature analysis	Overall KOL interview analysis	<b><u>Overall evaluation</u></b>
f	g	h	$(f + g + (\frac{h}{2}))$

Since the statements of the physicians were very different and very individual and the physicians often only considered the clinical aspect with regard to the weak spot and drew less conclusions on the technical aspect, only half of the sum of the interview evaluation was included in the final evaluation matrix.



## **4 Results**

This chapter presents the number of weak spots collected during the expert interviews and the results of the individual evaluations of the seven weak spots that achieved a 'high' in the interim rating.

The results of the evaluations on the weak spots that have achieved 'medium' and 'low' interim ratings can be found in appendix 13.4 and 13.5.

### **4.1 Identified weak spots**

In discussions with various internal experts in the field of DES, a total of 33 weak spots were identified. The weak spots collected were divided into the categories stent, catheter and packaging according to their respective topics. Some already known and investigated topics of the IIB institute were also taken up, as all inputs from the expert interviews were included in the first interim rating.

All collected weak spots are listed in tables according to their categories and topic and can be found in appendix 13.2.

### **4.2 Evaluation of weak spots**

#### **4.2.1 First interim rating**

After all weak spots from the expert interviews had been recorded, the first interim rating was performed. Table 14 lists the evaluation of the weak spots that reached a 'high' in the interim rating and were thus included in a more detailed external literary research as well as in the interview phase with selected physicians.

Table 14: Results of the first interim rating including all seven weak spots that have reached a 'high' (high = 10 - 14)

<b>First interim rating</b>						
Weak spot	Potential of market differentiation	Expert feedback	Realizability in project	Internal test methods & results available	Competitor comparison	<b><u>Total</u></b>
Cell size/ side branch too small, Side branch accessibility	2	2	1	1	2	<b>10</b>
Stent performance in overdilated condition	2	2	1	1	2	<b>10</b>
Stent strut malapposition behaviour	3	2	1	1	2	<b>12</b>
Narrowing side branch	2	2	1	1	2	<b>10</b>
Buckling susceptibility	1	2	1	2	2	<b>10</b>
Torsions behaviour for higher requirements than standard specification	2	2	1	1	2	<b>10</b>
Pullback until necking	1	2	1	2	2	<b>10</b>

The weak spots 'Cell size/ side branch too small, Side branch accessibility' to 'Narrowing side branch' represent weak spots that belong to the category *stent*, while the weak spots 'Buckling susceptibility' to 'Pullback behaviour' represent weak spots from the category *catheter*.

A brief explanation of the seven weak spots can be found in appendix 13.3.

#### **4.2.2 External literature analysis**

Table 15 shows the evaluation of the literature found on the seven weak spots.



Table 15: Results of the external literature analysis on the seven weak spots

<b>External literature analysis</b>				
Weak spot	Occurrence	Severity	Quality	<b><u>Total</u></b>
Cell size/ side branch too small, Side branch accessibility	1	2	1	<b>4</b>
Stent performance in overdila- tated condition	1	2	2	<b>5</b>
Stent strut malapposition behav- iour	1	2	2	<b>5</b>
Narrowing side branch	1	2	1	<b>4</b>
Buckling susceptibility	3	1	3	<b>7</b>
Torsions behaviour for higher requirements than standard spec- ification	3	1	3	<b>7</b>
Pullback until necking	1	1	2	<b>4</b>

### 4.2.3 Interview analysis

After all interviews with the physicians had been carried out, the evaluations of the respective weak spots were summed up. Table 16 shows the overall evaluations from the interviews on the seven weak spots.

Table 16: Results of the overall interview analysis with the KOL on the respective weak spots

<b>Overall KOL interview analysis</b>				
Weak spot	Known/possible problem	Occurrence	Severity	<b><u>Total</u></b>
Cell size/ side branch too small, Side branch accessibility	14	6	6	<b>26</b>
Stent performance in overdila- tated condition	13	7	7	<b>27</b>

Stent strut malapposition behaviour	11	8	7	<b>26</b>
Narrowing side branch	10	3	3	<b>16</b>
Buckling susceptibility	9	2	2	<b>13</b>
Torsions behaviour for higher requirements than standard specification	10	3	2	<b>15</b>
Pullback until necking	13	8	7	<b>28</b>

#### 4.2.4 Overall evaluation

The evaluations of the first interim rating, the literature found and the entire interviews with the physicians resulted in the overall evaluation listed in Table 17 for the respective weak spots. It must be mentioned once again that only half of the results of the overall interviews is included in the overall evaluation.

Table 17: Overall evaluation of the seven weak spots

Weak spot	First interim rating	External literature analysis	Overall KOL interview analysis	<u>Overall evaluation</u>
Cell size/ side branch too small, Side branch accessibility	10	4	13	<b>27</b>
<b>Stent performance in overdilatated condition</b>	<b>10</b>	<b>5</b>	<b>13.5</b>	<b><u>28.5</u></b>
<b>Stent strut malapposition behaviour</b>	<b>12</b>	<b>5</b>	<b>13</b>	<b><u>30</u></b>
Narrowing side branch	10	4	8	<b>22</b>
Buckling susceptibility	10	7	6.5	<b>23.5</b>
Torsions behaviour for higher requirements than standard specification	10	7	7.5	<b>24.5</b>
Pullback until necking	10	4	14	<b>28</b>

On the basis of the results of the first interim rating, the literature found on the weak spots and the results of the entire physician interviews, the weak spots 'Stent performance in overdilatated condition' and 'Stent strut malapposition behaviour' achieved the highest values, **28.5** and **30**.

Based on the results of the final overall evaluation, a new test method for these two weak spots will be developed in Part II according to the previously selected competitor products.



## 5 Discussion

The following chapter discusses the results of the individual evaluations and the outcome of the overall evaluation of the weak spots collected. In addition, the results obtained are used to justify for which two of the weak spots collected a new test method is to be developed in Part II.

### 5.1 First interim rating

The evaluation of all 33 collected weak spots with the developed evaluation matrix of the first interim rating showed that only weak spots from the category stent and catheter reached a rating 'high'. On the one hand, this was due to the fact that weak spots collected regarding packaging did not represent enough potential for a market differentiation of Biotronik's DES Orsiro in comparison to the other competing products and, on the other hand, that the development of a new test method in this category by internal experts did not attract as much interest as it did for the categories stent and catheter.

Considering the results of the 'high'-rated weak spots in the first interim rating in Table 14, chapter 4.2.1, it can be seen that based on internal experts feedback the 'Stent strut malapposition behaviour' weak spot represents the highest potential for market differentiation with rating high (3), while the 'Buckling susceptibility' and 'Pull-back until necking' weak spots represent the lowest potential with rating low (1). The reason for this assessment was that Orsiro's special helix structure design [20] may allow it to stand out from other competitor designs in terms of 'Stent strut malapposition behaviour'.

The evaluation categories 'Expert feedback' and 'Realizability in project' had the highest influence on the interim rating, as they represented the internal interest in investigating the weak spots and the feasibility of the test method to be developed in the context of this work and were therefore multiplied by the sum of the values of 'Potential of market differentiation', 'Internal test methods & results available' and 'Competitor comparison', as can be seen in Table 2, chapter 3.2.1. For all seven weak spots that reached a 'high' in the first interim rating, there was an internal interest in a further investigation and were therefore rated with 2 in the category 'Expert feed-

back', as can be seen in Table 14, chapter 4.2.1. In the category 'Realizability in project', the weak spots also received the highest rating with Yes (1) as the development of a new test method for the individual weak spots would be feasible within the time frame of the work.

When looking at the ratings for the categories 'Internal test methods & results available' and 'Competitor comparison', Table 14, chapter 4.2.1, shows that for five of the seven weak spots there are already internal investigations (rated with 1) but no competitor comparisons were carried out (rated with 2). For the weak spot 'Stent strut malapposition behaviour', for example, first investigations were carried out in which the conformability and apposition behaviour of the stent struts to a silicone stenosis was investigated. However, these tests were only carried out in a single study and no comparisons were made with competitor products. Only for the two weak spots 'Buckling susceptibility' and 'Pullback until necking' there are no internal test methods yet and were therefore rated with 2 - no internal test methods and results available.

The overall results of the first interim rating listed in Table 14 (chapter 4.2.1) show that the 'Stent strut malapposition behaviour' weak spot had received the highest assessment with an overall rating of 12. The other six weak spots were each assessed with a total score of 10. Although the experts were interested in investigating all weak spots further, the evaluation for 'Potential of market differentiation' and 'Internal test methods & results available' for some weak spots, such as 'Cell size/ side branch too small, Side branch accessibility', was rated with 'medium' (rated with 2) and 'Yes' (rated with 1). This evaluation can be justified by the fact that, on the one hand, the cell size of Orsiro stent belongs to the smaller ones and thus leads to restricted side branch access in comparison to the larger cell sizes of the competitor products, thus lacking the potential for market differentiation. On the other hand, there are already internal test methods in which the cell size is examined [22].

## **5.2 External literature analysis**

During the external literary research for the seven 'high'-rated weak spots, various literature references were found for almost all weak spots.

The weak spot 'Cell size/ side branch too small, Side branch accessibility', for example, received an overall result of 4, as shown in Table 15, chapter 4.2.2, as various

reports were found in which the side branch accessibility of different stents was investigated in bifurcations using different PCI techniques [31–33].

For the weak spot 'Stent performance in overdilatated condition' an overall rating of 5 was the result, as listed in Table 15, chapter 4.2.2, due the fact that Foin et al. already investigated how the stent cells and the individual stent struts behave after overdilatation was performed [27]. In another study, the best technique to achieve overexpansion and how it affects the mechanical behaviour of the stent platform was investigated [34].

For the weak spot 'Stent strut malapposition behaviour' mainly clinical studies were found. For example, Lindsay et al. investigated the behaviour of stent strut malapposition in relation to calcium distribution by OCT technique, while another clinical study investigates how OCT guided PCI reduces the number of malapposed struts [35, 36]. All clinical studies found investigate the stent strut malapposition behaviour using different techniques, however, no technical conclusion of the behaviour based on the stent design can be drawn. Only limited data on stent mechanical properties and stent apposition behaviour is available. During the entire literary research, only one report showed first investigations of the apposition behaviour of different DES in a test method developed for this purpose [3]. The resulted behaviour of the stent platforms, however, was attributed to the materials of the stents and not to their designs. For this reason and on the basis of the other literature found, a rating of 5 (Table 15, chapter 4.2.2) was reached for the weak spot 'Stent strut malapposition behaviour' in the total external literature evaluation.

The weak spots 'Narrowing side branch' as well as 'Pullback until necking' both reached a rating of 4 in the overall evaluation of the literary research, listed in Table 15, chapter 4.2.2. Both represent weak spots that have been discussed and investigated in the literature several times. For example, Gwon et al. investigated the influence that various PCI techniques can have on side branch narrowing or occlusion [37]. On the other hand, Seo et al. examines the predictors for side branch failure during PCI [38]. The weak spot 'Pullback until necking' was the subject of several studies and reports of true cases in which, for example, the treatment in case of a stent system getting stuck was discussed. [39]

During the entire literary research, no suitable literature was found on the weak spots 'Buckling susceptibility' and 'Torsions behaviour for higher requirements than stand-

ard specification'. Thus, external literature could not be used to prove how and whether the weak spots affect product performance and to what extent. Therefore, both became more relevant as no external literature and thus test methods currently exist and therefore received the highest overall rating with a rating of 7 respectively as listed in Table 15, chapter 4.2.2.

### **5.3 KOL interview analysis**

The interviews with eight interventional cardiologists have shown that the physicians have very different opinions on the individual weak spots.

For instance, the statements regarding the weak spot 'Cell size/ side branch too small, Side branch accessibility' differed greatly. For some of the cardiologists, the inadequate side branch accessibility of individual DES products due to small cell sizes represents one of the major problems during PCI and also led to complications and thus to prolongations of the intervention, while others see no problem with this weak spot and have therefore never had problems during PCI. All collected opinions from the physicians on this weak spot resulted in an overall rating of 26, as listed in Table 16, chapter 4.2.3.

On the subject of overdilatation of stents and thus on the weak spot 'Stent performance in overdilatated condition', the opinions of all physicians surveyed were almost identical. Most dilate during PCI above the maximum allowed labelled overdilatation diameter to ensure sufficient stent apposition to the vascular wall. Many see the maximum labelled overdilatation diameter as a major weak spot of some commercially available DES products and therefore choose stents that can be overdilatated further, especially in larger vessels. Some are critical about overdilatating stents and argued that they would never dilate more than 10% above this maximum labelled diameter because the risk of stent recoil is too high and thus would lead to a prolongation of the procedure by performing post-dilatation. The result of these statements of the physicians resulted in the second highest evaluation of the collected opinions with a sum of 27 (see Table 16, chapter 4.2.3).

With the weak spot 'Stent strut malapposition behaviour' the opinions of the physicians were again very different. For most of the physicians interviewed, the stent strut malapposition behaviour is a known problem, but for most it depends less on the de-



sign of the stents and more on the applied PCI technique. An adequate apposition of the stent struts to the vessel wall is one of the most important characteristics of a successful PCI for all physicians interviewed. Many therefore dilate, as already mentioned above, over the maximum labelled diameter of the stents to ensure this apposition of the struts to the vessel. However, some of the physicians also reported that despite overdilatation after control by angiography, the blood supply at the constricted site in the vessel was not present, which often led to an extension of the procedure. These and all other statements of the cardiologists on the weak spot 'Stent strut malapposition behaviour' led to an overall assessment of 26, as can be seen in Table 16, chapter 4.2.3.

Considering the weak spot 'Pullback until necking', which reached the highest rating of 28 after compiling all interviews in Table 16, chapter 4.2.3, the occurrence and severity of this weak spot during PCI, according the statements of physicians, led to this high number of points. Almost all of the physicians surveyed have already experienced problems with the return of the system, for example by the catheter system getting stuck on previously implanted stents. This led to an extension of the procedure for all of them. The physicians, who have never had problems with the weak spots so far, however, argued that everything depended on the right technique used during PCI and adequate preparation.

The weak spots 'Narrowing side branch', 'Buckling susceptibility' and 'Torsions behaviour for higher requirements than standard specifications' received the lowest scores when looking at the results in Table 16, chapter 4.2.3 with a sum of 16, 13 and 15 respectively. In the case of 'Narrowing side branch', almost all physicians were of the opinion that the weak spot is dependent on the correctly applied PCI technology. Whereas the weak spots 'Buckling susceptibility' and 'Torsions behaviour for higher requirements than standard specifications' were not even known to most of the cardiologists interviewed, nor would they have ever led to a problem during PCI.

## **5.4 Overall evaluation**

The weak spot 'Stent strut malapposition behaviour' achieved the highest overall evaluation with a total value of **30**, as can be seen in Table 17, chapter 4.2.4. In particular, the evaluation of the first interim rating showed the highest value compared to

the other six weak spots, as potential market differentiation may be possible due to the special Orsiro stent design with regard to stent apposition behaviour according to internal expert feedbacks. The evaluations of the external literary research as well as the physician interviews also resulted in high overall evaluations. However, despite the literature found, how different stent designs affect the apposition of the stent struts to the vessel wall is still an insufficiently understood topic. Even during the interviews with the physicians, opinions varied regarding better apposition behaviour of certain stents due to their designs. The divergent opinions of the physicians as well as the limited amount of data contributed significantly to the fact that the 'Stent strut malapposition behaviour' achieved the highest total number of points in the final overall evaluation and thus lead to a high interest of being investigated.

The second-highest overall evaluation with a rating of **28.5** was achieved for the weak spot 'Stent Performance in overdilatated condition'. Although different studies and reports regarding overdilatation of stents were found in which DES systems were examined after overdilatation, questions regarding stent overdilatation capacity and performance remain mostly open. In particular, the explanation for some of the maximum labelled diameters being much higher than others and what effect these over-expansion differences of the manufacturers have on performance is mostly unclear. This fact as well as the fact that it has become a normal practice of the interventional cardiologists to post-dilate the stents often above their maximum labelled overexpansion diameters without knowing the performance of the devices above this diameter labelled, has mainly contributed to the fact that this weak spot achieved the second-highest evaluation value.

## 6 Conclusion

The analysis of current-generation DES systems regarding acute weak spots with direct link to the clinical intervention has been proven to be more difficult and more comprehensive than expected. Nowadays, there are hardly any properties of commercially available DES systems that do not have to be investigated in existing test methods by the approval authorities. The identification of distinctive weak spots in DES therefore required a comprehensive expertise in the field of coronary stent systems as well as in properties of equivalent competitor products.

The external analysis of the literature provided important insights into the individual weak spots and was therefore essential to figure out what literature respectively test methods already exist with regard to the weak spots collected.

The evaluation of the weak spots on the basis of statements by interventional cardiologists proved to be a challenging aspect in finding weak spots for which a new test method shall be developed. Thus, the opinions of the experts sometimes deviated strongly from each other and it became apparent that some of the physicians questioned were more technically affine than others. While some of the cardiologists were able to draw a technical conclusion from the weak spots to the stent design of individual products, others only discussed the clinical aspect and could not assess the impact of the technical construction of the stent on the weak spots. Some of the physicians also did not intend to provide any statements about the performance of competitor products with regard to the weak spots, while others listed their favourites for various types of interventions. Based on the individual opinions of the practising physicians, only half of the interview ratings were included in the overall rating.

Based on the overall evaluation the 'Stent strut malapposition behaviour' and 'Stent Performance in overdilatated condition' represent the weak spots for which, according to evaluations by internal experts, analysis of external literature and statements by various physicians, the greatest interest exists in examining these topics in a defined test method. For this reason, a new test method is being developed in Part II as a basis for acquiring performance profiles of competitor devices.



## **Part II. Development of a new test method**

### **7 Introduction**

In order to be able to develop a suitable new test method according to the weak spots 'Stent strut malapposition behaviour' and 'Stent performance in overdilatated condition' defined in Part I, it is essential to have an understanding of both weak spots and to the literature existing on them. For this reason, an explanation of both is given in this chapter.

#### **7.1 Malapposition behaviour**

The stent malapposition is defined as the incomplete stent strut apposition to the arterial wall. This malapposition behaviour represents one of the greatest risk factors for late stent thrombosis and restenosis. Lindsay et al. correlate the stent strut malapposition with an incomplete stent expansion during PCI. OCT guided interventions and the use of other intracoronary diagnostic techniques should help to assess strut malapposition. [35]

Based on statements made by cardiologists, adequate apposition of the stent struts is one of the most important characteristics of an ideal stent. According to the physicians, the examination of an optimal apposition during PCI is carried out by various imaging procedures such as OCT, in which both the renewed correct blood flow and the position of the struts in relation to the vessel wall are examined.

#### **7.2 Overdilatation behaviour**

The weak spot 'Stent performance in overdilatated condition' is understood as the behaviour of the products after executing expansion of the stents above their maximum labelled expandable diameter. Because of difference in lumen diameter between the artery and the stent size, especially in some cases of bifurcation treatment where the distal and proximal lumen diameter differs, a proximal post-expansion of the stent is necessary in order to match the proximal reference diameter of the vessel and to ensure an optimal stent apposition. An incomplete apposition of the stent

struts (= malapposition) to the arterial wall is associated with increased risk of stent thrombosis and stent restenosis. In order to avoid these incidences, a stent post-dilatation is commonly performed using a large post-dilatation balloon. Based on reports found in the literature, post-dilatations and therefore overdilatations above the maximum labelled diameter of stents are increasingly performed in the left main coronary artery. [27, 40]

These findings about the post-dilatation in left main bifurcations found in the literature were also confirmed by statements of the physicians during the interviews. According to their statements and the fact that for the treatment of bifurcation lesions it is recommended to select the stent diameter close to the distal vessel diameter, most post-dilatations are performed in the proximal area of bifurcations to ensure optimal stent apposition [40]. Based on the argument of one cardiologist, the performance of post-dilatation especially for lesions located in the RIVA area is necessary, as the diameter differs greatly from the distal area in front of the RD bifurcation.

## **8 Methods and materials**

The following chapter describes the methods and the materials used to develop a new test method that is specifically adapted to the two weak spots. The test method will be developed according to the profiles of the seven selected competitor products with the aim of investigating the stents apposition and overdilatation behaviour.

Due the fact that no internal test methods for evaluating the apposition of stent struts to the vessel wall and for examining the stent platform after overdilatation of stents above their maximum labelled diameters are available, a selective test program is defined in which the methodology and the test scope are determined. For this purpose, an artificial coronary arterial lesion model in which stents of the chosen competitors should be implanted is determined and developed.

The following points explain in detail on which basis the compliant coronary lesion models were defined and developed in order to obtain clinically traceable silicone vessels and thus to create a basis for acquiring performance profiles of the competitor products according to apposition and overdilatation behaviour. In addition, in order to check the dimensions and mechanical behaviour of the silicone vessels developed, the performance of a test method verification is described and the methodology applied as well as the materials used are explained in detail. Furthermore, the entire test setup as well as the procedure for implanting the stents into the so-called mock vessels is described. Finally, the procedure for the investigation and evaluation of the apposition and overdilatation behaviour using Micro-CT is discussed and the required test setup described.

### **8.1 Definition of a selective test program**

In order to create a basis for evaluating the mechanical performance of the competitor products selected in Part I regarding apposition and overdilatation behaviour, a selective test program must be defined. This test program describes how the stents are to be examined for the two weak spots and to what extent the measurements are to be carried out.

The following chapter describes the basis on which the area in the arterial vascular system to be simulated by the mock vessel was decided. Furthermore, it explains how a test program was defined based on the profiles of the competitor products to

be tested. In addition, it demonstrates at which sections in the artificial vascular model apposition and overdilatation behaviour should be tested.

### **8.1.1 Imitation area of mock vessels**

To investigate the apposition and overdilatation behaviour of the stents simultaneously, both are to be tested in a benchmark test under clinically relevant conditions in a simulated artificial vessel model, the so-called mock vessel. The mock vessel should simulate a realistic clinical area in the arterial vascular system in which both the apposition and overdilatation behaviour of the stents can be investigated.

Considering the fact that post-dilatations are mostly performed in proximal areas of bifurcations in the left coronary artery as well as the fact that cardiologists interviewed overdilate often in bifurcation lesions in the area of RIVA in order to be able to carry out an adequate PCI, an idealised artificial vascular coronary vessel model is being developed in the context of this work that is intended to emulate the RIVA as well as the RD1 bifurcation.

Due the fact that the investigation of apposition/malapposition behaviour is recommended at stenosis, following the investigations of Foin et al. [3], a 3D-printed stenosis is integrated in the distal part of the RIVA.

### **8.1.2 Establishment of customized mock vessels**

In order to be able to test the selected DES of the seven manufacturers for overdilatation, the maximum allowed and labelled overexpansion diameter of each product had to be identified. As each manufacturer provides different sizes of stents, the size to be tested had to be selected in order to identify the maximum labelled diameter. Since the typical diameters of coronary vessels range from 2 to 4.5 mm and the most common diameters of coronary stents are between 2.5 and 4 mm, it was decided to test stents with a nominal diameter of 3 mm [9].

Table 18 lists all major diameters and the maximum available length as indicated by each manufacturer in their compliance chart and in the instructions for use for 3 mm diameter stents.



Table 18: Labelled limitation sizes for 3.00 mm stents of the seven competitor products

<b>Company &amp; product name</b>	<b>Diameter (@NP) [mm]</b>	<b>Diameter (@RBP) [mm]</b>	<b>Max. length [mm]</b>	<b>Overexpansion diameter [mm]</b>
BIOTRONIK Orsi-ro	3.00	3.33	40	3.50
Boston Scientific Synergy	3.00	3.27	38*	4.24
Abbott Xience Sierra	3.00	3.13	38	3.75
Medtronic Resolute Onyx	3.00	3.25	38	3.75
Terumo Ultimas-ter	3.00	3.20	38	3.50
Cordis Elunir	3.00	3.28	33	3.75
B.Braun Coroflex ISAR NEO	3.00	3.55	38	3.50

\*maximum available stent length is 48 mm. So that the models for all stents are approximately of the same length, it was decided to choose one size below and thus the 38 mm long stent.

To keep the proximal area in which the stents are to be tested for overdilatation large enough and due the fact that LAD/RIVA can range between 10 mm and 40 mm in length, the clinical vessel models are modified to the maximum lengths available for the 3.00 mm stents of the competitors. These vary, as shown in Table 18, between 33 mm, 38 mm and 40 mm depending on the manufacturer. The diameter at NP represents the inner diameter of the stent when inflating the stent under nominal pressure. The nominal pressure is the pressure required to dilate the stent to its nominal diameter. The Rated Burst Pressure (RBP), on the other hand, represents the next labelled pressure limit and is already referred to by most manufacturers as a limit value that must not be exceeded during PCI [28, 29].

Nevertheless, if the deployed stent size is still inadequate with respect to the vessel wall after performing expansions under NP and RBP, a post-dilatation with a high-pressure non-compliant balloon system may be performed [40]. In order to avoid de-

formation of the stent struts during post-dilatation and thus endangering the mechanical properties of the stents, each manufacturer specifies its maximum possible over-dilatation diameter to which the stent may be dilated. Although the manufacturers strictly advise against exceeding this value, according to the cardiologists interviewed, overdilatations are carried out very frequently in order to guarantee adequate apposition of the stent to the vessel wall. As can be seen in Table 18, these overexpansion diameters of stents labelled by the seven manufacturers vary between 3.50 mm, 3.75 mm and 4.25 mm.

In order to investigate the behaviour of the stent platforms when these overdilatation values are exceeded, three different artificial vessel models are developed as part of the test method development which have different inner diameters in the proximal part of the RIVA corresponding to the three different maximum labelled diameters of the seven competitors. While the inner diameter between transition zone (TZ) and proximal part is modified to the maximum overexpansion diameter (OExD) of the seven manufacturers, the inner diameter at the end of the proximal part of the RIVA is adjusted to the maximum labelled overexpansion diameter + 10% (OExD+10%). This results in the proximal inner diameters listed in Table 19 for the three differently labelled maximum diameters of the seven manufacturers.

Table 19: Selected proximal inner diameters of the three mock vessels to be developed

<b>Company &amp; product name</b>	<b>Overexpansion diameter (OExD) [mm]</b>	<b>Overexpansion diameter + 10% (OExD+10%) [mm]</b>
BIOTRONIK Orsiro	3.50	<b>3.85</b>
Terumo Ultimaster		
B.Braun Coroflex ISAR NEO		
Abbott Xience Sierra	3.75	<b>4.13</b>
Medtronic Resolute Onyx		
Cordis Elunir		
Boston Scientific Synergy	4.24	<b>4.66</b>

Figure 6 illustrates the longitudinal cross section of the mock vessel and depicts the areas of the different proximal inner diameters as "OExD" and "OExD+10%". The inner diameters in the distal section of the RIVA, however, remain the same for all models, as the nominal diameter of the stents of the seven competitors is the same and thus have a value of 3.00 mm, illustrated as "ND". The diameter at the transition between distal and TZ was selected from the rounded mean of the seven RBP labelled diameters of the manufacturers with 3.25 mm and is marked as "RBP" in Figure 6.

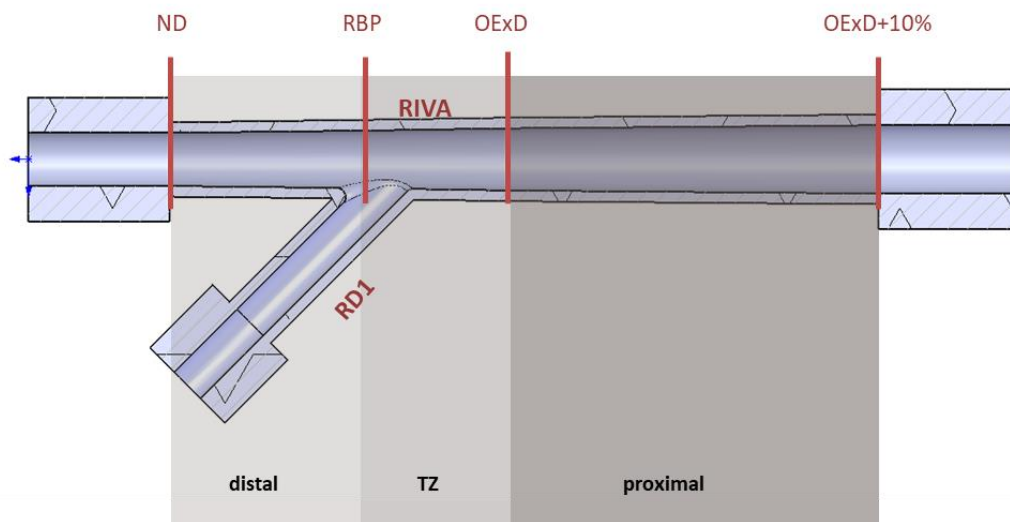


Figure 6: Simulation of the mock vessel to be developed with marked areas of different diameters

### 8.1.3 Test program for investigating weak spots

The idea of how and in which part of the mock vessels the selected stents should be examined for apposition and overdistalation behaviour is illustrated in Figure 7. The model represents one of the mock vessels to be developed, which contains a 3D-printed stenosis in the distal region. The apposition behaviour will be investigated in the distal part at the 3D-printed stenosis, while in the proximal section of the artificial artery an overexpansion will be performed to evaluate the behaviour of the stent platform. The RD1 branch remains free and was designed exclusively to simulate a bifurcation. The bars at the sides of the mock vessel and at the end of the branch were integrated only for the purpose of better fixation of the mock vessel during stent implantation. They are also referred to as 'holders'.

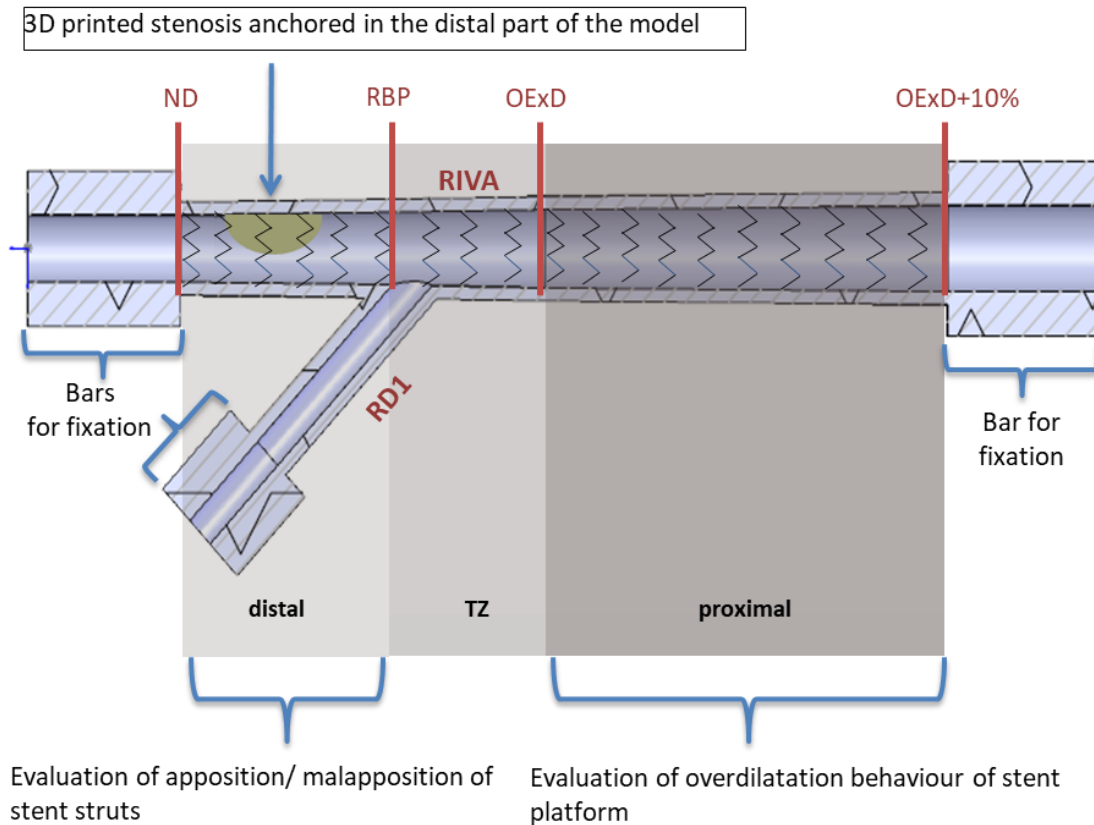


Figure 7: Simulation of the evaluation of the mock vessels to be developed. The zigzag pattern drawn in the vertical area simulates the stent implanted in the RIVA, the main stem

After expansion of the stents and post-dilatation in the proximal area to the respective over-dilatation diameter + 10%, the aim is to investigate the apposition behaviour in the distal area at the integrated 3D-printed stenosis and the over-dilatation behaviour in the proximal area.

The evaluation of the apposition behaviour at the stenosis in the distal area as well as the behaviour of the stent platform after an overexpansion will be carried out by Micro-CT technique. After scanning the samples, the following evaluations should be performed:

- Evaluation of strut malapposition
- Evaluation of residual stenosis
- Evaluation of over-dilatation behaviour

## 8.2 Design of mock vessels

The development of mock vessels for the medical sector is widely used and indispensable for evaluating various mechanical properties of medical devices in a realistic vessel model. The use of mock vessels in medical device studies represents an alternative to using animal vessels. In order to perform the testing of stents in such mock vessels as realistic as possible, these artificial vessels must possess approximately the same characteristics as real blood vessels. [41]

For this purpose, this chapter describes which investigations were used to determine the geometry of the bifurcation, i.e. the RD1, in order to manufacture a realistic clinical arterial model simulating part of the RIVA and the first branching. In addition, it is explained on what basis the degree and anatomy of the stenosis, which is to be simulated by a 3D-printed model and implanted into the mock vessel, was identified and determined. Furthermore, standards and guidelines are explained which have been followed to determine a suitable material and thus to select dimension of wall thickness in order to simulate the physical and mechanical properties of biological vessels for the mock vessels to be manufactured.

### 8.2.1 Bifurcation geometry

Although a multitude of bifurcations and trifurcations are present in the coronary arterial vessel system, no bifurcation geometry can be compared with any other. This is mainly due to large anatomical differences in diameters of bifurcations, angles between branches, accumulation and location of plaque and much more. [42]

Nevertheless, bifurcations can be classified according to the angulation between the main stem, also called main vessel (MV) or main branch (MB), and the side branch (SB). If the angle between the MB and the SB is  $> 70^\circ$ , it is called "T-angulation", while an angle of  $< 70^\circ$ , on the other hand, is known as "Y-angulation". Waksman et al. also maintain that the angle between MB and SB and the appearance and anatomy of plaque are closely related. [32, 42]

Various clinical studies have already been conducted to investigate the natural scattering of bifurcation angles in main coronary arteries. The study by Pflederer et al. revealed an mean bifurcation angle between LAD/RIVA and RD1 of  $46 \pm 19^\circ$  [43]. On the basis of this result and due to a simpler implementation in the construction, it was

decided to choose an angle of 45° between RIVA and RD1 for the mock vessels.

The relation between flow and diameter of the coronary bifurcation anatomy was already described by Murray more than 90 years ago. By combining the conservation of mass with the power law relation between flow and diameter, Murray was able to propose a relation as demonstrated in Figure 8. In his geometric relation, the proximal MB (D1) must equal the sum of the diameters of the distal MB (D2) and the SB (D3). By incorporating the laminar flow through the vessel, Murray's law contains an exponent of 3. This exponent was replaced both theoretically and experimentally years later by Huo-Kassab (HK) with an exponent of 7/3. While Murray's and HK's law is based on the conservation of mass, another formula introduced by Finet represents a simplification without including the conservation of mass. [33, 44]

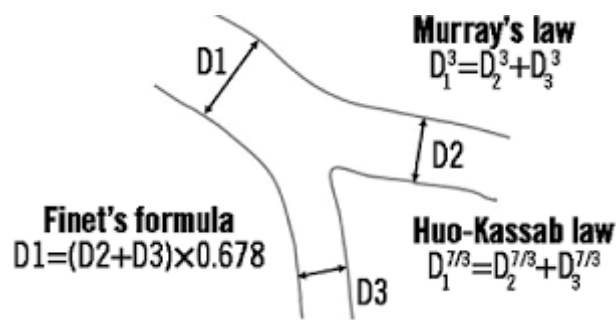


Figure 8: Different scaling laws for determining bifurcation diameters [33]

Since the HK law regards the entire coronary vessel system as an integrated whole where downstream resistances can influence the entire flow and Murray's law cannot experimentally support its exponent of 3 and considers individual vessels isolated, the diameter of the RD1 SB is determined by means of the HK law [44]. Converting the HK formula according to  $D_3$  to determine the SB diameter provides the following formula (1):

$$D_3 = \sqrt[7/3]{D_1^{7/3} - D_2^{7/3}} \quad (1)$$

Using the inner diameters previously defined in chapter 8.1.2, Table 18, for the distal MB (D2), illustrated in Figure 6 as "ND", and the proximal MB (D1) given as "OExD" (chapter 8.1.2, Table 19), the RD1 inner diameters listed in Table 20 results for the 3 mock vessels to be developed.

Table 20: Diameters of the distal (D2) and proximal (D1) MB used to calculate the expected SB diameter (D3)

<b>Distal MB diameter (D2) [mm]</b>	<b>Proximal MB diameter (D1) [mm]</b>	<b>SB diameter (D3) [mm]</b>
3.00	3.50	<b>2.10</b>
3.00	3.75	<b>2.55</b>
3.00	4.25	<b>3.30</b>

### 8.2.2 Stenosis anatomy

In order to imitate a clinically relevant indication for the selected area in the left coronary artery, the anatomy of a stenosis that is integrated into the artificial vascular model has to be defined.

According to the European Bifurcation Club (EBC), a bifurcation lesion is defined as “a coronary artery narrowing occurring adjacent to, and/or involving, the origin of a significant side branch” [45]. Bifurcation lesions typically occur at or near a division of major coronary arteries, whereby the lesion morphology can be divided into three segments: proximal MB, distal MB and SB. A bifurcation lesion is defined as significant if the stenosis causes a reduction of the vessels lumen diameter by at least 50%. To characterize coronary bifurcation lesions, many classification schemes in the field of interventional cardiology have already been published. The Medina classification represents one of the simplest and most commonly used classification schemes. In this classification, the three segments proximal MB, distal MB and SB are each assigned a value of '1' in the presence and '0' in the absence of a stenosis, as shown in Figure 9. [46]

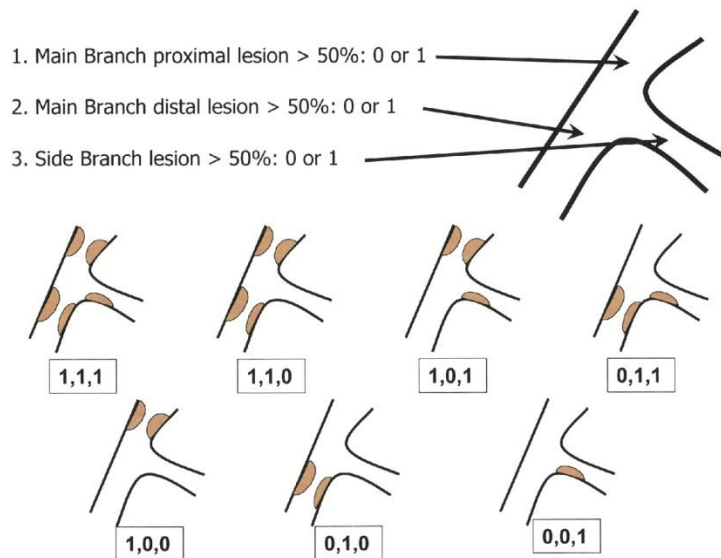


Figure 9: Medina's classification of coronary bifurcation lesions [46]

Since the apposition in the distal area of the RIVA is to be investigated, the lesion '0,1,0' in accordance with Medina classification was selected for the test method.

The anatomy of the stenosis was selected on the basis of results from clinical investigations of bifurcation lesions. In these studies, the length of stenosis in the LAD varied between 4.32 mm and 11.85 mm with a lumen reduction between 47% and 61.3% [42]. Since a total length of 40 mm was selected for the RIVA and the distal area of it occupies 11 mm, a stenosis length of 7 mm was selected due to the fact that cardiologists place the stent typically  $2 \pm 1$  mm beyond the stenosis. In addition, the stenosis is modified to cause a diameter lumen reduction of 50% at its maximum point simulating a significant lesion [46].

### 8.2.3 Wall thickness dimensions

One of the most important properties in the development of realistic artificial vessel models is the so-called radial compliance. The radial compliance determines the load on the vessel. [47]

Previous published studies have shown that the radial compliance of biological vessels is typically in the range of 4 - 7% [41]. According to DIN EN ISO 7198 (*Cardiovascular implants and extracorporeal systems – Tubular vascular grafts and vascular patches*) and DIN EN ISO 25539-1 (*Cardiovascular implants – Endovascular devices – Part 1: Endovascular prostheses*), artificially produced vessels must meet the required



compliance of the blood vessel to be depicted so that the implanted stent can be tested realistically. Radial compliance can be calculated according to formula (2). The change in the inner diameter of a vessel due to cyclic pressure changes is determined. [48, 49]

$$\% \text{ Compliance/ } 100 \text{ mmHg} = \frac{(D_{p2} - D_{p1}) \cdot 10^4}{D_{p1} \cdot (p_2 - p_1)} \quad (2)$$

where:

$D_{p1}$  = inner diameter at the pressure of  $p_1$  [mm]

$D_{p2}$  = inner diameter at the pressure of  $p_2$  [mm]

$P_1$  = lower pressure value (diastolic) [mmHg]

$P_2$  = higher pressure value (systolic) [mmHg]

As can be seen in formula (2), the calculated radial compliance must be given as a percentage of the diameter change per 100 mmHg according to standards. [49]

The radial compliance is mainly determined by the material used and the selected dimensions of the mock vessel. A correct determination of these two parameters is therefore essential for developing a biologically realistic mock vessel. In several earlier studies silicones are used for the production of mock vessels. Due to their transparent and biocompatible properties, they have proven effective for testing stents [41].

The modulus of elasticity (also called Young's modulus) of materials represents an important parameter in the selection of a suitable material as it can be used to predict the properties of materials. The Young's modulus of blood vessels is difficult to determine due to the complex composition of tissue. However, based on results of Hardung et al., who performed elasticity measurements on blood vessels in their study, an elastic modulus of 1.68 MPa can be assumed for human arteries. [50]

In order to find a suitable silicone for the manufacture of mock vessels, their modulus of elasticity must be determined. In literature there are different approaches to define the modulus of elasticity of silicones. One of the simplest models is represented by the Neo-Hooke model. In this model, the shear modulus  $G$  is first calculated from the Shore-A hardness  $H_A$  of the silicone using formula (3). [51]

$$G = \frac{0.07515 \cdot H_A + 0.549}{(4.1 + 3.9 \cdot e^{-1.397 \cdot h}) \cdot (0.395 \cdot h + 0.315 \cdot h^2)} \quad (3)$$

with

$$h = 0.025 \cdot (100 - H_A) \quad (4)$$

Based on the shear modulus  $G$  the Neo-Hooke parameter  $C_{10}$  given in formula (5) can be determined.

$$C_{10} = \frac{G}{2} \quad (5)$$

The modulus of elasticity  $E$  can then be calculated using the relation (6).

$$E = C_{10} \cdot 6 \quad (6)$$

Since the silicone Elastosil M4546 from Wacker Chemie AG is already used by Biotronik AG for the production of artificial cardiac aorta, the Young's modulus is calculated from the hardness value in order to find out whether this corresponds to the Young's modulus of biological coronary vessels. When using formulas (3) to (6) and the given Shore-A hardness of 40, an Young modulus of 1.78 MPa results for this silicone. As the Young's modulus of Elastosil differs from the Young's modulus of biological arteries by less than 6% and the radial compliance depends not only on the material properties but also on the vessel dimensions, this silicone is used in the context of this thesis for the production of mock vessels.

In order to dimension the wall thickness of the artificial vessel model when using the material Elastosil in such a way that it corresponds to the compliance of arteries, Hook's law (7) is used in combination with Barlow's formula (8) [51–53]. Whereby  $\sigma$  in Hook's law represents the stress tensor,  $\varepsilon$  the strain tensor and  $E$  the Young's modulus.

$$\sigma = \varepsilon \cdot E \quad (7)$$

In Barlow's formula, variable  $p$  denotes the pressure that is applied to the inner wall of the vessel,  $d$  the inner diameter of the vessel and  $S$  the wall thickness.

$$\sigma = \frac{p \cdot (d + S)}{2 \cdot S} \quad (8)$$

If one equates Hook's law with Barlow's formula and reshapes it to  $S$ , formula 9 is

obtained for determining the mock vessel wall thickness.

$$S = \frac{d \cdot p}{(2 \cdot \varepsilon \cdot E) - p} \quad (9)$$

Considering that according to DIN EN ISO 7198 [49] the radial compliance should be measured at an internal pressure of 100 mmHg and the biological radial compliance of vessels represented by variable  $\varepsilon$  lies between 4 - 7%, the wall thickness can be determined. Using the distal inner diameter of 3 mm defined in chapter 8.1.2, Table 18, the Young's modulus of Elastosil with a value of 1.78 MPa and a compliance of 5%, a wall thickness of 0.24 mm results at an inner pressure of 100 mmHg.

### **8.3 Manufacture of mock vessels**

In this chapter the production processes for the manufacture of mock vessels are discussed in detail and the design and functionality of individual parts of the rig are explained.

#### **8.3.1 Mock vessel rig design and functionality**

For the production of mock vessels, the casting process is used. In this process, the liquid silicone is poured into a mould, which represents the dimensions of the artificial arterial vessel to be formed.

In order to produce the three different mock vessels defined in chapter 8.1.2 with the selected dimensions, three different construction rigs (= moulds) were designed using the CAD software SolidWorks (Dassault Systèmes SolidWorks Corporation, Massachusetts, USA). A rig consists of two outer shells, depicting the component to be filled, an inner mandrel which consists of the RIVA and the RD1 branch and is placed inside the shells and a cover for fixation of all parts. As a wall thickness of 0.24 mm represents a dimension that renders it almost impossible to remove the vessel after cross-linking from the moulds, the wall thickness had to be adapted in order to enable a constantly adequate and artefact-free production. On the basis of studies by Colombo et al. [54] who designed mock arteries with a wall thickness of 0.4 mm and the fact that one of the leading manufacturers of artificial arterial vessel models produces

mock vessels that have a wall thickness of 0.7 mm, the decision was made to use the mean value of 0.6 mm as dimension of wall thickness. Figure 10 represents the dimensions of one of the three designed mock vessels to be developed using the casting process in moulds developed for this purpose. As can be seen in the figure, the inner and outer diameters have been dimensioned exactly to obtain a wall thickness of 0.6 mm. The diameters that differ between the three mock vessel designs are marked red in Figure 10 and listed in Table 21.

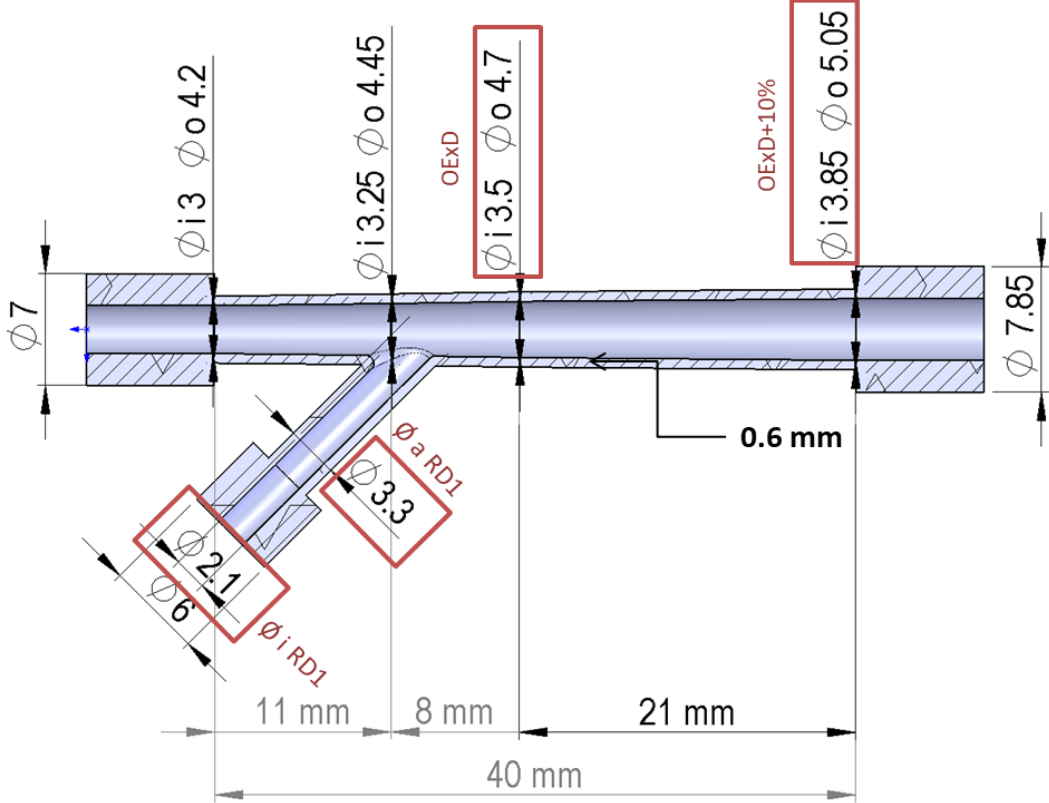


Figure 10: Dimensions of the mock vessel design 1

Table 21: Dimensions of the three mock vessel designs that differ

Mock vessel design	OExD [mm]		OExD+10% [mm]		RD1 [mm]	
	$\varnothing_i$	$\varnothing_a$	$\varnothing_i$	$\varnothing_a$	$\varnothing_i$	$\varnothing_a$
1	3.50	4.70	3.85	5.05	2.10	3.30
2	3.75	4.95	4.13	5.33	2.55	3.70
3	4.24	5.44	4.66	5.86	3.30	4.50

In order to obtain the three mock vessels with the selected dimensions, the two outer shells as well as the inner mandrel of each rig were constructed exactly in such a way that the cavity to be filled in at a concentric position of the mandrel is 0.6 mm in thickness. A cover was designed to fix the two outer shells together with the inner mandrel as well as to ensure that the inner mandrel is centered exactly as such that the resulting mock vessel has a uniform thickness along its length. Figure 11 illustrates one of the three drawn construction rigs, which consists of five components. Where 1 and 2 represent the two outer shells, 3 the RIVA, 4 the RD1 branch and 5 the cover.

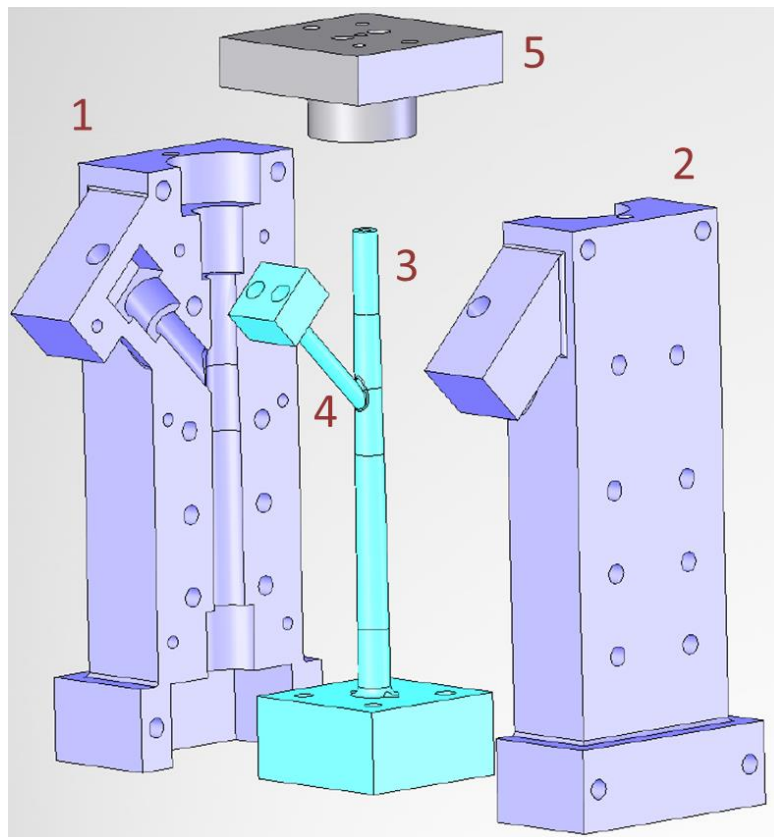


Figure 11: Construction rig for the manufacturing of mock vessel design 1

In order to optimally seal the two outer shells after insertion of the inner mandrel and fixing by the cover and thus to prevent the penetration of air bubbles, they were connected to each other by additional screws. The holes illustrated in Figure 11 in components 1 and 2 simulate the holes designed for fixing the screws. The ends of the outer shells and cover have been constructed with additional exit holes to allow the transfer of silicone through these channels during the casting process and to ensure

that air can escape from the holes during the cross-linking process.

To integrate the stenosis into the silicone models after they have been manufactured, one outer shell was designed with the device marked red in Figure 12. This device kept a part in the distal region of the mock vessels silicone-free during the casting process and enabled the stenosis to be inserted exactly at this point with the holder, marked red in Figure 13, which was constructed on the top of the stenosis.

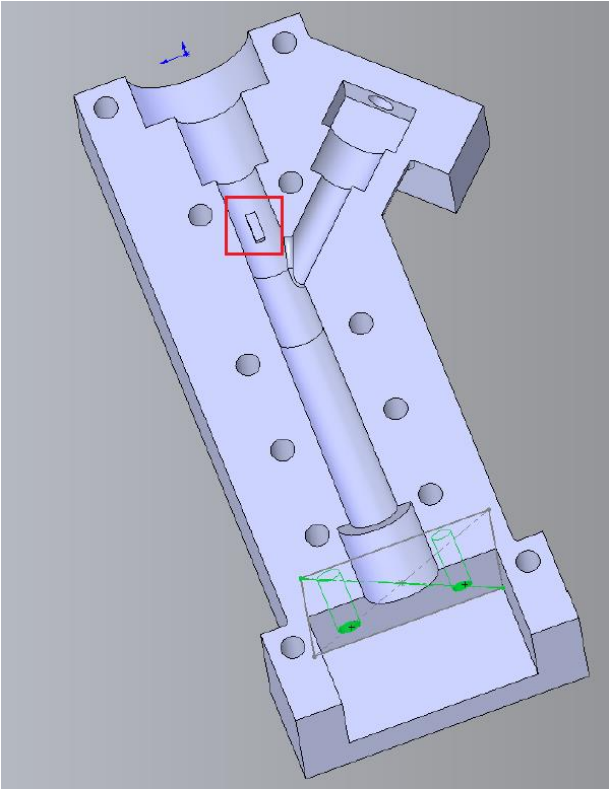


Figure 12: Device for enabling stenosis fixation in the silicone mock vessels

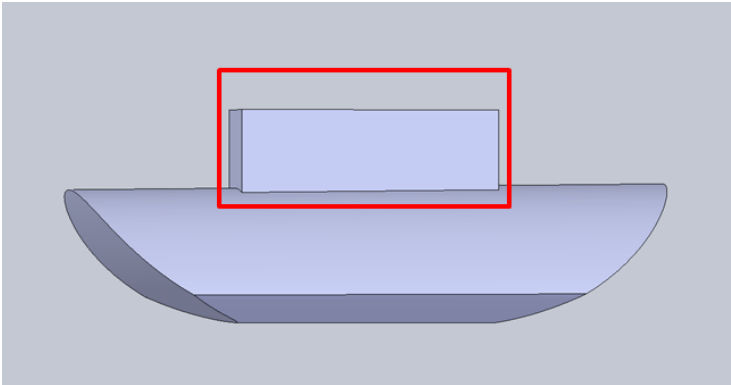


Figure 13: Design of the defined stenosis with the holder attached to the top for fixation in the mock vessel

For the manufacture of mock vessels, only the construction rig with the dimensions of mock vessel design 1, which represents the dimensions of Biotronik's DES Orsiro, was 3D-printed in an external workshop. The printshop uses the method of stereolithography, whereby the models can be built with a layer thickness between 0.05 mm and 0.1 mm [55]. The designed stenosis (Figure 13), which is supposed to cause a 50% diameter lumen reduction after implantation into the silicone vessels, was also 3D-printed using the same rigid material. The material, Accura® Xtreme [55], with a Shore D hardness of 86 and a Young's modulus of about 2000 MPa represents an ideal material for moulds and additionally corresponds to properties of materials used in a study to simulate real calcifications [56].

The CAD drawings of the components of the rig of mock vessel design 1 can be found in appendix 13.7.

### **8.3.2 Silicone mock vessel production**

The manufacture of mock vessels can basically be divided into three phases: the preparation of the construction rig and the materials to be used, the casting of the moulds and the post-processing of the mock vessels as well as of the construction rig.

During the preparation phase, each component of the construction rig was first cleaned and then coated uniformly with a wax-based release agent (Achem SG-1008S, Angewandte Chemie GmbH, Ganderkesee, Germany). This release agent facilitates the release of the mock vessel off the inner mandrel as well as off the outer shells once the silicone had cured. Once the components had been coated, they were assembled using pins and screws and afterwards mounted on a vice for the casting process as shown in Figure 14.

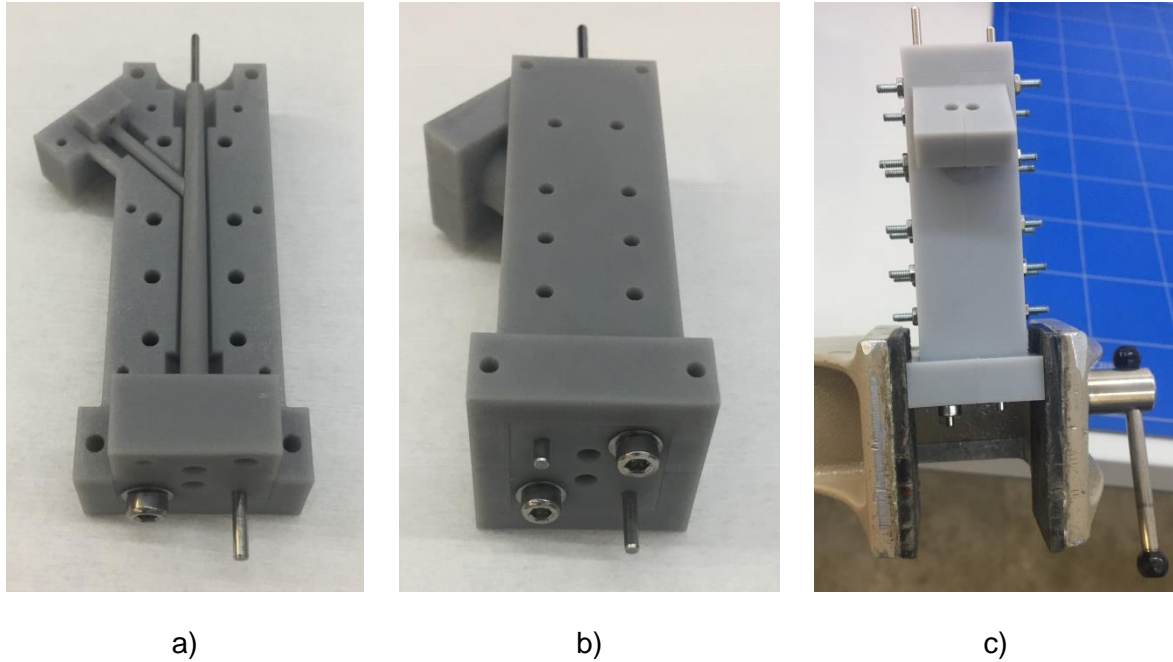


Figure 14: Assembly of rig. a) Mounting the inner mandrel to the first outer shell b) Attaching the second outer shell to the inner mandrel followed by mounting the cover c) Fastening the entire construction rig to a vice

Before the casting process could begin, the silicone had to be prepared. The silicone Elastosil M4645 (Elastosil M4645 A/B, WACKER Chemie AG, München, Germany), used in the context of this work, is a two-component rubber. During the cross-linking process, which can take place at room temperature or high-temperature, the plastic state is converted into an elastomeric rubber structure. According to the data sheet, components A and B were weighed in a ratio of 10:1 on a laboratory scale (Entris Sartorius, 220 g weighing capacity, 0.1 mg readability, Sartorius Lab Instruments GmbH & Co. KG, Goettingen, Germany) [57]. Subsequently, both components were mixed for seven minutes in a vacuum mixer (Wamix-Touch Injector, 100 – 550  $\text{min}^{-1}$  rotational speed, at least 5 bar compressed air supply, Wassermann Dental-Maschinen GmbH, Hamburg, Germany). During the mixing process, this vacuum mixer is able to remove the air bubbles that form in the mixture as a result of mixing [58].

Following the mixing process and vacuum drawing, the prepared Elastosil was injected via syringes into the injection holes constructed on the bottom of the inner mandrel. Although (according to the manufacturer) the silicone belongs to the group of silicones cross-linking at room temperature and thus requires a cross-linking time of 12 hours, the process can be accelerated enormously at elevated temperatures, fol-



lowing the manufacturer's data sheet [57]. For this reason, the system was placed in a furnace (Convection furnace, A. Hofmann, Ostfildern, Germany) at 60 °C for four hours.

Once the cross-linking time was over, the construction rig was taken out of the furnace and left to cool down for 30 minutes at ambient temperature. To remove the mock vessel from the mould, the cover was first removed, followed by the outer shells. The silicone vessel was subsequently slipped off the inner mandrel by gently unwinding it with a spiral movement, taking care not to damage it. The excess silicone residues on the mock vessel and in the components of the rig were then removed using needles and tweezers so that the vessel was ready for further processing and the construction rig could be used for further fabrications.

## 8.4 Mock vessel design and process verification

In order to evaluate geometric and mechanical properties of the artificial vessel models manufactured in the context of this work, test methods were developed and carried out.

According to DIN EN ISO 7198, there are already a number of test methods that allow the evaluation of artificial cardiovascular implants. In this context, however, it should be mentioned that the standards and test procedures listed are intended for cardiovascular implants that remain permanently in the human body replacing segments of the cardiovascular system [49]. Thus, standards and test procedures mentioned in DIN EN ISO 7198 do not exactly reflect requirements for mock vessels for in-vitro testing. However, the specification of properties and development of test methods for verification mock vessels was oriented on this standard.

For characterizing geometric and mechanical properties of mock vessels the following tests were performed:

- Visual inspection for air bubbles
- Verification of relevant lengths, diameters and bifurcation angle
- Evaluation of reproducibility of stenosis placement and lumen reduction
- Determination of radial compliance
- Measurement of wall thickness

As part of this work, nine mock vessels were produced. Since destructive tests were planned for wall thickness measurements, but some of the mock vessels had to be used for stent implantations as well as for first Micro-CT scans in the following chapters 8.5 and 8.6, a test matrix was prepared in advance which divides the entire test procedure into destructive tests and non-destructive tests. Table 22 lists the test matrix including tests to be performed in both categories.

Table 22: Developed test matrix for testing the manufactured mock vessels for geometric and mechanical properties

Test category	Visual inspection for air bubbles	Verification of relevant lengths, diameters and bifurcation angle	Evaluation of reproducibility of stenosis placement and lumen reduction	Determination of radial compliance	Measurement of wall thickness	Stent implantation including further investigations <sup>*</sup>
Non-destructive	X	X	X	X		X
Destructive	X	X		X	X	

<sup>\*</sup> performed and described in chapter 8.5

As can be seen in Table 22, in both categories the mock vessels are to be checked for air bubbles, verified for lengths, diameters and bifurcation angle between RIVA and RD1 and are determined in radial compliance. In addition, samples that are assigned to "non-destructive" category undergo stent implantations and are then subjected to further examinations, described in chapter 8.5.

In order to randomly assign the nine manufactured mock vessels to the two test categories, a random sample was carried out using the statistical software Minitab (Minitab GmbH, München, Germany). It was decided to include three of the nine mock vessels in the non-destructive tests and thus in the stent implantations to be performed in chapter 8.5 and to carry out non-destructive tests and thus wall thickness measurements on the remaining six. The random sample test thus revealed the assignment of mock vessels to the two test categories listed in Table 23.

Table 23: Randomized assignment of the nine manufactured mock vessels to the two defined test categories

Mock vessel no.	Test category
1	Destructive
4	
9	
2	
3	
6	
8	Non-destructive
5	
7	

In the following chapters, the individual performed test methods are explained in detail and the devices and materials used are explained. All test results obtained were recorded in test protocols.

#### 8.4.1 Visual inspection for air bubbles

The mock vessels were visually checked for air bubbles using the digital microscope Keyence VHX-500F (KEYENCE DEUTSCHLAND GmbH, 10 µm resolution, Neu-Isenburg, Germany). At this point it can be mentioned that all further mentions of measurements using the Keyence digital microscope refer to the model and the specification given here.

Each mock vessel was placed separately on the microscope stage (illustrated in Figure 15) and examined with magnification 20x. The visual inspection always started at the distal holder of the vessel and continued along the length of the RIVA to the proximal end of the vessel. Finally, the RD1 and its holder were examined for air bubbles.

The location and number of air bubbles found are recorded for each mock vessel.

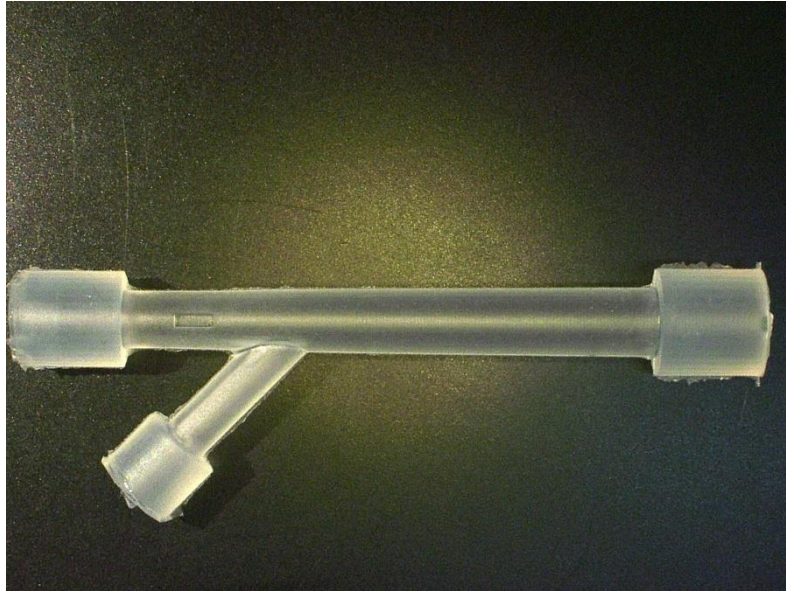


Figure 15: Placement of the mock vessels on the microscope stage for inspection for air bubbles

#### **8.4.2 Verification of relevant lengths, diameters and bifurcation angle**

##### **Length of the RIVA and the stenosis fixation**

For the verification of the lengths of the developed mock vessels it was decided to examine the length of the RIVA as well as the length of the stenosis fixation integrated in the vessel.

The length of the RIVA of each sample was measured visually using a ruler (shown in Figure 16), which can measure with a resolution of 0.5 mm.

One measured length was recorded per mock vessel and the arithmetic mean  $\bar{x}$  and standard deviation  $s$  of all sample lengths were calculated. The % deviation from the initially defined length value of the RIVA (40 mm) was calculated from the determined mean value of all lengths.

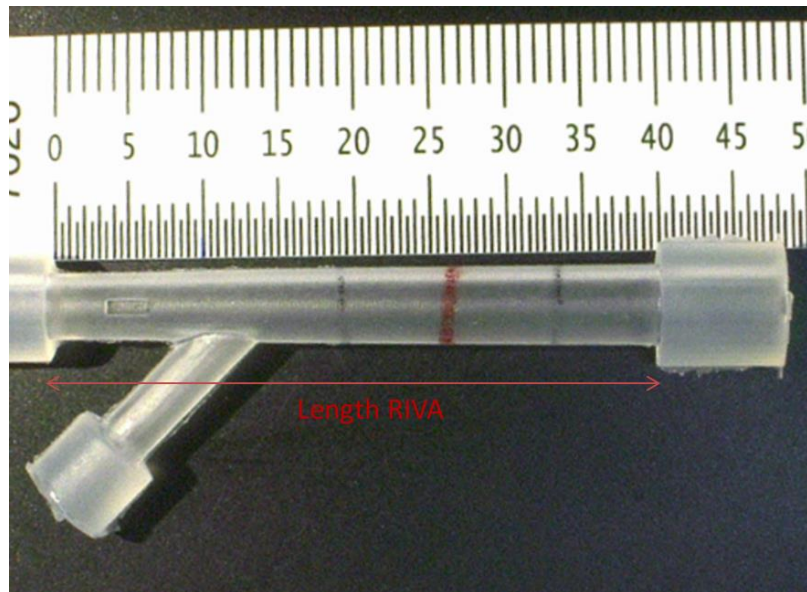


Figure 16: Measurement of the length of RIVA using ruler

The length of the stenosis fixation, initially defined as 3 mm, was measured with the digital microscope from Keyence GmbH. As shown in Figure 17, the measurement was carried out at three measuring points, two at each corner and one in the middle of the fixation, using the integrated measuring function of the digital microscope.

The arithmetic mean  $\bar{x}$  and the standard deviation  $s$  were calculated from all three measuring points of the respective mock vessels. In addition, the total mean value from all recorded measuring points and the corresponding standard deviation were calculated. This mean value was then compared with the initially defined length value of the stenosis fixation and the % deviation was recorded.

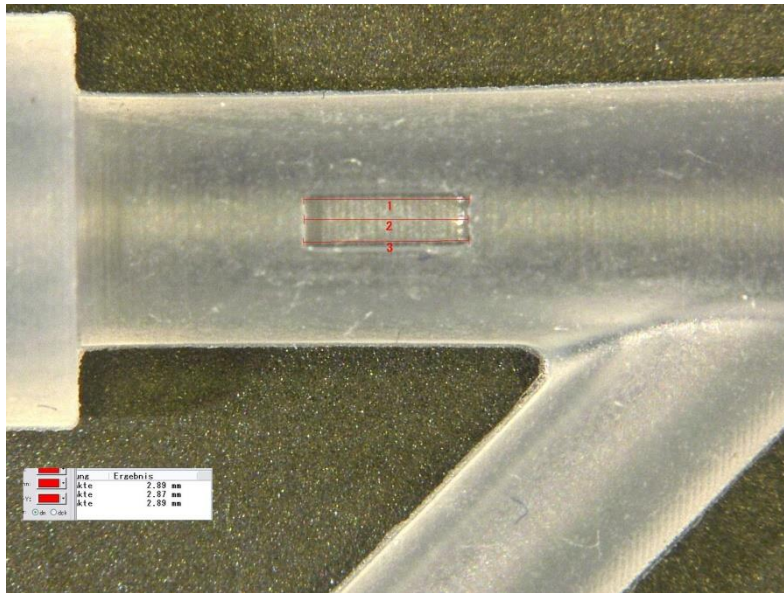


Figure 17: Measurement of the length of the stenosis fixation at 3 measuring points

### Bifurcation angle

The verification of the defined angle between RIVA and RD1 was performed by centrally placing each sample on the microscope stage and subsequently measuring it using the angle measurement function of the Keyence digital microscope.

For each mock vessel one line was drawn in the center of the RIVA and one in the center of the RD1 and the angle between the two was recorded, as illustrated in Figure 18. From the recorded values, the arithmetic mean  $\bar{x}$  and the standard deviation  $s$  were recorded. Finally, the % deviation of all values from the initially defined angle of  $45^\circ$  was determined.



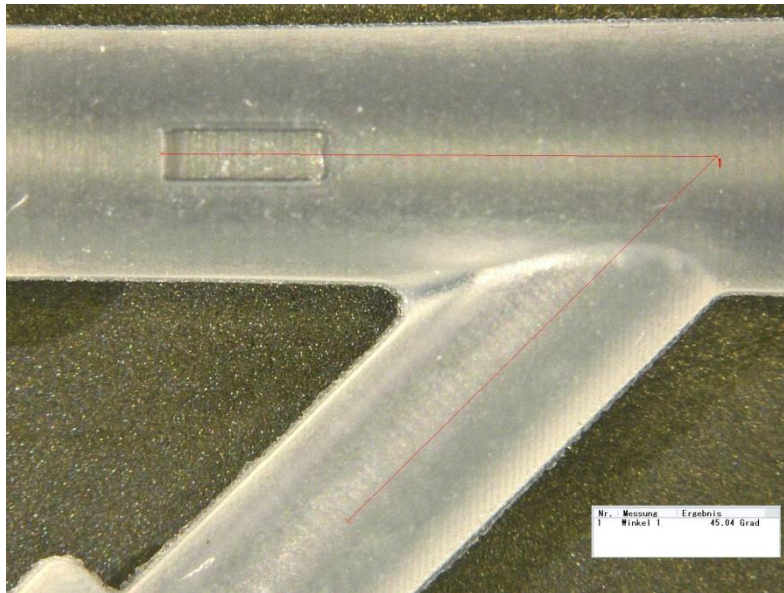


Figure 18: Measurement of the bifurcation angle

### Outer diameters

The outer diameters were verified at the measuring points "MP ND", "MP OExD", "MP OExD+10%" and "MP RD1". All four measuring points represent points whose diameters were defined during the construction of the mock vessel in chapter 8.1.2. In order to be able to measure the diameter of measuring point "MP OExD" at the precisely defined position, as illustrated in Figure 19, the position had to be measured out and marked on the mock vessels first. Since the distance of "MP OExD" to the measuring point "MP ND" is known from the construction, it was measured using the measuring function of the Keyence digital microscope and marked with a pen at position "MP OExD".

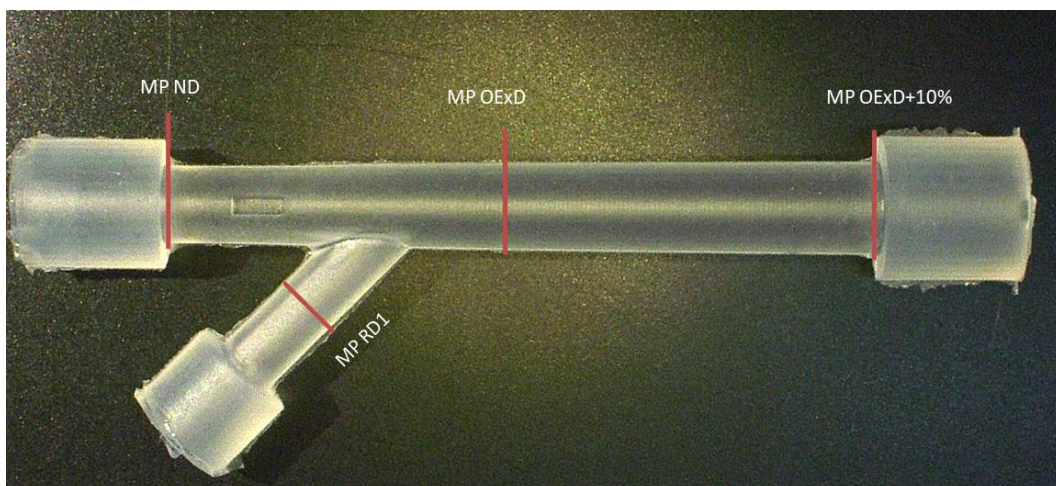


Figure 19: Illustration of measuring points at which the outer diameters were determined



The outer diameters were then measured per measuring point in two different orientations. These orientations were chosen in such a way that the scar, which is formed on the vessels during the cross-linking of the silicone due to the two outer shells, as shown in Figure 20, is not included in the measurement and thus leads to measurement errors.

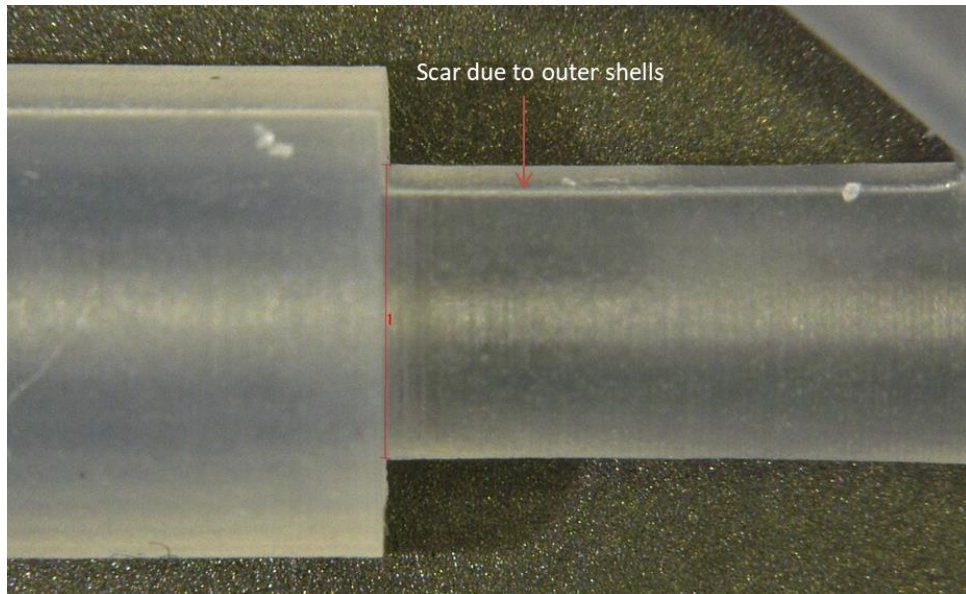


Figure 20: Measurement of the outer diameter at measuring point "MP ND" and illustration of the scar which results when cross-linking the silicone in the outer shells

At the measuring point "MP OExD" three measurements per orientation along the marked line were taken while at the measuring points "MP ND" and "MP OExD+10%" one measurement per orientation was taken, because the diameter exactly at this position corresponds to the predefined value and cannot vary as in the measuring point "MP OExD" due to marking with a pen. To determine the diameter of the RD1, three measurements were also carried out per orientation, as the diameter is the same over the entire length of the RD1 and to increase the number of measured values.

The arithmetic mean  $\bar{x}$  and the standard deviation  $s$  per mock vessel were then calculated from the measurements recorded in the two orientations. From the mean values of the measuring points "MP ND", "MP OExD", "MP OExD+10%" and "MP RD1" the total mean values and the standard deviations were determined. These mean values were then used to calculate the deviation from the initially defined outer diam-

eters of the respective measuring points, visible in Figure 10, chapter 8.3.1.

### **8.4.3 Evaluation of reproducibility of stenosis placement and lumen reduction**

The mock vessel was designed in such a way that the distance between the 3D-printed stenosis and the distal measuring point "MP ND" after implantation of the stenosis is exactly 2 mm. This dimension was chosen because, according to a cardiologist, the stent is typically placed 2 mm beyond the calcification in the vessel. In order to verify this distance, the 3D-printed stenoses were first inserted into the mock vessels to be tested. The device designed on the top of the stenoses allowed the stenoses to be ideally integrated into the silicone-free hole of the mock vessels.

For the distance measurement the mock vessels were placed on the Keyence microscope stage. Afterwards the distance between the stenosis edge and the measuring point "MP ND" was measured using the integrated measuring function of the digital microscope, as illustrated in Figure 21 by a red measuring line.

One distance measurement per mock vessel was recorded and the arithmetic mean  $\bar{x}$  and the standard deviation  $s$  were then determined from all measurements. The deviation from the initially defined distance (2 mm) was determined from the total mean value.

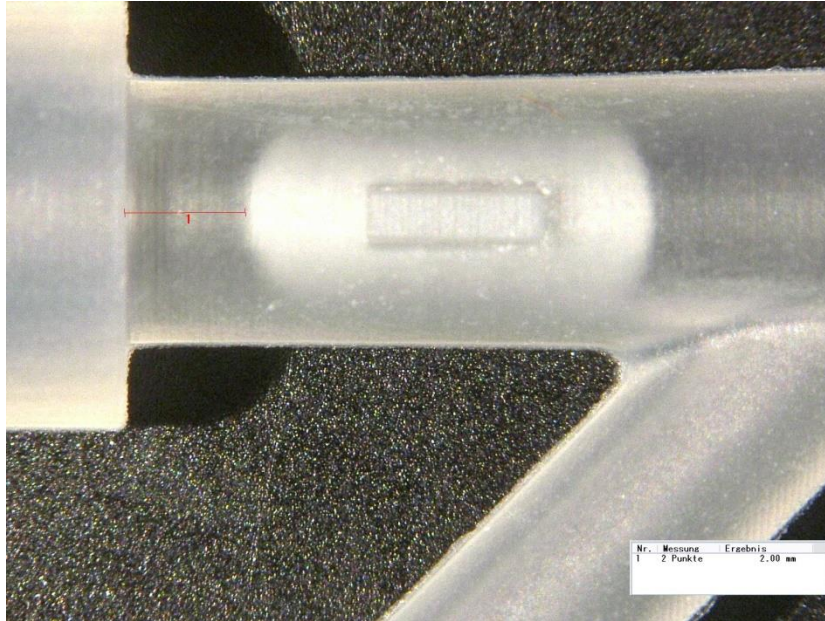


Figure 21: Measurement of the distance of the stenosis to the distal measuring point "MP ND" after fixing the 3D-printed stenosis in the constructed position in the mock vessel

For testing the lumen reduction caused by the implanted stenosis, test rods were used. Since the initial inner diameter of the vessel at the point where the stenosis should exhibit a 50% reduction of the lumen according to the constructed dimensions corresponds to a value of 3.14 mm, test rods of 1.56 mm and 1.57 mm in diameter were used. The test rod was carefully inserted into the mock vessel up to the anchored stenosis. If the stenosis could be passed without applying great pressure and deformation of the vessel, the diameter lumen reduction was calculated using formula 10 based on the diameter of the test rod  $D_r$  used and the known initial inner diameter  $D_i$  of the vessel at this position.

$$\% \text{ diameter lumen reduction} = \frac{D_r}{D_i} \cdot 100 \quad (10)$$

#### 8.4.4 Determination of radial compliance

According to DIN EN ISO 7198, artificially manufactured vessels have to be tested for their dynamic radial compliance. This should be done by measuring the change in diameter under dynamic cyclic simulated vessel loading. [49]

Since, as previously mentioned, the test procedures defined in DIN EN ISO 7198 were developed for vascular implants remaining in the body and therefore do not fully

meet the requirements for mock vessels, a separate test method for determining radial compliance was developed which is, however, oriented to the standard.

In order to test the diameter change of the mock vessels under vessel loading, a dynamic pressure was applied to the inner side of the vessels. The inflation device (Festo Manometer 161126, Festo AG, 0.02 bar resolution, Lupfig, Switzerland) was attached to the proximal opening of the mock vessels while the distal end and the RD1 were closed during the measurement to maintain a constant pressure on the inside of the vessel. During the measurement process, the mock vessels were placed centrally in the fixture of a 1-axis laser device (Zumbach Electronic USYS, Zumbach Electronics AG, 1  $\mu\text{m}$  resolution, Orpund, Switzerland) in order to measure the outer diameter during dynamic pressure loading. For a test cycle, the mock vessel was pressurized from 0 mmHg to 150 mmHg in 75 mmHg steps while the outer diameter was simultaneously measured with the 1-axis laser scanner.

The measuring procedure was carried out at the following measuring points (MP) shown in Figure 22. To measure the change in diameter per applied pressure unit, the mock vessels were aligned in two directions, as already described in chapter 8.4.2 when measuring the outer diameter, so as not to falsify the measurement result by the scar in the mock vessels.

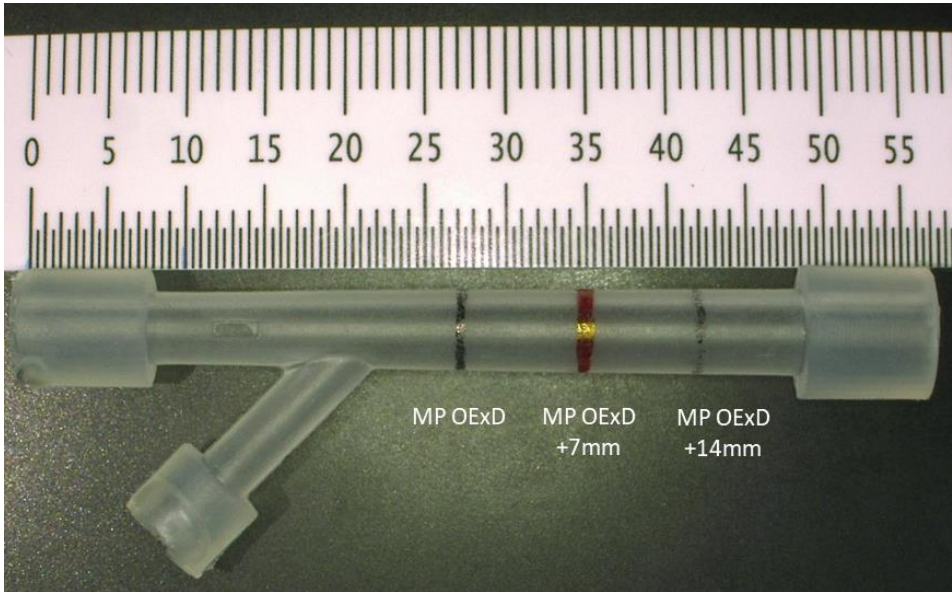


Figure 22: Measuring points at which diameter changes during dynamic pressure release were recorded

Since according to DIN EN ISO 7198 the radial compliance is defined as the change in inner diameter of a vessel due to pressure changes, the measured outer diameters had to be converted to the inner diameters [49]. This was done as shown in formula 11, from the outer diameter  $D_{po}$  at the respective pressure delivery and the wall thickness  $t$  provided from the destructive tests.

$$D_{pi} = D_{po} - 2 \cdot t \quad (11)$$

Once the inner diameters  $D_{pi}$  in the specified pressure range had been calculated the radial compliance could be calculated according to formula 2 depicted in chapter 8.2.3.

From the measured outer diameters and the calculated inner diameters per pressure unit, both the arithmetic mean values  $\bar{x}$  and the standard deviations  $s$  were determined for each mock vessel per measuring point. The radial compliance per mock vessels was determined from the calculated inner diameters at the respective measuring points. From all determined results of the outer and inner diameters as well as the radial compliance at the respective measuring points, the total mean values and standard deviations were calculated. To determine the total radial compliance per mock vessel, all mean values and standard deviations were summarized. Finally, the overall radial compliance of all mock vessels was calculated from the determined mean values and standard deviations.

#### **8.4.5 Measurement of wall thickness**

The wall thickness measurements were performed to both determine the concentricity of the developed mock vessels and to obtain the inner diameters of the vessels required for the calculation of the radial compliance, as given in chapter 8.4.4. The wall thicknesses were therefore measured at the same measuring points (see Figure 22, chapter 8.4.4) where the diameter changes were measured to determine radial compliance. For this purpose, thin discs were cut out at these exact positions using a scalpel and examined by means of the Keyence digital microscope. As shown in Figure 23, the wall thicknesses were measured at two positions in the x- and y-axis using the integrated measuring function of the digital microscope.



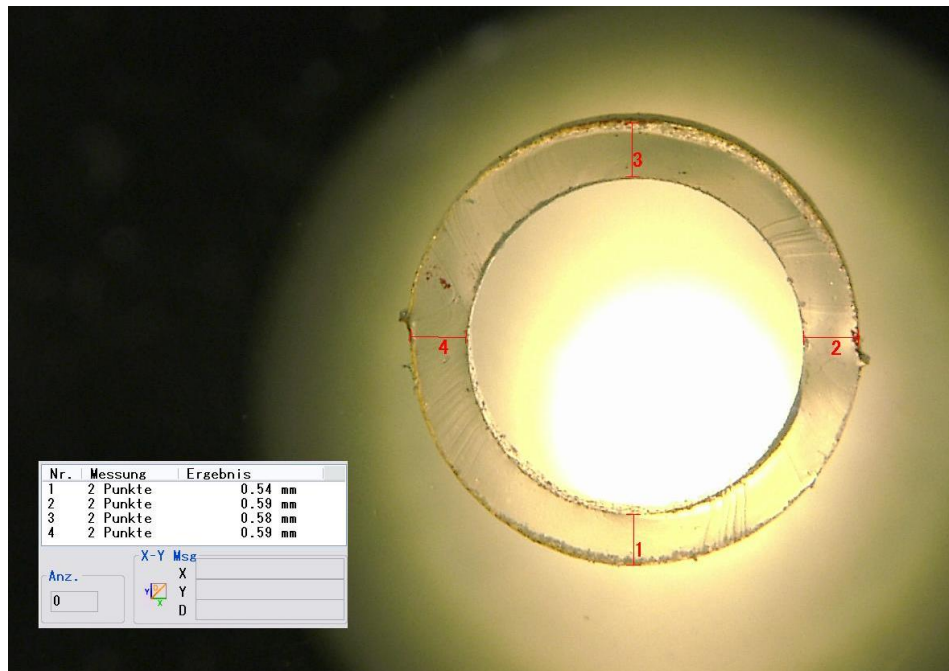


Figure 23: Measurement of wall thicknesses from cross sections at two measuring points in x-direction and at two in y-direction

For the determination of the concentricity  $C$ , the minimum  $t_{min}$  and maximum  $t_{max}$  wall thicknesses determined at the respective measuring points "MP OExD", "MP OExD+7mm" and "MP OExD+14mm" were used as depicted in formula 12. As can be seen in formula 12, the concentricity is given in %. A value of 100% indicates that the mock vessel is completely concentric [59].

$$\% C = \frac{t_{min}}{t_{max}} \cdot 100 \quad (12)$$

From the four measurements per measuring point and mock vessel, the minimum and maximum wall thicknesses were determined and the concentricity calculated. In addition, the arithmetic mean values  $\bar{x}$  and standard deviations  $s$  of all wall thickness measurements and concentricity determinations were calculated and the deviations from the initially defined values were determined.

## 8.5 Implantation of stents in mock vessels

To investigate the apposition behaviour of the stent struts to the vessel wall and to the integrated stenosis and to determine how the stent platform behaves after overdistention, the stents first had to be implanted into the artificial vessel models. As already mentioned in chapter 8.4, a random sample test resulted in stents being implanted in mock vessel no. 5, 7 and 8 within the scope of this work and in order to be able to carry out first investigations with Micro-CT technology.

Since the manufactured mock vessels corresponded to the dimensions of Biotronik's DES Orsiro, the balloon-expandable stents (3x Orsiro 3.0/40, REF 391241, LOT 11185762, BIOTRONIK AG, Bülach, Switzerland) were implanted into the mock vessels. In order to be able to perform implantations, the entire test equipment required, including all materials and tools, had to be defined in advance. The following two chapters explain in detail which test equipment was used in order to perform implantations of Orsiro's into the three selected mock vessels and describes the test procedure performed. In addition, first examinations of the implanted stents in the mock vessels as well as how the elastic recoil of stents was calculated are described.

### 8.5.1 Test setup and implantation procedure

In order to simulate the implantation process as realistically as possible, an existing in-vitro model, shown in Figure 24, which is used by the IIB testing laboratory for trackability tests, was modified to the developed vessel model using the CAD software SolidWorks again. The so-called track model simulates the arterial coronary system and is based on the ASTM model F2394-07 (ASTM F2394-07 (2013), *Standard Guide for Measuring Securement of Balloon Expandable Vascular Stent Mounted on Delivery System*. ASTM International, West Conshohocken, PA.) [2].

As the developed mock vessels represents the RIVA and the RD1 branch, the path of the IIB model was only adopted up to the red mark shown in Figure 23. The modified track model is represented in Figure 25 and shows how the mock vessel had to be placed during implantation.

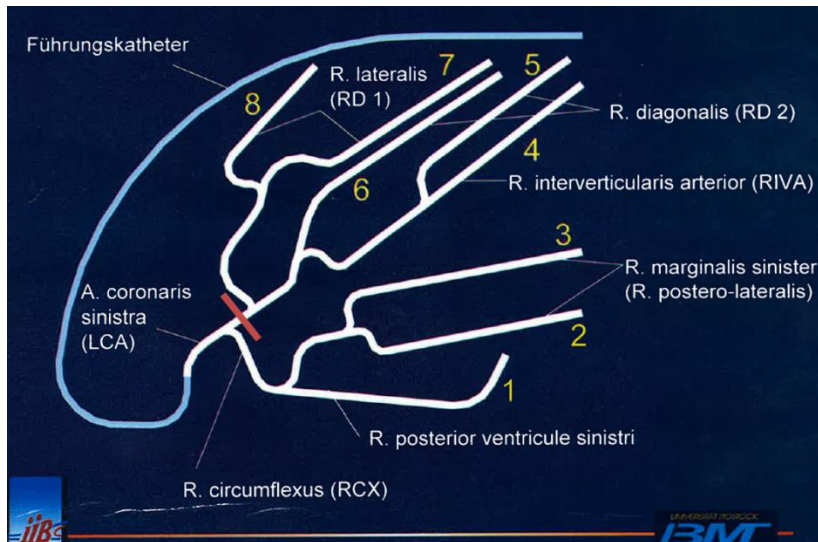


Figure 24: Illustration of the track model of the IIB testing institute for testing trackability of stents

The grey device in which the mock vessel is placed, illustrated in Figure 25, was also designed using SolidWorks and then 3D-printed (in the same printshop as mentioned in chapter 8.3.1) to ensure that the artificial vessel model remains optimally positioned in the track model during implantation without any risk of displacement.

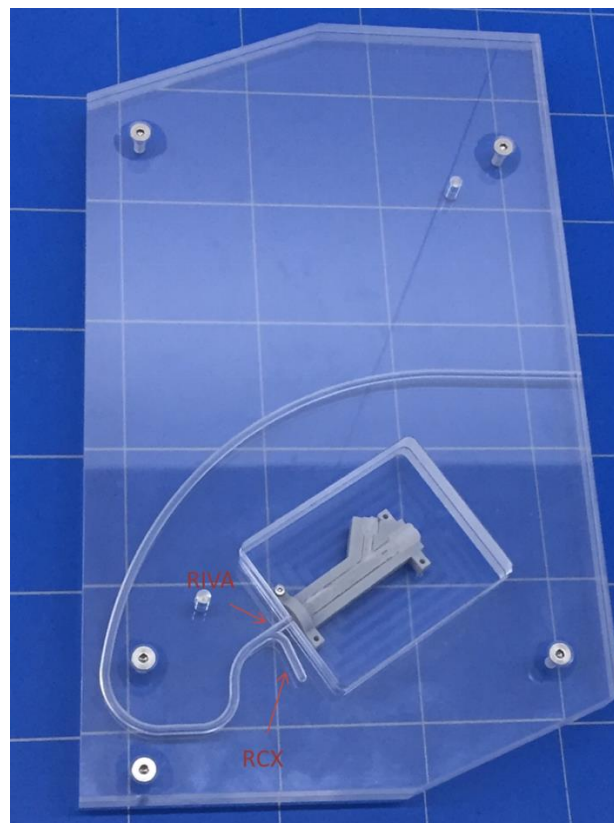


Figure 25: Modified track model for performing stent implantations in the developed mock vessels



The implantations were carried out in a water bath with a temperature of 37 °C. The developed track model was first placed in the water bath and then the guiding catheter (Cordis bride tip GE 5F), through which the delivery system is brought into the mock vessel, was inserted into the track model. The subsequent insertion of the guide wire Biotronik Galeo M (REF 406888, LOT 58006079, BIOTRONIK AG, Bülach, Switzerland) allowed the respective stent systems to be placed exactly between the distal and proximal ends of the vessel models as shown in Figure 26.



Figure 26: Optimal placement of the delivery system at the distal and proximal vessel ends

A manometer syringe with a mixture of 50% NaCl (0.5% NaCl methylene blue) and 50% X-ray contrast agent (Visipaque 320, GE healthcare AG) was used for the inflation of the balloon. As the mock vessels produced were constructed over their entire length with different diameters to imitate realistic cardiovascular vessels and to simulate an indication for overdilatation in the proximal region, the stents were initially expanded to the diameter of 3.25 mm defined in the measuring point "MD RBP" in order to ensure optimal apposition of the stent struts to the mock vessel wall in the distal region and to the integrated stenosis. According to the compliance chart of Biotronik's DES Orsiro, this diameter is reached at an inflation pressure of 14 atm [20]. After the stents were expanded to 14 atm the delivery system was removed.

Since the diameters in the proximal area of the mock vessels are beyond the dilated diameter of 3.25 mm, a post-dilatation with a non-compliant balloon was performed beginning at the measuring point "MP OExD". For this purpose, the balloon markers

of the used non-compliant balloon Pantera LEO (Pantera LEO 3.75/30, REF 367042, LOT 11184979, BIOTRONIK AG, Bülach, Switzerland) were placed exactly at the positions marked in Figure 27.

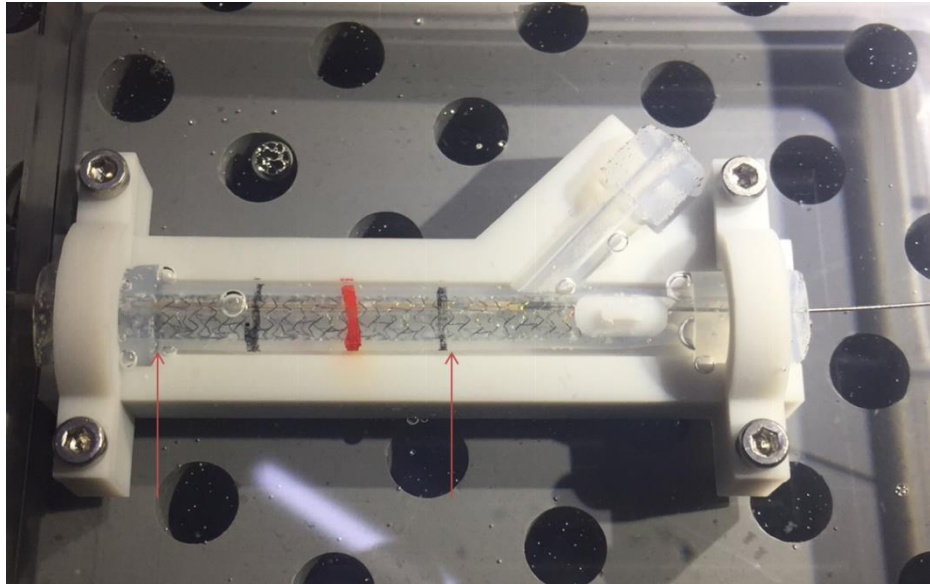


Figure 27: Placement of the non-compliant balloon Pantera LEO at the proximal measuring points "MP OExD+10%", marked by the first arrow, and "MP OExD" marked by the second arrow, for performing an optimal overdilatation

In order to dilate the stent to the diameter of the measuring point "MP OExD+10%" and thus to a value that is 10% above the maximum allowed dilatation diameter of Orsiro, the non-compliant balloon was inflated to 3.85 mm at an inflation pressure of 18 atm. The entire process of overdilatation in the proximal area of the mock vessels was performed twice for all three stent implantations to ensure optimal stent apposition to the vessel wall.

Figure 28 shows the entire test setup.



Figure 28: Test setup for performing stent implantations

All CAD drawings of the components required for the implantations are listed in appendix 13.7. In addition, the test instruction which was specially developed to carry out the defined test procedure can be found in appendix 13.8.

### 8.5.2 Measurement of elastic recoil of stent

For the examination of the implanted Orsiro stents in the mock vessels the digital microscope from Keyence GmbH was used again. To determine the elastic recoil of stents, outer diameter measurements had to be performed. The outer diameters of the mock vessels after stent implantation were measured at the positions shown in Figure 29 using the integrated measuring function of the Keyence microscope.

The outer diameters were measured again in two directions to avoid the scar on the vessel wall. At the two measuring points "MP OExD" and "MP OExD+7mm", which were marked with a pen on the mock vessel, three measuring points per orientation

were recorded, while at the measuring point “MP OExD+10%” one measurement per orientation was carried out.

By using formula 13, the elastic recoil could be calculated [2].

$$\% \text{ Recoil} = \frac{D_{p1} - D_{p0}}{D_{p1}} \cdot 100 \quad (13)$$

$D_{p1}$  represents the outer diameter that is achieved during expansion and  $D_{p0}$  the outer diameter after the balloon is deflated.

As no direct measurements of the outer diameter were performed during the implantation of stents, the parameter  $D_{p1}$  for the calculation of the recoil is based on ideal outer diameter values which are expected during the expansion of the stents to 3.85 mm. With inflation of the stents to an inner diameter of 3.85 mm, a known strut thickness  $t_{strut}$  of Orsiro of 60  $\mu\text{m}$  [20] and a vessel wall thickness  $t$  of 0.6 mm, the outer diameter  $D_{p1}$  was calculated as follows:

$$D_{p1} = 3.85 \text{ mm} + (2 \cdot t_{strut}) + (2 \cdot t) \quad (14)$$

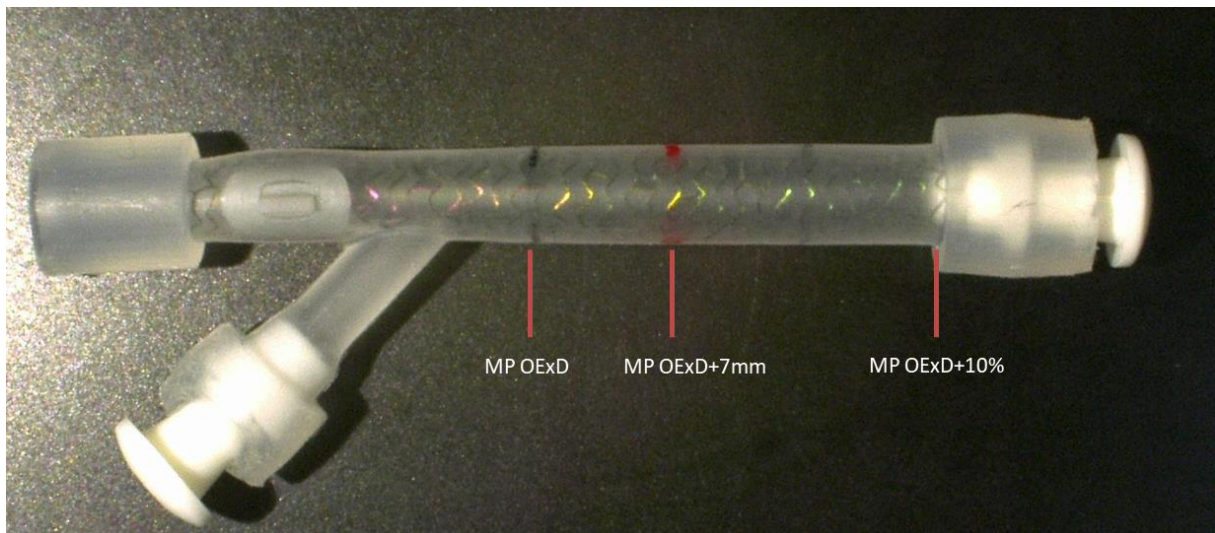


Figure 29: Measurement points for determining the outer diameters  $D_{p0}$  after stent expansion

The arithmetic mean values  $\bar{x}$  and the standard deviations  $s$  were calculated from the measured outer diameters  $D_{p0}$  per measuring point of the mock vessels. From the averaged outer diameters and the calculated ideal outer diameter during expansion

$D_{p1}$ , the recoils could be calculated for each mock vessel at the respective measuring points. The total recoil per measuring point could then be calculated from all outer diameters of the three measured mock vessels.

## **8.6 Micro-CT scanning of mock vessel**

In order to examine the implanted stents for apposition and overdilatation behaviour, it was decided to use the x-ray microtomography technique. The use of Micro-CT technique enables a 3D reconstruction of the scanned sample and thus allows a precise examination of individual segments of interest [60].

Since the Biotronik site in Bülach does not offer such x-ray microscopy, the scans were performed at the subsidiary Cortronik GmbH in Rostock-Warnemünde, Germany. In order to not exceed the scope of this work and for the results to be evaluated, it was decided to carry out Micro-CT scans on only one sample.

In the following, the general microtomography procedure is briefly described and the scanner properties used are given. In addition, the evaluation of the reconstruction images and the methodology developed to investigate the apposition and overdilatation behaviour are discussed.

### **8.6.1 X-ray microtomography procedure and used scanner settings**

As the Micro-CT scans of the sample were performed by colleagues at Cortronik GmbH, this chapter briefly describes the procedure of x-ray tomography in general and explains the parameters and filter settings used.

In order to obtain a 3D reconstruction of the sample, shadow images or so-called transmission images are first taken from different angular positions after optimal placement of the sample in the x-ray tomography scanner (SkyScan 1172, SkyScan N.V., Aartselaar, Belgium). After acquiring all angular projections the images are saved as 16 bit TIFF files on a disk. The obtained shadow images saved on these disks are then used for the reconstruction. In the reconstruction a raw data cross section is generated. By using this cross section, images with 256 grey values (8 bit) are created. [60]



Figure 30 illustrates the required steps for the reconstruction of the cross section image.

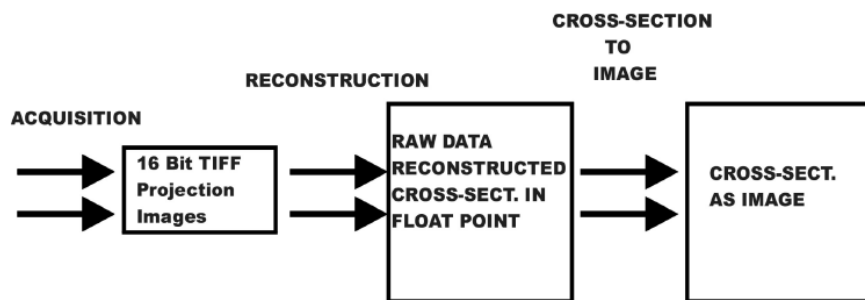


Figure 30: Micro-CT procedure for generating cross section image [60]

Important parameters and filter settings were made in advance in order to obtain optimal, high-quality images. For example, the following settings were used:

- Frame Averaging
- Random Movement
- Geometrical Correction
- Median Filtering

Since the scanning of cobalt-chromium stents in particular causes strong metal artefacts due to the high x-ray density of the material, additional optimizations had to be made. In addition to using an aluminium filter placed in front of the camera, the mock vessel was filled during the scanning process with contrast agent (Visipaque 320, GE healthcare AG) to suppress the strong metal artefacts in the best possible way.

### 8.6.2 Evaluation of apposition and overdilatation behaviour

After receiving all scanned 3D data sets of the mock vessel, they could be visualized and examined with the help of the analysis program CTAn (CT-Analyser, Bruker Corporation, Massachusetts, USA). The program is able to display the corresponding cross sections at precisely selected positions on the reconstruction image of the scanned sample. This enabled measurements to be performed on the internal microstructure of the sample.

The positions on the mock vessel at which the stent has to be examined for

apposition and overdilatation behaviour were already defined in chapter 8.1.3, Figure 7. Figure 31 depicts the five measuring points in the distal area of the vessel at which the stent was examined for apposition behaviour. The behaviour of the stent platform on overdilatation was investigated in the proximal part of the vessel.

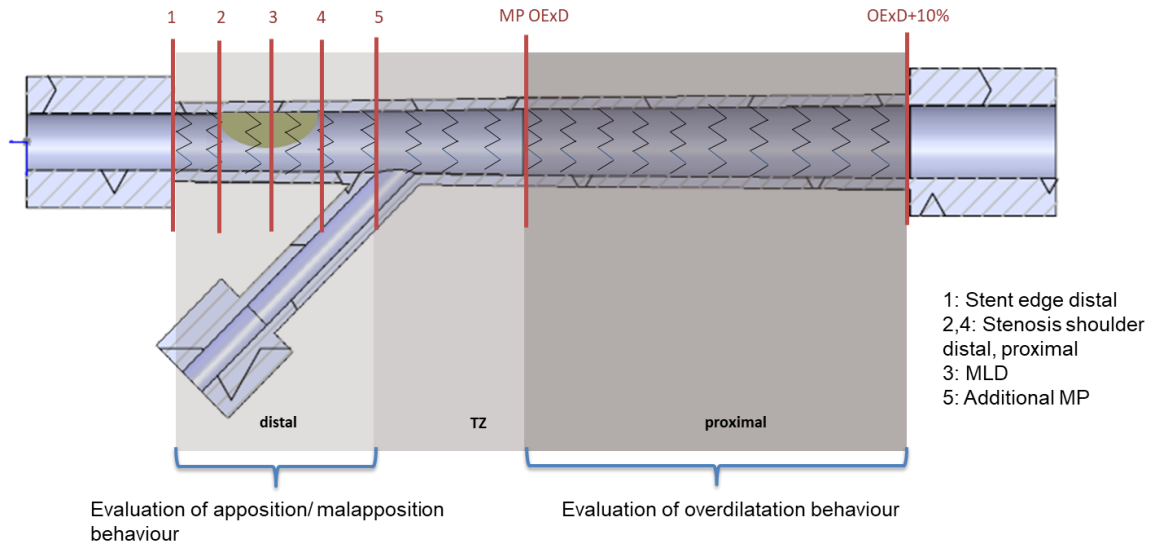


Figure 31: Predefined measuring points and areas in which the stent should be examined for apposition and overdilatation behaviour

The following investigations were carried out:

- % strut malapposition
- % residual stenosis

In order to determine the stent strut malapposition, each cross sectional representation of the five measuring points was examined for struts that were not exactly attached to the vessel wall or the integrated stenosis. The calculation of the strut malapposition and the residual stenosis diameter was based on the methodology defined by Foin [3]. The % strut malapposition (formula 15) could be calculated by recording both the malapposed struts and the total number of existing struts in the cross section.

$$\% \text{ strut malapposition} = \frac{\text{Number of malapposed struts}}{\text{Total number of struts in cross section}} \cdot 100 \quad (15)$$

Of all five cross sectional representations, the number of malapposed struts as well as the total number of struts present in the cross sections was recorded and the % strut malapposition measured.

To determine the residual restenosis, the minimum lumen diameter (MLD) in the cross section of measuring point 3, which represents the point of the initially defined maximum lumen reduction, was measured with an integrated measurement function of the CTAn software. Figure 32 shows the measurement of the MLD in the cross sectional representation of measuring point 3 (Figure 32 b)) and the corresponding projection image (Figure 32 a)). The residual stenosis was then calculated as follows:

$$\% \text{ residual stenosis diameter} = \frac{(\text{Reference vessel diameter} - \text{MLD})}{\text{Reference vessel diameter}} \cdot 100 \quad (16)$$

The initial inner diameter at measuring point 3 (3.14 mm), according Figure 31, was selected as the reference vessel diameter.

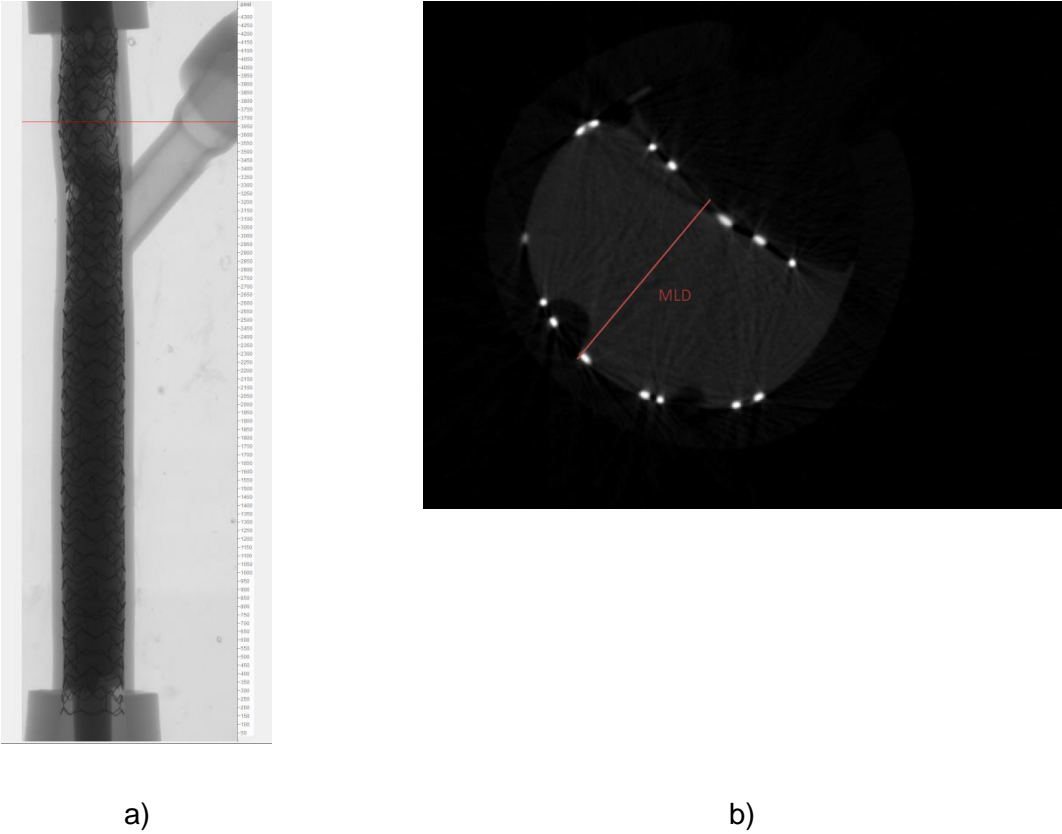


Figure 32: Projection image including marking of the cross section position, b) Cross section image of measuring point 3 showing the MLD measurement. White dots represent the stent struts and the black semicircle the stenosis.

In order to evaluate the overdilatation behaviour of the stent platform, the proximal part of the stent from measuring point “MP OExD” to “MP OExD+10%”, as marked in Figure 31, was examined. The projection image was used to investigate the strut behaviour visually. The struts were examined for cracks and deformations.



## 9 Results

In the following chapter all results obtained during the investigations are presented. The results obtained during the verification of the mock vessels will be discussed as well as the results obtained after implantation of the stents. In addition, the results established after scanning one of the mock vessels and the subsequent investigation are presented.

### 9.1 Verification of manufactured mock vessels

#### 9.1.1 Air bubbles and overall dimensions

##### Air bubbles

The visual inspection results of the mock vessels are listed in Table 24.

Table 24: Results of all air bubbles found in the nine mock vessels manufactured including the location of their occurrence

Mock vessel no.	Number of air bubbles	Location
1	1	Distal holder
2	0	-
3	1	Proximal holder
4	1	Distal holder
	1	RD1 holder
5	0	-
6	1	Distal holder
	1	RD1 holder
7	1	RD1 holder
8	0	-
9	1	Distal holder
	1	RD1 holder

As shown in Table 24, air bubbles were only detected in the holders. Whereby four were found in the distal holder, four in the holder of the RD1 and only one air bubble in the holder of the proximal side. The air bubble found in the proximal holder of the mock vessel 3 is visible in Figure 33.

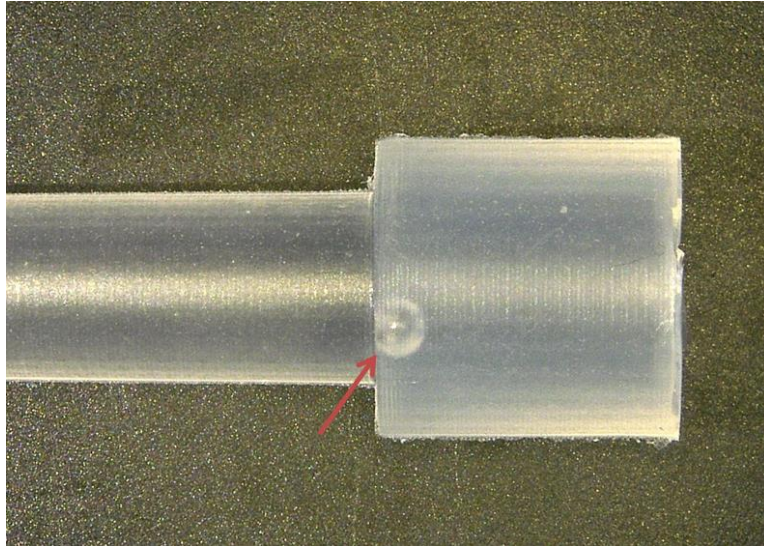


Figure 33: Air bubble in mock vessel no. 3 in the proximal holder

### RIVA and stenosis fixation length and bifurcation angle

Table 25 shows the recorded and calculated length values of the RIVA and the stenosis fixation as well as the determined angle values of the individual vessels. In addition, the arithmetic mean values as well as the standard deviation from the total determined values of the mock vessels,  $\bar{x} \pm s$  (total), are listed. The deviation from the initially defined values (IDV) was then derived from these average values.

Table 25: Measured and calculated length and angle values of the developed mock vessels as well as their deviation from the IDV

Mock vessel no.	Length RIVA [mm]	Length stenosis fixation, $\bar{x} \pm s$ [mm]	Bifurcation angle [°]
1	39.50	$2.93 \pm 0.01$	45.08
2	39.50	$2.92 \pm 0.02$	45.07
3	40	$2.95 \pm 0.01$	45.06
4	40	$2.88 \pm 0.01$	45.07
5	40	$2.89 \pm 0.05$	45.05
6	40	$2.92 \pm 0.01$	45.04
7	39.50	$2.88 \pm 0.01$	45.06
8	40	$2.91 \pm 0.02$	45.08

9	39.50	2.93 ± 0.03	45.02
$\bar{x} \pm s$ (total)	39.78 ± 0.26	2.91 ± 0.03	45.06 ± 0.02
Deviation from IDV [%]	<b>0.56</b>	<b>2.90</b>	<b>0.13</b>

### Outer diameters

In Table 26 the arithmetic mean values  $\bar{x}$  and standard deviations  $s$  of all measurements of the outer diameters  $D_o$  performed at the measuring points "MP RD1", "MP ND", "MP OExD" and "MP OExD+10%" are listed per mock vessel. In addition, the total mean values determined for each measuring point, such as the standard deviations,  $\bar{x} \pm s$  (total), and the deviations of the averaged outer diameters from the initially defined outer diameters (ID) of the individual measuring points can be found in Table 26.

Table 26: Mean values and standard deviations of the  $D_o$  of the individual measuring points as well as the deviations from the ID

Mock vessel no.	MP RD1	MP ND	MP OExD	MP OExD+10%
	$D_o, \bar{x} \pm s$ [mm]			
1	3.33 ± 0.01	4.21 ± 0.01	4.69 ± 0.03	5.04 ± 0.01
2	3.30 ± 0.01	4.19 ± 0.01	4.69 ± 0.02	4.99 ± 0.01
3	3.31 ± 0.01	4.18 ± 0.02	4.69 ± 0.03	4.99 ± 0.05
4	3.30 ± 0.01	4.16 ± 0.01	4.68 ± 0.04	5.01 ± 0.02
5	3.28 ± 0.02	4.16 ± 0.01	4.63 ± 0.03	4.94 ± 0.01
6	3.28 ± 0.06	4.18 ± 0.04	4.63 ± 0.07	4.94 ± 0.04
7	3.31 ± 0.02	4.16 ± 0.01	4.61 ± 0.04	4.94 ± 0.04
8	3.30 ± 0.01	4.15 ± 0.00	4.64 ± 0.05	4.95 ± 0.04
9	3.30 ± 0.05	4.16 ± 0.06	4.62 ± 0.04	4.98 ± 0.04
$\bar{x} \pm s$ (total)	3.30 ± 0.03	4.17 ± 0.03	4.65 ± 0.05	4.97 ± 0.04
Deviation from ID [%]	<b>0.03</b>	<b>0.74</b>	<b>1.02</b>	<b>1.52</b>

Figure 34 shows all measured outer diameters per measuring point as well as the initially defined diameter of the individual measuring points in a box plot.

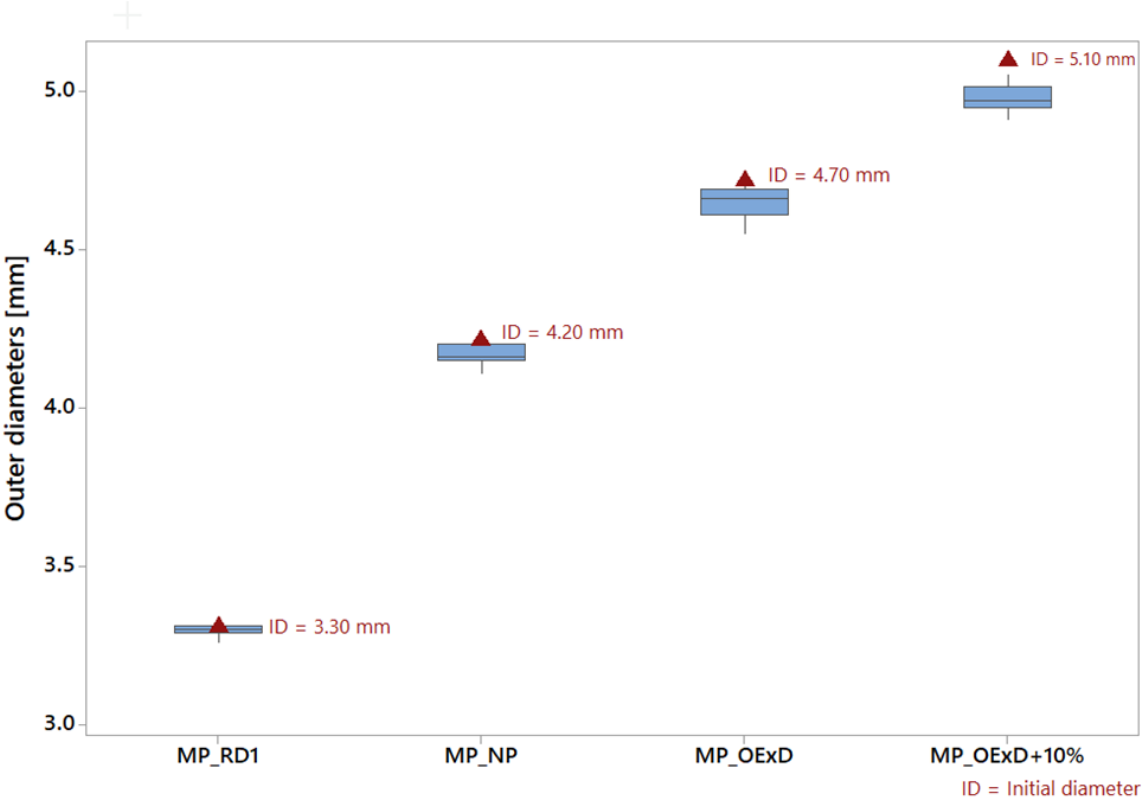


Figure 34: Measured outer diameters per measuring point and its initially defined diameter value

**9.1.2 Stenosis placement and lumen reduction**

Table 27 shows the distance measurements of the stenosis to the measuring point "MP ND" measured per mock vessel. The arithmetic mean value from all distance measurements as well as the standard deviation,  $\bar{x} \pm s$  (total), and the deviation of the total determined mean value from the initial defined value (IDV) are shown in Table 27.

Table 27: Stenosis distance measurements as well as its calculated  $\bar{x}$  and  $s$  and the deviation to the IDV

Mock vessel no.	Stenosis distance [mm]
1	1.97
2	1.98

3	1.97
4	1.98
6	1.96
9	1.99
$\bar{x} \pm s$ (total)	$1.98 \pm 0.01$
Deviation from IDV [%]	<b>1.25</b>

The testing of the lumen reduction at the maximum point of the stenosis in the mock vessels was done with two test rods with different diameters. After the initial defined inner diameter of the mock vessel at the point where the stenosis reaches its maximum has a value of 3.14 mm, a test rod with a diameter of 1.56 mm was first used. Since the passage with the 1.56 mm test rod was carried out without applying great pressure and performing deformation, the 1.57 mm test rod was used next. All mock vessels tested showed that it was possible to pass up by using a test rod with a diameter of 1.57 mm. Thus, for all mock vessels, the diameter of the 1.57 mm test rod was used to calculate the diameter lumen reduction. By applying formula 10 from chapter 8.4.3, and using 1.57 mm for the diameter of the test rod  $D_r$  and 3.14 mm for the initial inner diameter  $D_i$ , all mock vessels showed a 50% lumen reduction in diameter due to the stenosis integrated in the vessel wall.

### 9.1.3 Radial compliance and wall thickness

#### Radial compliance

Table 28 to 30 lists the measured outer diameters  $D_o$  as well as the calculated inner diameters  $D_i$  and the determined radial compliance of the inner diameters  $C_i$  per pressure unit and mock vessel of the respective measuring points "MP OExD", "MP OExD+7mm" and "MP OExD+14mm" as arithmetic mean values and standard deviations,  $\bar{x} \pm s$ . At the end of the tables the total mean values and standard deviations,  $\bar{x} \pm s$  (total), of all determined diameters and compliances are listed.

Table 28: Mean values and standard deviations of outer and inner diameters as well as of the radial compliances at the measuring point "MP OExD"

Mock ves- sel no.	MP OExD				
	D <sub>o</sub> , 75 mmHG [mm]	D <sub>o</sub> , 150 mmHG [mm]	D <sub>i</sub> , 75 mmHG [mm]	D <sub>i</sub> , 150 mmHG [mm]	C <sub>i</sub> , 150/ 75mmHg [%/ 100 mmHg]
1	4.74 ± 0.01	4.80 ± 0.02	3.56 ± 0.01	3.62 ± 0.02	2.25 ± 0.26
2	4.70 ± 0.00	4.77 ± 0.00	3.53 ± 0.00	3.59 ± 0.00	2.36 ± 0.08
3	4.67 ± 0.00	4.76 ± 0.01	3.50 ± 0.00	3.58 ± 0.01	3.14 ± 0.46
4	4.70 ± 0.00	4.76 ± 0.00	3.53 ± 0.00	3.59 ± 0.00	2.31 ± 0.32
5	4.66 ± 0.01	4.74 ± 0.02	3.48 ± 0.01	3.56 ± 0.02	3.06 ± 0.31
6	4.66 ± 0.01	4.74 ± 0.01	3.49 ± 0.01	3.57 ± 0.01	3.08 ± 0.80
7	4.63 ± 0.06	4.69 ± 0.06	3.45 ± 0.06	3.52 ± 0.06	2.49 ± 0.10
8	4.66 ± 0.03	4.74 ± 0.02	3.49 ± 0.03	3.56 ± 0.02	2.81 ± 0.32
9	4.62 ± 0.02	4.69 ± 0.01	3.44 ± 0.02	3.51 ± 0.01	2.73 ± 0.37
<b><math>\bar{x} \pm s</math> (total)</b>	<b>4.67 ± 0.04</b>	<b>4.74 ± 0.04</b>	<b>3.50 ± 0.04</b>	<b>3.57 ± 0.04</b>	<b>2.69 ± 0.45</b>

Table 29: Mean values and standard deviations of outer and inner diameters as well as of the radial compliances at the measuring point "MP OExD+7mm"

Mock ves- sel no.	MP OExD+7mm				
	D <sub>o</sub> , 75 mmHG [mm]	D <sub>o</sub> , 150 mmHG [mm]	D <sub>i</sub> , 75 mmHG [mm]	D <sub>i</sub> , 150 mmHG [mm]	C <sub>i</sub> , 150/ 75mmHg [%/ 100 mmHg]
1	4.82 ± 0.00	4.90 ± 0.00	3.65 ± 0.00	3.72 ± 0.00	2.63 ± 0.00
2	4.80 ± 0.01	4.88 ± 0.01	3.63 ± 0.01	3.71 ± 0.01	3.05 ± 0.27
3	4.76 ± 0.01	4.86 ± 0.01	3.58 ± 0.01	3.68 ± 0.01	3.59 ± 0.07
4	4.78 ± 0.01	4.86 ± 0.01	3.60 ± 0.01	3.69 ± 0.01	3.20 ± 0.14
5	4.77 ± 0.02	4.83 ± 0.01	3.59 ± 0.02	3.66 ± 0.01	2.47 ± 0.35

6	4.77 ± 0.00	4.86 ± 0.00	3.60 ± 0.00	3.69 ± 0.00	3.39 ± 0.19
7	4.75 ± 0.04	4.82 ± 0.05	3.58 ± 0.04	3.65 ± 0.05	2.44 ± 0.05
8	4.76 ± 0.04	4.84 ± 0.02	3.59 ± 0.04	3.67 ± 0.02	2.98 ± 0.66
9	4.72 ± 0.01	4.81 ± 0.01	3.55 ± 0.01	3.64 ± 0.01	3.21 ± 0.15
$\bar{x} \pm s$ (total)	<b>4.77 ± 0.03</b>	<b>4.85 ± 0.03</b>	<b>3.60 ± 0.03</b>	<b>3.68 ± 0.03</b>	<b>3.00 ± 0.44</b>

Table 30: Mean values and standard deviations of outer and inner diameters as well as of the radial compliances at the measuring point "MP OExD+14mm"

Mock ves- sel no.	MP OExD+14mm				
	$D_o$ , 75 mmHG [mm]	$D_o$ , 150 mmHG [mm]	$D_i$ , 75 mmHG [mm]	$D_i$ , 150 mmHG [mm]	$C_i$ , 150/ 75mmHg [%/ 100 mmHg]
1	4.95 ± 0.01	5.03 ± 0.01	3.78 ± 0.01	3.85 ± 0.01	2.70 ± 0.03
2	4.92 ± 0.01	4.99 ± 0.02	3.75 ± 0.01	3.82 ± 0.02	2.54 ± 0.47
3	4.85 ± 0.07	4.95 ± 0.08	3.68 ± 0.07	3.77 ± 0.08	3.46 ± 0.11
4	4.92 ± 0.00	5.00 ± 0.00	3.75 ± 0.00	3.83 ± 0.00	2.90 ± 0.03
5	4.91 ± 0.02	4.98 ± 0.02	3.73 ± 0.02	3.81 ± 0.02	2.61 ± 0.07
6	4.91 ± 0.02	5.01 ± 0.02	3.74 ± 0.02	3.83 ± 0.02	3.39 ± 0.12
7	4.89 ± 0.04	4.95 ± 0.04	3.71 ± 0.04	3.78 ± 0.04	2.46 ± 0.21
8	4.89 ± 0.02	4.98 ± 0.01	3.72 ± 0.02	3.80 ± 0.01	3.03 ± 0.35
9	4.87 ± 0.01	4.96 ± 0.00	3.70 ± 0.01	3.78 ± 0.00	3.06 ± 0.06
$\bar{x} \pm s$ (total)	<b>4.90 ± 0.04</b>	<b>4.98 ± 0.03</b>	<b>3.73 ± 0.04</b>	<b>3.81 ± 0.03</b>	<b>2.91 ± 0.38</b>

Figure 35 shows the box plot representation of all determined radial compliance values  $C_i$  divided into the three measuring points "MP OExD", "MP OExD+7mm" and "MP OExD+14mm".

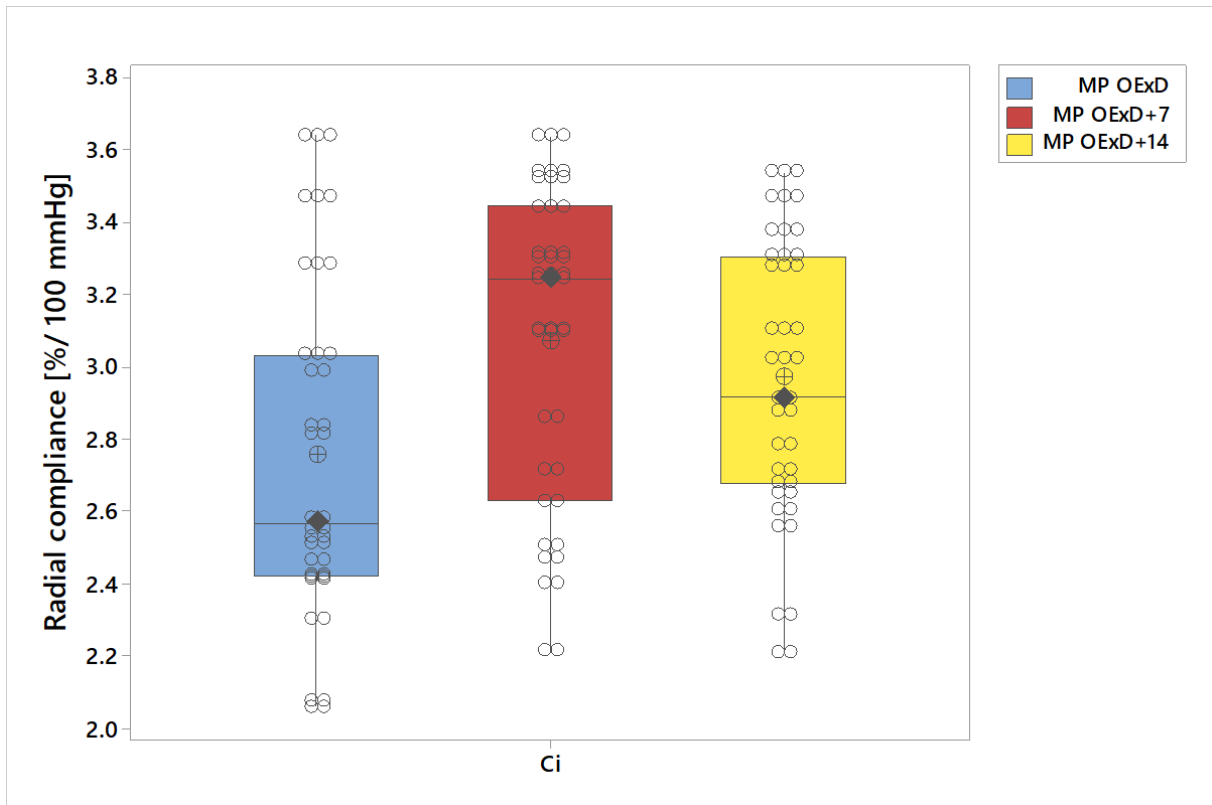


Figure 35: Radial compliance at the measuring points "MP OExD", "MP OExD+7mm" and "MP OExD+14mm"

Table 31 lists the total mean values and standard deviations ( $\bar{x} \pm s$ ) of all results of the nine mock vessels. In addition, the overall radial compliance calculated from the mean values of all results can be found.

Table 31: Total radial compliance per mock vessel as well as the overall radial compliance of all mock vessels manufactured

Mock vessel no.	$C_{i, 150/75\text{mmHg}}$ [%/ 100 mmHg]	$C_{i, \text{overall}}$ [%/ 100 mmHg]
1	$2.53 \pm 0.25$	<b><math>2.86 \pm 0.44</math></b>
2	$2.65 \pm 0.40$	
3	$3.40 \pm 0.30$	
4	$2.80 \pm 0.44$	
5	$2.71 \pm 0.35$	
6	$3.29 \pm 0.40$	
7	$2.46 \pm 0.11$	



8	2.94 ± 0.38	
9	3.00 ± 0.28	

### Wall thickness

Table 32 presents the minimum and maximum wall thicknesses determined and the corresponding concentricity calculations at the measuring points "MP OExD", "MP OExD+7mm" and "MP OExD+14mm" of the mock vessels. In addition, the total mean values and standard deviations ( $\bar{x} \pm s$  (total)) of the determined wall thicknesses and calculated concentricity's are listed for each measuring point. At the end of the table the deviation of the total mean values from the initially defined values (IDV) is shown.

Table 32: Minimum and maximum wall thicknesses determined as well as calculated concentricity of the respective measuring points of the mock vessel and their deviations from the IDV

Mock ves- sel no.	MP OExD			MP OExD+7mm			MP OExD+14mm		
	t <sub>min</sub> [mm]	t <sub>max</sub> [mm]	C [%]	t <sub>min</sub> [mm]	t <sub>max</sub> [mm]	C [%]	t <sub>min</sub> [mm]	t <sub>max</sub> [mm]	C [%]
1	0.58	0.61	95.08	0.54	0.60	91.53	0.59	0.60	98.33
2	0.58	0.65	89.23	0.56	0.62	90.32	0.57	0.63	90.48
3	0.55	0.62	88.71	0.55	0.62	88.71	0.55	0.63	87.30
4	0.58	0.64	90.63	0.54	0.63	85.71	0.56	0.65	86.15
6	0.55	0.60	91.67	0.55	0.62	88.71	0.56	0.61	91.80
9	0.51	0.60	85.00	0.54	0.59	91.53	0.56	0.62	90.32
$\bar{x} \pm s$ (total)	0.58 ± 0.03		90.05 ± 3.35	0.58 ± 0.03		89.42 ± 2.21	0.59 ± 0.03		90.73 ± 4.29
Deviation from IDV [%]	<b>2.64</b>		<b>9.95</b>	<b>2.85</b>		<b>10.58</b>	<b>1.11</b>		<b>9.27</b>

## 9.2 Elastic recoil of stent

Table 33 lists all measured outer diameters  $D_{p0}$  at the respective measuring points of the three mock vessels as arithmetic mean values and standard deviations ( $\bar{x} \pm s$ ). Furthermore, the calculated value of parameter  $D_{p1}$  and the calculated recoils per mock vessel and per measuring point are presented. At the end of the table the total mean values as well as standard deviations,  $\bar{x} \pm s$  (total), of the outside diameters and the calculated recoils of the respective measuring point are listed.

Table 33: Mean values and standard deviations of the measured outer diameters as well as indication of the determined  $D_{p1}$  and the calculated recoils

Mock vessel no.	MP OExD			MP OExD+7mm			MP OExD+10%		
	$D_{p0}$ [mm]	$D_{p1}$ [mm]	Recoil [%]	$D_{p0}$ [mm]	$D_{p1}$ [mm]	Recoil [%]	$D_{p0}$ [mm]	$D_{p1}$ [mm]	Recoil [%]
5	4.92 ± 0.02	5.17	4.93	4.95 ± 0.07	5.17	4.32	5.00 ± 0.08	5.17	3.29
7	4.84 ± 0.04		6.48	4.91 ± 0.01		5.03	4.99 ± 0.01		3.58
8	4.89 ± 0.06		5.51	4.92 ± 0.02		4.93	5.01 ± 0.04		3.09
$\bar{x} \pm s$ (total)	4.88 ± 0.05	5.17	<b>5.64</b>	4.92 ± 0.04	5.17	<b>4.76</b>	5.00 ± 0.04	5.17	<b>3.32</b>

## 9.3 Apposition and overdilatation behaviour

### 9.3.1 Strut malapposition

Table 34 shows the number of struts that were not precisely attached to the mock vessel wall as well as the total number of struts per cross section of the five measuring points. From these two values the % strut malapposition was calculated and can also be seen in Table 34.

Table 34: Number of malapposed struts as well as total number of struts in cross section per measuring point and the resulting % strut malapposition

Measuring points	Number of malapposed struts	Total number of struts in cross section	Strut malapposition [%]
1	4	14	28.57
2	1	11	9.10
3	1	15	6.67
4	2	9	22.22
5	0	12	0

Figure 36 shows the struts that are not exactly apposed to the mock vessel wall at measuring point 1.

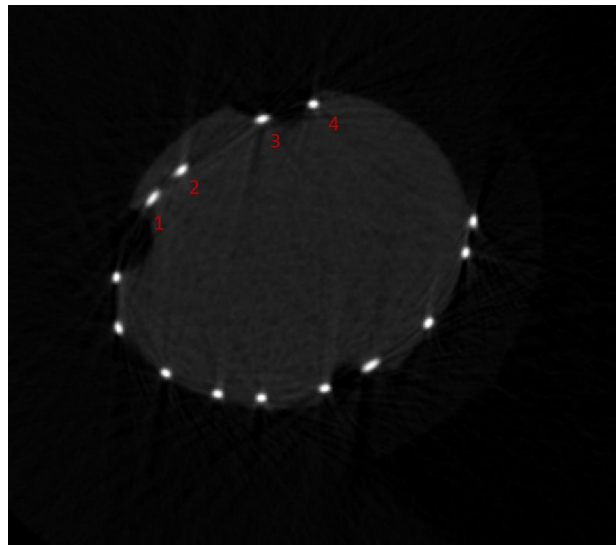


Figure 36: Malapposed struts in cross section of measuring point 1. The black circles visible at points 1, 3 and 4 represent air bubbles introduced by the contrast medium

### 9.3.2 Residual stenosis

The measurement of the MLD was difficult because the exact corner point of the edge of the vessel and of the stenosis was not clearly visible due to the metal artefacts of the cobalt-chromium stent, as can be seen in Figure 37.

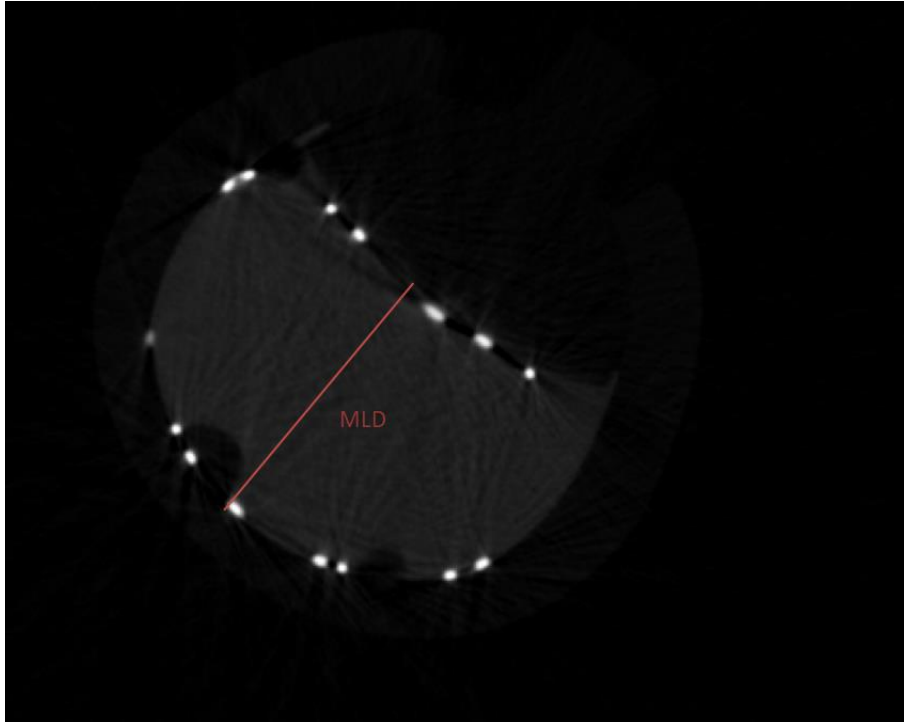


Figure 37: Measurement of the MLD at the maximum point of the stenosis. Metal artefacts can be identified by black stripes in the cross section

After an MLD of 2.32 mm could be measured out of the cross-sectional representation of measuring point 3 and the initial vessel inner diameter of this measuring point of 3.14 mm (known from the drawings of the mock vessel) was selected as the reference vessel diameter, a residual stenosis of 26.18% was calculated using Formula 16 from chapter 8.6.2.

### 9.3.3 Preliminary results of stent strut behaviour after overexpansion

The examination of the projection images for deformations in the proximal overdilated section between the measuring points “MP OExD” and “MP OExD+10%” showed no abnormalities such as deformations or cracks of the struts, as can be seen in Figure 38.

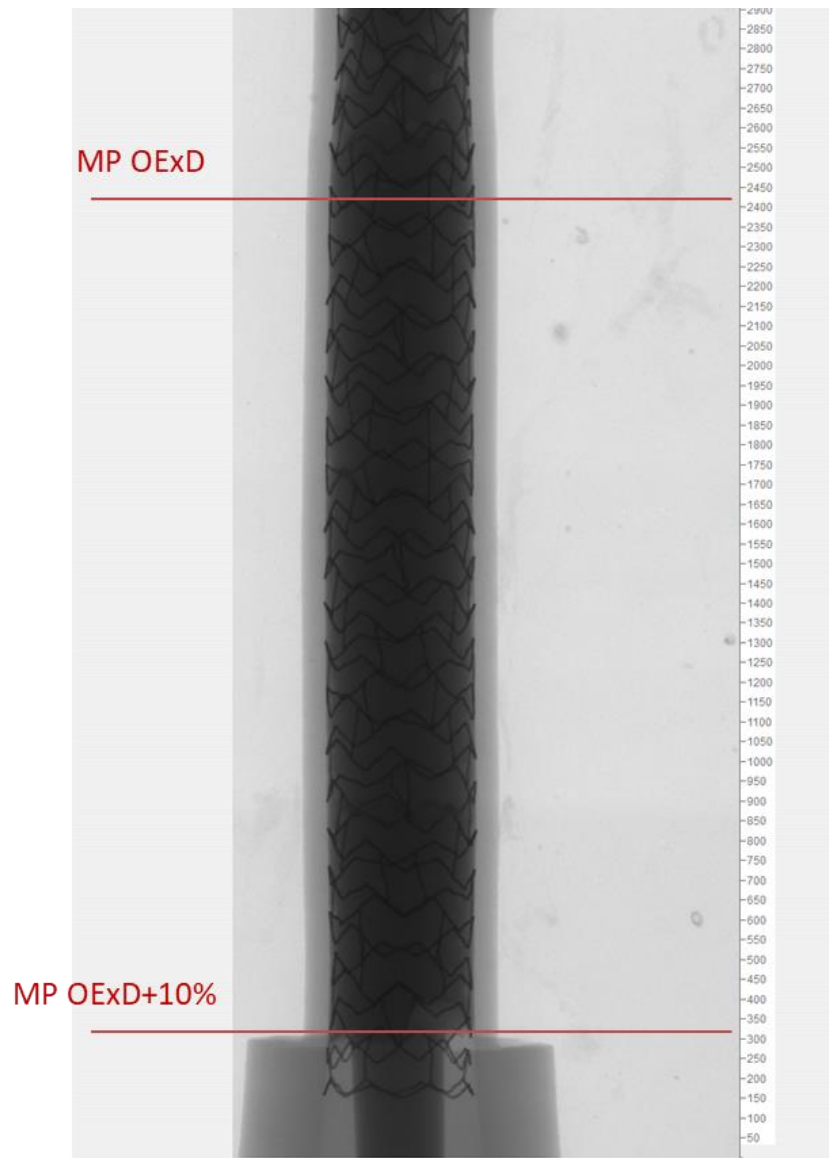


Figure 38: Projection image of the proximal section of the mock vessel for examination of overdilatation behaviour. Scale in pixel, image pixel size: 1 pixel = 9.99  $\mu\text{m}$



## **10 Discussion**

In the following chapter, the achieved results are evaluated and discussed. The results of the verification of the individual dimensions of the developed mock vessels are discussed and the findings are explained. Furthermore, the elastic recoil of the stents after implantation into the mock vessels as well as the results of the Micro-CT measurements is discussed.

### **10.1 Verification of mock vessels**

#### **10.1.1 Air bubbles and overall dimensions**

##### **Air bubbles**

When investigating the mock vessels for air bubbles, no bubbles were found in three of the mock vessels (mock vessel no. 2, 5 and 8), while in the other six (mock vessel no. 1, 3, 4, 6, 7 and 9) either one (mock vessel no. 1, 3 and 7) or two (mock vessel 4, 6 and 9), were found, as listed in Table 24, chapter 9.1.1. The air bubbles found were only located in the holders of the mock vessels, whereby most of them were found in the RD1 and distal holder (four air bubbles each) and only one in the proximal holder. The reason that four air bubbles were found in the RD1 holder was that the outer shells in the area of the RD1 could not be fully closed, as can be seen in Figure 39, and thus a minimal gap resulted. This gap allowed air to enter the silicone mold during the cross-linking process, creating air bubbles.

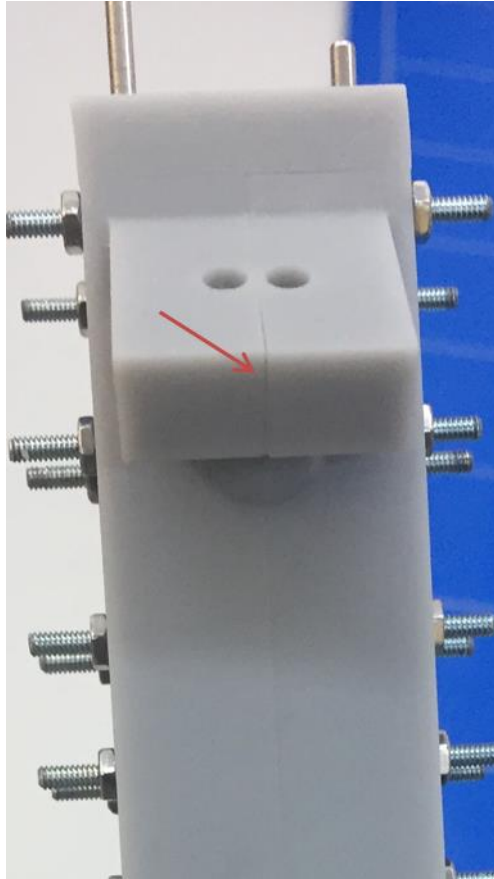


Figure 39: Minimum gap resulting after assembly of the rig

The air bubbles in the distal and proximal holder can be justified in such a way that the cross-linking of the silicone, which in the case of Elastosil M4645 is 80 minutes at 23 °C according to the data sheet [57], was greatly accelerated by cross-linking in the furnace and the air bubbles could no longer escape via the exit points before the complete cross-linking occurred.

However, despite the air bubbles found in the holders, none were found in the area of the RIVA or RD1 branch section. Thus, the relevant areas of the silicone vessels such as the RIVA, in which the stent remains after implantation, were free of air bubbles.

In order to avoid the occurrence of air bubbles in the entire mock vessel in the future, various measures can be taken. Firstly, additional screws or clamping tools can be attached to the RD1 branch to ensure correct closing of the outer shells and thus prevent the penetration of air bubbles. Furthermore, the exit holes constructed on the cover and end of the RD1 branch could be sized larger to facilitate the escape of air. Another possibility could be to cross-link the silicone vessels in vacuum furnaces in



the future. There, the final vacuum takes place automatically over the entire cross-linking time. However, this would initially require the purchase of such furnaces.

### **Length of RIVA**

The measurement of the length of the RIVA using a ruler showed a length of exactly 40 mm for five of the nine artificial vessels and a length of 39.5 mm for the other four, as listed in Table 25, chapter 9.1.1. Considering the relative deviation of the originally defined length of 40 mm from the mean value of all measurements of  $39.78 \text{ mm} \pm 0.26 \text{ mm}$ , it can be seen that the mock vessels produced were 0.56% (absolute difference: - 0.22 mm) shorter than originally designed. With regard to measuring methods using a ruler, it must be mentioned that the determination of the length was only possible with a resolution of 0.5 mm.

To measure the mock vessels with a higher accuracy one could also use the measuring function of a digital microscope. However, as there was no calibration for the existing Keyence digital microscope for a magnification of 5x, which would have been needed to measure the entire length under the microscope, in the timeframe of the work, the measurements were performed using a ruler.

### **Length of stenosis fixation**

The length measurement of the stenosis fixation, represented by the integrated opening in the distal section of the mock vessels, resulted in a total mean value of  $2.91 \text{ mm} \pm 0.03 \text{ mm}$  when measured with the Keyence digital microscope. The relative deviation of 2.90% (absolute difference: - 0.09 mm) of the measured lengths from the initial defined length of 3 mm indicates that the resulting stenosis fixation turned out to be smaller.

As mentioned in chapter 8.3.1, Figure 12 and 13, the opening and thus the stenosis fixation on the mock vessels is caused by the device designed on one side of the outer shell to keep this part free of silicone during the casting process in order to enable the 3D-printed stenosis to be inserted at this part. The outer shell with the device designed on it, as well as all other drawn components, were 3D-printed by an external printer. Considering the layer thickness of 0.05 mm to 0.1 mm with which the printer produces the models [55], it can be concluded that this had an effect on the

manufacturing accuracy of the device on the outer shell and thus on the resulting length of the stenosis fixation.

In order to incorporate this 3D printing accuracy into future models that are to be printed, the dimensions of the components must be increased by the applied layer thickness of the printers of at least 0.05 mm.

### **Bifurcation angle**

The measurement of the bifurcation angle between RIVA and RD1 resulted in a mean value of  $45.06^\circ \pm 0.02^\circ$  for the nine mock vessels. The angle value thus obtained lay 0.13% (absolute difference:  $+ 0.06^\circ$ ) above the initially defined bifurcation angle of  $45^\circ$ .

Since the measured angles of the mock vessels showed only minimal differences ( $0.02^\circ$ ), it can be concluded that all correspond to the predefined angle value of  $45^\circ$ .

### **Outer diameters**

If one considers the measurement results of the outer diameters at the four defined measuring points in comparison to the initially defined diameters, it can be seen that all except the outer diameter of the RD1 ( $3.30 \text{ mm} \pm 0.03 \text{ mm}$ ) are lower. As can be seen in Figure 34, chapter 9.1.1, the outer diameter at the measuring point "MP OExD+10%" ( $4.97 \text{ mm} \pm 0.04 \text{ mm}$ ) deviates the most with 1.52% (absolute difference:  $- 0.08 \text{ mm}$ ) from the initially defined diameter of 5.1 mm. Looking at the standard deviations among the individual measuring points of the mock vessels, there is no significant difference or outliers in the individual measured values. Thus the standard deviations of the individual measuring points vary between 0.03 mm (MP RD1) and 0.05 mm (MP OExD).

The reason why almost all measured diameters are below the initially defined diameter can be explained, on the one hand, by the printer accuracy of the 3D printer. Thus, the inner dimensions of the outer shells as well as the inner mandrel were designed with exactly the desired defined dimensions represented in chapter 8.3.1, Figure 10, without taking into account the applied layer thickness of the 3D printer. This layer thickness becomes visible again in a reduced profile of the mock vessels. On the other hand, the release agent applied to the components to facilitate the detach-

ment of the silicone vessels may have contributed to a reduced profile.

In order to avoid these reductions in the profiles of the mock vessels in the future, the dimensions of the moulds must be increased by the applied layer thickness of the 3D print shop as well as the layer reduced by the release spray.

### **10.1.2 Stenosis placement and lumen reduction**

After measuring the distance between the distal edge of the implanted stenosis in the mock vessels and the measuring point "MP ND", the reproducibility of stenosis placement was checked and almost the same distance was obtained for all nine mock vessels. The mean value of all measured distances was  $1.98 \text{ mm} \pm 0.01 \text{ mm}$ . This calculated total distance thus deviates by 1.25% (absolute difference: - 0.03 mm) from the initially defined distance of 2 mm. Based on these results, it can be assumed that the stenosis always occupied the same position in the nine developed vessel models after it had been integrated and was thus positioned exactly as originally designed.

By testing the lumen reduction of the implanted stenosis at its maximum point in the mock vessels using two different test rods and taking into account that the vessels at this maximum point have a diameter of 3.14 mm, a 50% loss of vessel diameter in all mock vessels resulted. The implanted stenosis thus exhibited the desired and defined 50% lumen intake in each mock vessel.

### **10.1.3 Radial compliance and wall thickness**

#### **Radial compliance**

The results of the radial compliance determinations, listed in Table 28 to 30, chapter 9.1.3, show that the total mean values of the mock vessels vary between the three measuring points by means of  $2.69 \pm 0.45\% / 100 \text{ mmHg}$  at "MP OExD",  $3.00 \pm 0.44\% / 100 \text{ mmHg}$  at "MP OExD+7mm" and  $2.91 \pm 0.38\% / 100 \text{ mmHg}$  at "MP OExD+14mm". Looking at the individual diameter determinations at the three measuring points under different pressure loads, individual standard deviations between 0.03 mm and 0.04 mm show no significant difference or outliers. For this reason it can be assumed that the partial large deviations in the radial compliance values are not traceable to the developed mock vessels themselves. Thus, the deviations in the

radial compliance values can rather be attributed to the applied measuring method itself.

If one considers the test method procedure developed in this thesis for the determination of radial compliance, optimisation possibilities can be derived from it in order to avoid measurement inaccuracies. On the one hand, the manual position during measurement as well as the pressure control could be optimized by the acquisition of automated measuring methods which simultaneously measure the dynamic pressure release as well as the diameter change. On the other hand, the measurements could be performed under clinical conditions in a water bath according to DIN EN ISO 7198 at 37 °C in order to create a constant ambient condition for the highly temperature-dependent properties of silicone elastomers [49, 51].

By comparing the total radial compliance from the mean values of the individual mock vessels,  **$2.86 \pm 0.44\%$**  / 100 mmHg, with those of real healthy arterial vessels which, according to Ramesh et al. [41], lie in a range between 4 – 7%, it becomes apparent that the determined compliance is lower. As already mentioned in chapter 8.2.3, the radial compliance that results from the change in inner diameter due to applied pressure changes strongly depends on the choice of material and the dimensions of the vessel. From the calculation of the modulus of elasticity for the available silicone Elastosil M4546, performed in chapter 8.2.3, it was found that with a value of 1.78 MPa it was higher than that of human blood vessels (1.68 MPa) [50]. The idea was to compensate this relative deviation of 5.95% (0.1 MPa) by appropriate selection of mock vessel dimensions such as wall thickness. However, it has been shown (chapter 8.2.3) that the wall thickness determined in order to achieve a radial compliance of 5%, for example, would have to be 0.25 mm for a material with a Young's modulus of 1.78 MPa and an inner diameter of 3 mm at a pressure range of 100 mmHg, which is used. When using the casting process for the production of mock vessels, however, this wall thickness was not feasible, as it would have been almost impossible to release the vessel from the rig without causing cracks or other defects. For the first production of such artificial vessel models, it was thus decided to adapt the wall thickness of the vessels to sizes used in studies already published [55]. Considering possible limitations in radial compliance, a wall thickness of 0.6 mm was chosen.

In order to be able to use this wall thickness and still be in the radial compliance range of human arteries, one would have to use a material with a lower modulus of

elasticity than Elastosil when considering the formula (9) in chapter 8.2.3.

### **Wall thickness**

From the wall thickness measurements at the respective measuring points of the mock vessels it can be deduced that the wall thickness are almost identical with values of  $0.58 \text{ mm} \pm 0.03 \text{ mm}$  at measuring point “MP OExD”,  $0.58 \text{ mm} \pm 0.03 \text{ mm}$  at measuring point “MP OExD+7mm” and  $0.59 \text{ mm} \pm 0.03 \text{ mm}$  at measuring point “MP OExD+14mm”. With deviations between 1.11% (absolute difference: - 0.01 mm) and 2.64% (absolute difference: - 0.02 mm) to the initially defined wall thickness, it can be assumed that the restrictions of the outer diameter as mentioned in chapter 10.1.1 due to 3D printing accuracy also affected the production of the inner mandrel and thus led to an almost constant wall thickness of the manufactured mock vessels.

The concentricity calculations from the measured minimum and maximum wall thicknesses of the mock vessels resulted in a concentricity of 90.05% (absolute difference: -9.95%) at measuring point “MP OExD”, of 89.42% (absolute difference: - 10.58%) at measuring point “MP OExD+7mm” and of 90.73% (absolute difference: - 9.27% at measuring point “MP OExD+14mm”. From these results it can be derived that the design of the rig and thus of its components almost meets its requirements and that the inner mandrel was placed almost perfectly concentrically in the outer shells over all measurements on the nine mock vessels.

## **10.2 Elastic recoil of stent**

Since it was not possible to directly measure the outer diameter of the mock vessels during the stent implantation in the track bath within the scope of the work, the calculated outer diameter  $D_{p1}$  of the vessels at the pressure load applied was used for the calculation of the recoil, as explained in chapter 8.5.2. The measurement of the outer diameters after expansion  $D_{p0}$  was recorded for all three mock vessels at the measuring points and resulted in diameter values of  $4.88 \text{ mm} \pm 0.05 \text{ mm}$  at measuring point “MP OExD”,  $4.92 \text{ mm} \pm 0.04 \text{ mm}$  at measuring point “MP OExD+7mm” and  $5.00 \text{ mm} \pm 0.04 \text{ mm}$  at measuring point “MP OExD+10%”. Based on these measured values and the ideal diameter assumed to be 5.17 mm at all three measuring points after overdilatation (as listed in Table 33, chapter 9.2), a stent recoil decreas-

ing to the proximal side was obtained at the measuring points. Thus, the recoil at the measuring point “MP OExD” was still 5.64%, whereas it was only 3.32% at the measuring point “MP OExD+10%”. This decrease of the recoil can be explained by the fact that the initial diameter at the measuring point “MP OExD” is smaller than the diameter at the measuring point “MP OExD+10%” and thus the resistance by the vessel wall on the expanded stent was therefore higher than in the more proximal section of the vessel.

If one compares the measured recoils at the three measuring points with the recoil of Orsiro known from internal studies of 4.18% [22], deviations can be seen (absolute differences: + 1.46% at “MP OExD”, + 0.58 % at “MP OExD+7mm” and – 0.86% at “MP OExD+10%”). The deviations can be explained on the one hand by the fact that in the test method of the IIB laboratory the stents are not expanded in artificial vessel models but contactless in a water bath. On the other hand, the IIB laboratory automatically measures the outer diameter during expansion and after expansion. [22]

### **10.3 Apposition and overdilatation behaviour**

#### **Strut malapposition**

From the cross sectional representations of the five predefined measuring points, struts that were not exactly attached to the vessel wall or to the stenosis integrated in the mock vessel were analysed at all measuring points except at measuring point 5. The number of malapposed struts at measuring points 2, 3 and 4 can be traced more accurately than the recorded malapposition at measurement point 1 due to the presence of stenosis at these measurement points.

The number of four malapposed struts of total of 14 struts at measuring point 1 and the resulting strut malapposition of 28.57% (Table 34, chapter 9.3.1) can have various reasons. On the one hand, this malapposition of the struts at the distal edge of the stent and thus at the distal end of the RIVA could have been caused by preparations of the sample for shipment to the Micro-CT examination, since this measuring point was located precisely at the transition to the distal holder and the sample was fixed there for transport. On the other hand, it could also have been caused during the preparation of the sample for Micro-CT measurement.

The malapposed struts at measuring points 2, 3, and 4 can be explained by the tran-

sition of the stent struts from the vessel wall to the stenosis (measuring points 2 and 4) and by the adaptation of the struts to the maximum point of stenosis (measuring point 3).

### **Residual stenosis**

Measuring the residual stenosis from the cross sectional view at the maximum point of the integrated stenosis proved to be difficult and error-prone despite the use of additional filters and contrast medium-filled mock vessels. The metal artefacts caused by the cobalt-chromium alloy of the stent platform could not be completely eliminated despite additional settings.

If one compares the resulting residual stenosis of 26.18% despite measurement uncertainty, with the original lumen diameter reduction of the stenosis at this measuring point 3 being 50%, it can be seen that the vessel loss due to the stenosis was reduced after stent expansion, but not completely eliminated. During a clinical intervention in such a case, angiography would have to be used to check whether the blood flow is sufficient or whether post-dilatation and thus extended expansion of the stent is necessary [40].

In order to further reduce restenosis in this case, the stent could have been dilated up to 3.50 mm in the distal section according to Orsiro's instructions for use [20]. However, according to the defined test method, overdilatation was only planned in the proximal section of the mock vessel.

With regard to the stenosis material used in 3D printing, future investigations would have to question whether the material is transferable to the simulation of real calcification in arterial vessels and can thus be used to investigate the apposition behaviour of stents.

To perform Micro-CTs on cobalt-chromium stents in the future without encountering metal artefacts, better filter settings and optimization possibilities would have to be sought. On the one hand, the use of a contrast agent with a higher iodine concentration and thus a better property for suppressing artefacts could contribute to improving the resulting scans. On the other hand, other imaging techniques such as OCT could be used, which (according to literature) is used to investigate the apposition of struts to the vessel wall during clinical application [35]. However, this would require the pur-

chase of such a device and the required expertise to use it.

### **Evaluation of the overdilatation behaviour of stents**

The examination of the proximal section of the stent for cracks and deformations as a result of overdilatation did not reveal any visible abnormalities when the projection images were examined using the CTAn software. The investigation was, however, limited because only 2D views of the scanned model were possible with the CTAn software and therefore the mock vessel could not be examined as a 3D model. Thus, only one side of the scanned stent could be examined for overdilatation behaviour.

However, if the results are interpreted, it can be concluded that Biotronik's DES Orsi-ro does not show any cracks or deformations even with dilatation of up to 10% above the maximum allowed labelled diameter.

In order to improve the examination of the mock vessels for overdilatation, a visualization program would have to be used that is capable of displaying the entire scanned model in 3D view. This would allow each section of the model to be examined for cracks and deformations in different views and angles.



## 11 Conclusion and Outlook

The production of artificial vascular models for the investigation of the apposition and overdilatation behaviour of stents has shown that many different aspects influence the geometric and mechanical properties of the vessel models.

It has been shown that the 3D-printed moulds had an influence on the reduced dimensions of the silicone vessels produced. The release agent applied to the inner side of the outer moulds could also be mentioned as a potential cause of the reduced profiles of the vessels. In order to avoid reductions of the cross sections, the coating thickness of the release agent would have to be investigated and adapt the dimensions as offset to the mould dimensions.

The results of the radial compliance measurements have shown that when using the selected silicone Elastosil M4645 and a wall thickness of 0.6 mm, the resulting radial compliance is below that of human arteries. Considering the formula (9) used to calculate the wall thickness in chapter 8.2.3, it can be concluded that the radial compliance could be increased by reducing the wall thickness of the mock vessel or the Young's modulus of the silicone. Furthermore, it should be mentioned that there is still room for improvements when looking at the measurement procedure. If one orients on the test method that is prescribed according to DIN ISO 7198 [49] for implants that remain permanently in the body, the measurement would have to be carried out in a track bath at 37 °C using automated measuring instruments for simultaneous measurement of the pressure load and the resulting outer diameter. In addition, an inflation device should be used in future that has a pressure unit with improved resolution in order to be able to regulate the pressure ranges used more precisely. These optimization possibilities, however, were not feasible within the timeframe of this work and are therefore included in the outlook.

In the determination of the apposition and overdilatation behaviour of stents using Micro-CT technology, a number of improvement possibilities have been identified. Up to now no solution could be found to completely eliminate the metal artefacts caused by the cobalt-chromium alloy of the stent platform, which made the measurements of the residual stenosis more difficult. The reduction of artefacts would require further research in the field of artefact reduction in imaging and test experiments in which, for example, contrast agents of different iodine concentrations are used to further reduce the artefacts. In addition, further examination possibilities such as the use of

the OCT technique or other imaging techniques could be evaluated prospectively. For future investigations, besides the general recording of the number of malapposed struts, the measuring of the exact distance of the malapposed strut to the vessel wall would be interesting. This would allow conclusions to be drawn about the risk of restenosis. Furthermore, for the exact determination of the overdilatation behaviour of the stents in the entire proximal area, a better software would be required that would allow a 3D representation of the entire scanned model.

In conclusion, it can be said that the first production of such artificial arterial vessel models at Biotronik AG can be evaluated as a successful production. By integrating a 3D-printed stenosis into the silicone vessels, a clinical indication in the area of the left coronary artery could be simulated. With some minor adaptation of the rig and the material to be used for the mock vessels it would be possible to generate artificial vessels that mimic the characteristics of natural human arteries even more closely. Furthermore, if the Micro-CT measurements can be optimized to provide artefact-free scans, all seven competitor products selected in Part I could be tested for apposition and overdilatation behaviour with the developed test method and thus the performance profile of all products could be recorded.

## 12 References

- [1] World Health Organization (WHO), "Cardiovascular diseases (CVDs)," May. 2017. [Online] Available: [https://www.who.int/en/news-room/fact-sheets/detail/cardiovascular-diseases-\(cvds\)](https://www.who.int/en/news-room/fact-sheets/detail/cardiovascular-diseases-(cvds)).
- [2] T. Schmidt and Abbott, J., D., "Coronary Stents: History, Design, and Construction," 2018.
- [3] N. Foin *et al.*, "Impact of Stent Structural Design and Deployment Pressure on Strut Apposition and Recoil," 2012.
- [4] D. C. Gaze, *The Cardiovascular System - Physiology, Diagnostics and Clinical Implications*: INTECH Open Access Publisher, 2012.
- [5] B. Praveen, "Cardiovascular System Anatomy," Aug. 2014. [Online] Available: <https://emedicine.medscape.com/article/1948510-overview#showall>.
- [6] K. Rogers, *The Cardiovascular System*. Chicago: Britannica Educational Pub, 2011.
- [7] S. Whittemore, *The Circulatory System*. Philadelphia: Chelsea House Publishers, 2004.
- [8] P. Pavone, M. Fioranelli, and D. A. Dowe., *CT Evaluation of Coronary Artery Disease*, 1st ed. s.l.: Springer Verlag Italia, 2009.
- [9] R. Klinge, Ed., *Das Elektrokardiogramm*. Stuttgart: Georg Thieme Verlag, 2015.
- [10] A. Fortier, V. Gullapalli, and R. A. Mirshams, "Review of biomechanical studies of arteries and their effect on stent performance," 2014.
- [11] C. Souilhol, Harmsen, M., C., Evans, P., C., and G. Krenning, "Endothelial-mesenchymal transition in atherosclerosis," 2018.
- [12] R. Erbel, B. Pflücht, P. Kahlert, and T. Konorza, *Herzkatheter-Manual: Diagnostik und interventionelle Therapie ; mit 211 Tabellen ; Patientenbroschüren und das Handbuch des Herzinfarktverbundes Essen auf CD-ROM ; [mit CD-ROM]*. Köln: Dt. Ärzte-Verl., 2012.
- [13] Singh, A., K., V. Chawla, Saraf, S., K., and Keshari, A., K., "Different Chemical, Biological and Molecular Approaches for Anti-Hyperlipidemic Therapy with Special Emphasis on Anti-Hyperlipidemic Agents of Natural Origin," Sep. 2014.
- [14] Eggebrecht and R. Erbel, "PTCA (Koronarangioplastie)," [Online] Available: <https://www.cardio-guide.com/therapie/ptca/#>.
- [15] M. Picichè, Ed., *Dawn and Evolution of Cardiac Procedures: Research Avenues in Cardiac Surgery and Interventional Cardiology*. Milano: Springer, 2013.
- [16] Medgurus, "Angioplasty Stenting - Best Hospitals, Doctors & Cost in India," 2018. [Online] Available: <http://www.medgurus.org/angioplasty-stents-cost-and-best-hospitals/>.
- [17] Hess, O., M. and Simon, R., W., R., *Herzkatheter: Einsatz in Diagnostik und Therapie*. Berlin, Heidelberg, s.l.: Springer Berlin Heidelberg, 2000.
- [18] T. Bonzel and Hammer, C., W., *Leitfaden Herzkatheter*. Heidelberg: Steinkopff, 2009.
- [19] I. Krakau and H. Lapp, *Das Herzkatheterbuch: Diagnostische und interventionelle Kathetertechniken ; [inklusive CD-ROM]*, 2nd ed. Stuttgart: Thieme, 2005.
- [20] Biotronik AG, "Drug Eluting Stent System Orsiro," 2018.
- [21] Noad, R., L., Hanratty, C., G., and Walsh, S., J., "Clinical Impact of Stent Design," Apr. 2014.
- [22] W. Schmidt and P. Behrens, "Comparative investigation of Coronary stent systems (DES)," Aug. 2018.
- [23] Terumo, "Ultimaster," 2018.
- [24] B. Braun AG, "Coroflex® ISAR NEO: Sirolimus-freisetzendes Polymer-freies koronares Stentsystem," 2017.
- [25] Abbott, "Introducing Xience Sierra," 2017.
- [26] Cordis, "EluNIR™ Ridaforolimus Eluting Coronary Stent System: Instructions for Use," 2017.
- [27] J. Ng *et al.*, "Over-expansion capacity and stent design model: An update with contemporary DES platforms," 2016.
- [28] Medtronic, "Resolute Onyx™ Zotarolimus-Eluting Coronary Stent System: Rapid Exchange and Over-the-Wire Delivery Systems," 2016.
- [29] Boston Scientific, "Synergy™ Monorail™: Everolimus-Eluting Platinum Chromium Coronary Stent System," 2016.
- [30] Bundesministerium des Inneren, "Handbuch für Organisationsuntersuchungen und Personalbedarfsermittlungen," Feb. 2018.
- [31] F. Burzotta, P. Mortier, and C. Trani, "Characteristics of drug-eluting stent platforms potentially influencing bifurcated lesion provisional stenting procedure," (eng), *EuroIntervention : journal of EuroPCR in collaboration with the Working Group on Interventional Cardiology of the European Society of Cardiology*, vol. 10, no. 1, pp. 124–132, 2014.
- [32] N. Melikian and C. Di Mario, "Treatment of Bifurcation Coronary Lesions: A Review of Current Techniques and Outcome," 2003.
- [33] Lassen, J., F. *et al.*, "Percutaneous coronary intervention for the left main stem and other bifurca-

- tion lesions: 12th consensus document from the European Bifurcation Club,” (eng), *EuroIntervention : journal of EuroPCR in collaboration with the Working Group on Interventional Cardiology of the European Society of Cardiology*, vol. 13, no. 13, pp. 1540–1553, 2018.
- [34] Fam, J., M., De Beule, M., N. van Mieghem, and R. Diletti, “Defining Optimal Stent Overexpansion Strategies for Left Main PCI- Insights from bench testing,” 2015.
- [35] A. C. Lindsay *et al.*, “Predictors of Stent Strut Malapposition in Calcified Vessels Using Frequency-Domain Optical Coherence Tomography,” Sep. 2013.
- [36] E. Alegría-Barrero *et al.*, “Optical coherence tomography for guidance of distal cell recrossing in bifurcation stenting: Choosing the right cell matters,” (eng), *EuroIntervention : journal of EuroPCR in collaboration with the Working Group on Interventional Cardiology of the European Society of Cardiology*, vol. 8, no. 2, pp. 205–213, 2012.
- [37] H.-C. Gwon, Song, Y., B., and M. Pan, “The story of plaque shift and carina shift,” (eng), *EuroIntervention : journal of EuroPCR in collaboration with the Working Group on Interventional Cardiology of the European Society of Cardiology*, vol. 11 Suppl V, V75-7, 2015.
- [38] J.-B. Seo *et al.*, “Predictors for Side Branch Failure During Provisional Strategy of Coronary Intervention for Bifurcation Lesions (from the Korean Bifurcation Registry),” (eng), *The American journal of cardiology*, vol. 118, no. 6, pp. 797–803, 2016.
- [39] D. Locca *et al.*, “How should I treat an undeployed stent stuck in the proximal LAD? Going for another round,” (eng), *EuroIntervention : journal of EuroPCR in collaboration with the Working Group on Interventional Cardiology of the European Society of Cardiology*, vol. 10, no. 4, pp. 528–530, 2014.
- [40] N. Foin *et al.*, “Maximal expansion capacity with current DES platforms: a critical factor for stent selection in the treatment of left main bifurcations?,” 2012.
- [41] R. Ramesh, Strobe, E., R., Price, K., S., and Conti, “Frequency Dependent Hysteresis of Silicone and Latex Mock Arteries Used in Stent Testing,” 2005.
- [42] R. Waksman and Ormiston, J., A., *Bifurcation stenting*. Chichester, West Sussex, UK: Wiley-Blackwell, 2012.
- [43] T. Pflederer, J. Ludwig, D. Ropers, Daniel, W., G., and S. Achenbach, “Measurement of coronary artery bifurcation angles by multidetector computed tomography,” (eng), *Investigative radiology*, vol. 41, no. 11, pp. 793–798, 2006.
- [44] Kassab, G., S. and G. Finet, “Anatomy and function relation in the coronary tree: From bifurcations to myocardial flow and mass,” (eng), *EuroIntervention : journal of EuroPCR in collaboration with the Working Group on Interventional Cardiology of the European Society of Cardiology*, vol. 11 Suppl V, V13-7, 2015.
- [45] Y. Louvard *et al.*, “Classification of coronary artery bifurcation lesions and treatments: Time for a consensus!,” (eng), *Catheterization and cardiovascular interventions : official journal of the Society for Cardiac Angiography & Interventions*, vol. 71, no. 2, pp. 175–183, 2008.
- [46] J. Singh, J. Depta, and Y. Patel, “Bifurcation Lesions,” 2018. [Online] Available: <https://www.thecardiologyadvisor.com/cardiology/bifurcation-lesions/article/584040/>.
- [47] R. Ramesh *et al.*, “Comparison of Radial Expansion of Stents Within Mock Vessels Molded with a Target Bent Radius Versus Straight Mock Vessels Bent to a Target Radius,” Mar. 2011. [Online] Available: <https://dynateklabs.com/comparison-of-radial-expansion-of-stents-within-mock-vessels-molded-with/>.
- [48] *Kardiovaskuläre Implantate – Endovaskuläre Implantate – Teil 1: Endovaskuläre Prothesen*, DIN EN ISO 25539-1, 2018.
- [49] *Kardiovaskuläre Implantate und extrakorporale Systeme – Vaskuläre Prothesen – Tubulare vaskuläre Transplantate und Gefäßpatches*, DIN EN ISO 7198, 2017.
- [50] M. Wind and C. Schindler, *Numerische und experimentelle Analyse und Optimierung der technischen Eigenschaften eines selbstexpandierenden Stents*. Zugl.: Kaiserslautern, Techn. Univ., Diss., 2011. Kaiserslautern: Universitätsbibliothek Kaiserslautern, 2011.
- [51] B. Bertsche and W. Haas, “Kennwertermittlung für die FEM-Simulation,” Oct. 2012.
- [52] Kunz, Miacheli, Herrlich, and Land, *Kunststoffpraxis: Konstruktion*: WEKA MEDIA GmbH & Co. KG, 2004.
- [53] A. Ghajari, “An experimental study of Oil-Water flow in upwards inclined pipes,” 2005.
- [54] A. Colombo, H. Zahedmanesh, D. M. Toner, P. A. Cahill, and C. Lally, “A method to develop mock arteries suitable for cell seeding and in-vitro cell culture experiments,” (eng), *Journal of the mechanical behavior of biomedical materials*, vol. 3, no. 6, pp. 470–477, 2010.
- [55] 1zu1 Prototypen, “Stereolithografie (STL/SLA): Accura Xtreme, Accura 25, Somos WaterClear, Somos PerFORM, Somos ProtoTherm,” 2019. [Online] Available: [https://www.1zu1prototypen.com/3d-druck/stereolithografie.htm#tab\\_tab2-3753](https://www.1zu1prototypen.com/3d-druck/stereolithografie.htm#tab_tab2-3753).
- [56] Farooqi, K., M., *Rapid prototyping in cardiac disease: 3D printing the heart*. Cham, Switzerland: Springer, 2017.

- [57] WACKER Chemie AG, "Elastosil: An All-Rounder for Countless Applications," Nov. 2014. [Online] Available: <https://www.wacker.com/cms/en/products/brands/elastosil/elastosil.jsp>.
- [58] Wassermann Dental-Maschinen GmbH, "Vakuum-Anrührgerät Wamix-Touch Injector," [Online] Available: [https://www.wassermann.hamburg/de/produkte.html?tx\\_silproducts\\_kategorien%5Bkategorie%5D=16&tx\\_silproducts\\_geraete%5Bprodukt%5D=133&tx\\_silproducts\\_geraete%5Baction%5D=show&tx\\_silproducts\\_geraete%5Bcontroller%5D=Produkt&cHash=d3a51b191345281a6f7f8925c160075e](https://www.wassermann.hamburg/de/produkte.html?tx_silproducts_kategorien%5Bkategorie%5D=16&tx_silproducts_geraete%5Bprodukt%5D=133&tx_silproducts_geraete%5Baction%5D=show&tx_silproducts_geraete%5Bcontroller%5D=Produkt&cHash=d3a51b191345281a6f7f8925c160075e).
- [59] Science 19, "Wie man Konzentrität berechnet," [Online] Available: <https://science19.com/how-to-calculate-concentricity-7665>.
- [60] SkyScan, "Desktop X-ray microtomograph: Instruction Manual," Belgium, 2005.
- [61] W. Schmidt and C. Brandt-Wunderlich, "Investigation of Coronary Delivery Catheters: Particulate Evaluation after Simulated Use Tests," 2016.
- [62] W. Schmidt and C. Brandt-Wunderlich, "Investigation of Coronary Stent Systems: Acute and Chronic Coating Durability," 2015.



## 13 Appendix

### 13.1 Internal test methods

Table A1 represents the most frequently investigated topics dealt with in the IIB reports regarding DES systems and a brief description of the used test methods. The applied test methods of the IIB testing laboratory based on Council Directive 93/42/EEG and DIN EN ISO/IEC 17025 [22].

Table A1: Investigated topics of the IIB institute and their applied test methods [22, 61, 62]

Topics	Test methods
Photo documentation of package/ labelling, crimped stents, expanded stents (unstressed and stressed)	Investigation of detailed photographs of stents in crimped (original state) and expanded state as well as of package and labelling various competitors
Surface characterization and strut dimensions	Measurement and visualization of strut width and thickness as well as strut surface using Scanning Electron Microscopy (SEM)
Radiopacity of balloon marker, crimped and expanded stents	Quantitative analysis of the radiopacity of the balloon marker and the stents in crimped and expanded state using an X-ray device
Side branch accessibility	Assessment of the side branch accessibility through software-based acquisition of the largest cell in the central expanded stent
Bending stiffness of crimped and expanded stents and of the distal shaft	Measurement of the bending stiffness of crimped and expanded stents and of the distal shaft by using a load cell
Lesion entry profile	Determination of the lesion entry profile at the distal tip with the help of an image processing software
Outer contour of curved stent	Photo documentation of the outer contour of the curved stents and measurement of the distances between the distal and proximal stent ends and the balloon via an calibrated

	software integrated in an incident light microscope
Fishmouthing of tip	Measurement of the distance between the outer contour of the guidewire and the outer contour of the tip (called fishmouthing) via an calibrated software integrated in an incident light microscope
Tip length measurement	Determination of the length of the catheter tip from macro photographs using a software with measuring function
Trackability of the complete system	Measurement of the force required to track the stent/catheter system through a guiding catheter and an in-vitro vessel model using a 2-channel push device
Crossability of the complete system	Measurement of the force required to cross the stent/catheter system through an in-vitro vessel model which contains a simulated stenotic lesion at the end using a 2-channel push device
Pushability of the complete system	Measurement of the force required to push the stent/catheter system against a total occluded in-vitro vessel model using a 2-channel push device
Profile in the crimped state	Determination of the stent profile of crimped stents as mean values of the diameters over the entire stent length up to the distal shaft using a laser test system
Stent expansion, recoil, opening behaviour	Performing the stent expansion to nominal diameter with a control unit to record the opening behaviour of the stents and determine the stent recoil from the diameter in the expanded and non-expanded state
Stent length change	Determination of the stent length change by measuring stent length and diameter before



	and after the stent expansion using a 2-axis laser device
Balloon rewrap visually	Photo documentation of the balloon profiles after inflation to NP and deflation of the balloons by vacuum
Inflation/ Deflation time	Measurement of the inflation (is defined as the time required to completely fill the balloon with a mixture of liquids)/ deflation time (is defined as the time required to completely remove the liquid from the balloon) using a defined test setup and a stop watch
Stent preconditioning	Tracking the stent system three times through an in-vitro vessel model is defined as preconditioning
Stent dislodgement force after preconditioning	Determination of the force that is required to move the crimped stent on the evacuated balloon (=stent dislodgement force) after conclusion of the preconditioning using a universal test machine and a load cell
Balloon compliance and balloon burst	Assessment of the balloon compliance from measuring the balloon diameters as a function of the balloon pressure from NP to RBP using a control unit and a laser test system
Coating integrity	Investigation of the coating integrity of expanded stents using Scanning Electron Microscopy (SEM)
Particulate evaluation after simulated use test	Evaluation of particles in the test liquids obtained from different test solutions of the test path after performing the simulated use test (performing an balloon delivery through an in-vitro model) using a particle counter
Fatigue analysis	Inspection of stents using an incident light microscope after performing fatigue durability tests under radial loading

## 13.2 Identified weak spots

Table A2 to A4 represents the weak spots identified during discussions with various internal experts in the field of DES. The collected weak spots are divided into stent, catheter and packaging according to their respective topics.

Table A2: Identified weak spots related to the stent

<b>Stent</b>		
No	Topic	Weak spot
1	Radiopacity	Visibility is too weak
2	Stent cell size	Stent cell size for side branch too small
3	Side Branch Accessibility/ Bifurcation behaviour	Cell size/ side branch too small, Side branch accessibility
4	Overdilatation behaviour	Stent performance in overdilatated condition
5	Bending fatigue	Bending fatigue behaviour
6	Axial stiffness	Axial stiffness in different stent designs
7	Coating Integrity	Coating behaviour during implantation
8	Radial strength	Radial strength too low
9	Flow behaviour	Shear forces → risk of thrombosis (influences of strut thickness)
10	Apposition/ Malapposition	Stent strut malapposition behaviour
11	Recoil	Recoil at NP, RBP, overexpansion
12	Torsion	Torsion behaviour
13	Side Branch Protection	Narrowing side branch

Table A3: Identified weak spots related to the catheter

<b>Catheter</b>		
No	Topic	Weak spot
14	Balloon deflation time	Deflation time too long
15	Luer font size	Font size too small
16	Luer contour/ edge	Packaging damage/ position of luer
17	Luer – catheter transition	No kink protection
18	Hypotube/ FDA/ Transition zone	Buckling susceptibility
19	Tip length	Tip dimension

20	Fishmouthing tip	Too large fishmouth of tip in curvature
21	Catheter/ delivery system	Torsions behaviour for higher requirements than standard specification
22	Pullback behaviour	Pullback until necking
23	Guidewire section	Length distal part
24	Tube - distal part	Axial shaft compression in the distal region
25	Marker balloon	Clinical positioning accuracy
26	Balloon deformation	'Banana-shape' formation

Table A4: Identified weak spots related to the packaging

<b>Packaging</b>		
No	Topic	Weak spot
27	Compliance chart	Compliance chart containing all balloon/ stent sizes
28	Design outer packaging	Paint removal, Scan code - QR Code
29	Product counterfeiting	Protection too low
30	Inner packaging	Connection Luer - Dispenser too weak
31	Innermost packaging	Usability not ideal (misunderstandings)
32	Packaging wire	Protective cover → wire removal in front
33	Vacuum sealing process	Too high oxygen concentration in inner packaging

### 13.3 Explanation of the seven 'high'-rated weak spots

Table A5: Brief explanation of the 'high'-rated weak spots

Weak spot	Explanation
Cell size/ side branch too small, Side branch accessibility	The weak spot represents the issue of a too small cell size of the stent, which can lead to the cardiologist not being able to reach the side branch during bifurcation treatment.
Stent performance in overdilatated condition	The weak spot is understood as the behaviour of the products after executing expansion of the stents above their maximum labelled expandable diameter [27,

	40].
Stent strut malapposition behaviour	The stent malapposition is defined as the incomplete stent strut apposition to the arterial wall [35].
Narrowing side branch	The weak represents the issue of SB occlusion due to carina or plaque shift during stenting procedure [37].
Buckling susceptibility	The 'Buckling susceptibility' was defined as a weak spot due to the hypotube design of the Biotronik's DES Orsiro.
Torsions behaviour for higher requirements than standard specification	The weak spot defines the negative behaviour of the delivery system when more torque is applied to the system during PCI than allowed in the instructions for use.
Pullback until necking	The weak spot can be understood as the sticking of the delivery system during the pullback of the system from the arterial vascular system.

### 13.4 Evaluation of 'medium'-rated weak spots

Table A6 lists the evaluation of the weak spots that reached a 'medium' in the first interim rating.

Table A6: Results of the first interim rating including weak spots that have reached a 'medium' (medium = 5 – 9)

First interim rating						
Weak spot	Potential of market differentiation	Expert feedback	Realizability in project	Internal test methods & results available	Competitor comparison	<b>Total</b>

Coating behaviour during im-plantation	3	1	1	1	1	<b>5</b>
Radial strength low (competitors)	2	1	1	1	2	<b>5</b>
Recoil at NP, RBP, overexpan-sion	3	1	1	1	1	<b>5</b>
Packaging damage/ position of luer	2	1	1	1	2	<b>5</b>
No kink protection	1	1	1	2	2	<b>5</b>
Axial shaft compression in the distal region	1	1	1	2	2	<b>5</b>
Clinical positioning accuracy	2	1	1	2	2	<b>6</b>
'Banana-shape' formation	1	1	1	2	2	<b>5</b>
Connection Luer-Dispenser too weak	1	1	1	2	2	<b>5</b>
Usability not ideal (misunder-standings) --> with competing products	2	1	1	2	1	<b>5</b>
Protective cover --> wire remov-al in front	2	1	1	2	2	<b>6</b>

### 13.5 Evaluation of 'low'-rated weak spots

Table A7 lists the evaluation of the weak spots that reached a 'low' in the first interim rating.

Table A7: Results of the first interim rating including weak spots that have reached a 'low' (low = 0 - 4)

<b>First interim rating</b>						
Weak spot	Potential of market differentiation	Expert feedback	Realizability in pro-ject	Internal test methods & results available	Competitor compari-son	<b>Total</b>
Visibility in angiography too weak	1	1	1	1	1	<b>3</b>
Stent cell size for side branch too small	1	1	1	1	1	<b>3</b>
Bending fatigue behaviour	1	1	0	2	2	<b>0</b>
Axial stiffness in different stent designs	1	1	1	1	1	<b>3</b>
Shear forces --> risk of throm-	3	1	0	2	2	<b>0</b>

basis (influences of strut thickness)						
Torsion behaviour	2	1	0	2	2	<b>0</b>
Deflation time too long	1	1	1	1	1	<b>3</b>
Font size too small	1	1	1	1	1	<b>3</b>
Tip dimension	2	1	1	1	1	<b>4</b>
Too large fishmouth of tip in curvature	1	1	1	1	1	<b>3</b>
Length distal part	2	1	1	1	1	<b>4</b>
Adaptation to individual size	1	1	1	2	1	<b>4</b>
Paint removal, Scan code- QR Code, RFID (Logistics)	2	1	1	1	1	<b>4</b>
Protection too low	1	1	1	1	1	<b>3</b>
Too high oxygen concentration in inner packaging	1	1	1	1	2	<b>4</b>

## 13.6 Questionnaire for physician interviews

The following list shows the questionnaire which was prepared in advance according to the seven weak spots for the interviews with the physicians.

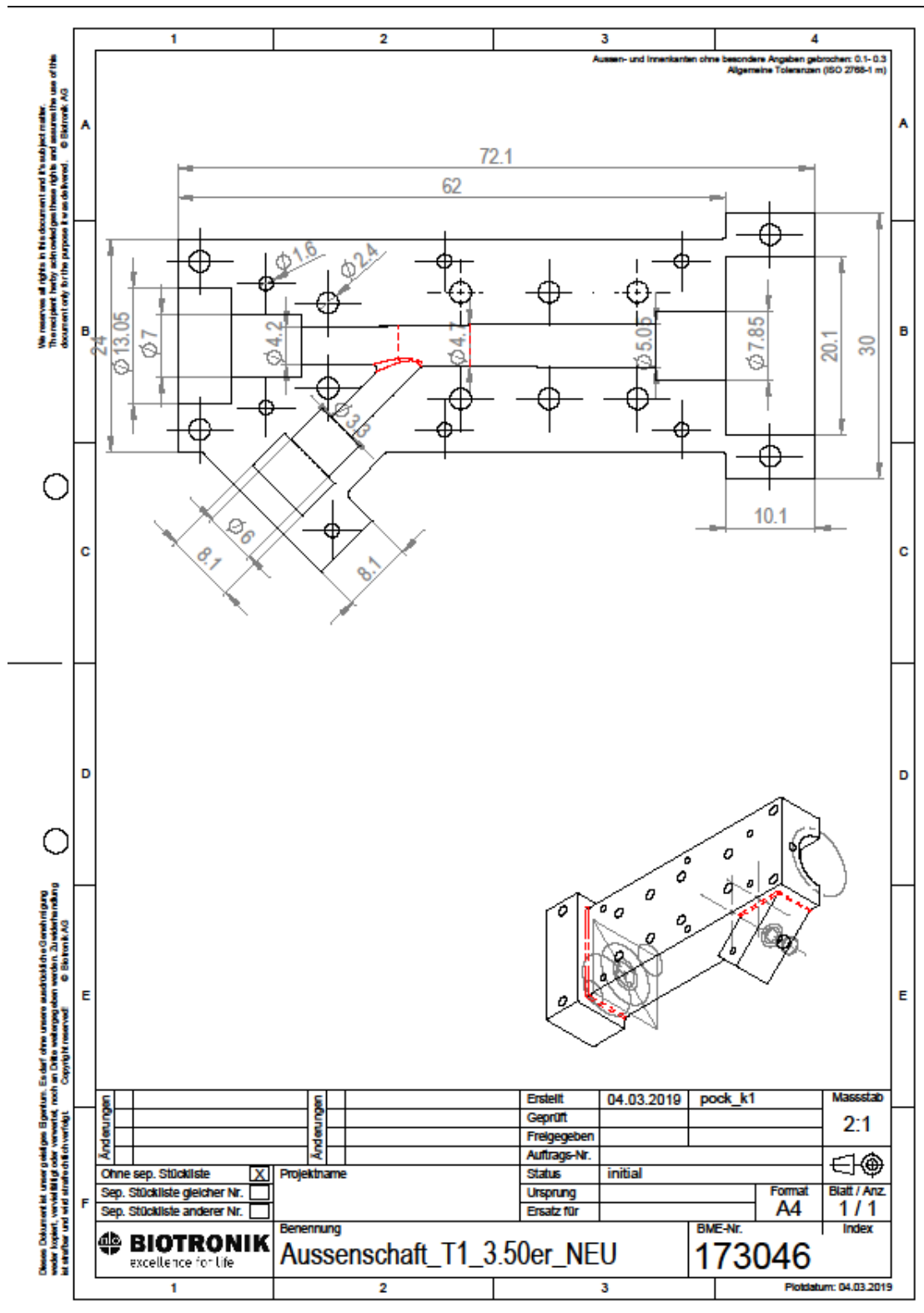
- Are there products that perform better than others in terms of side branch accessibility and side branch protection due to their design?
- Have there been any incidents during surgery where overdilatation of the stent (above its maximum labelled expandable diameter) had a negative effect on its performance?
- Have you ever noticed that specific stents have embedded better to stenosis/ the vascular wall than others due to their design?
- Are there products that tend to narrow side branch more quickly than others due to their construction? Is it possible to draw a technical conclusion on the design or is it dependent on the user/ technique?
- Has the delivery system ever had any anomalies with regard to buckling susceptibility?
- Is there a need to give torque to the delivery system in order to facilitate the passage of stenosis, for example? If so, how strong can this torque be?
- Have there ever been any problems with the return of the delivery system in terms of getting stuck or getting caught during interventions?



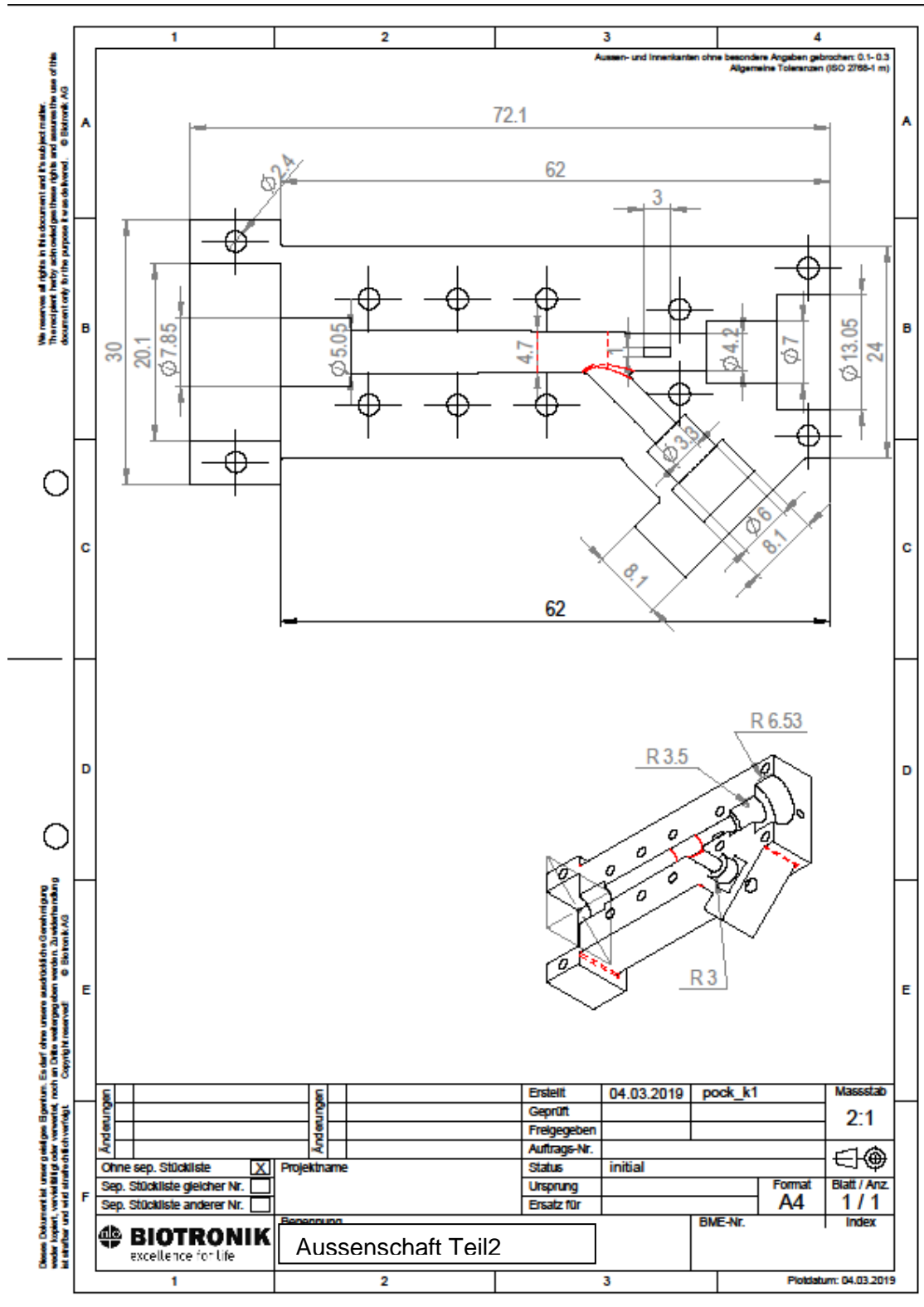


# 13.7 CAD drawings

## Outer shaft 1



# Outer shaft 2

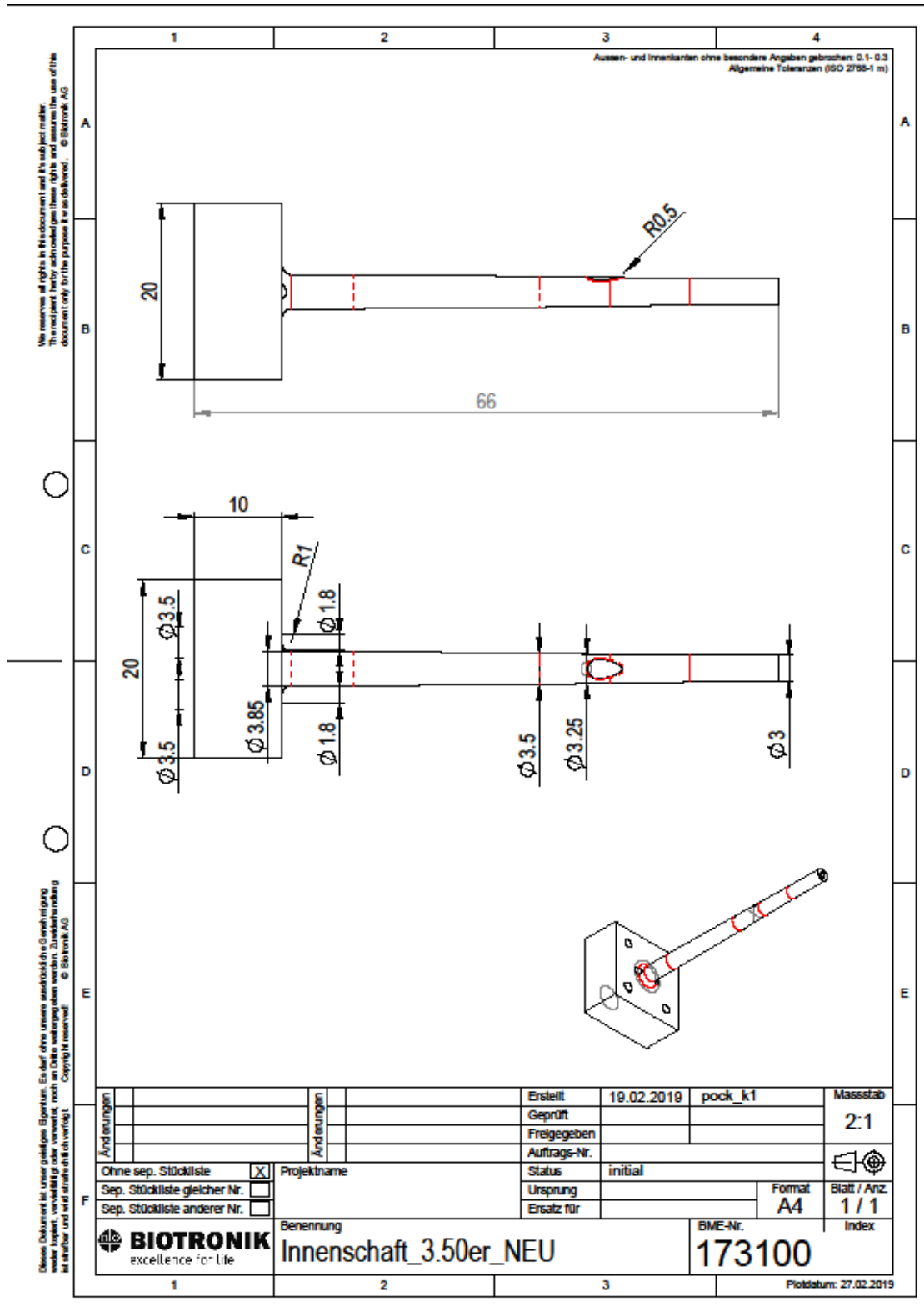


We reserve all rights in this document and its subject matter. The recipient hereby acknowledges these rights and assumes the use of this document only for the purpose for which it was delivered. © Biotronik AG

Dieses Dokument ist unser geistiges Eigentum. Es darf ohne unsere ausdrückliche Genehmigung weder kopiert, vervielfältigt oder verwendet, noch an Dritte weitergegeben werden. Zu jeder Handlung ist unsere und wird ausdrücklich verlangt. © Biotronik AG

Anderrungen		Anderrungen		Erstellt	04.03.2019	pock_k1	Massstab
				Gepf. /			2:1
				Freigegeben			
				Auftrags-Nr.			
Ohne sep. Stückliste <input checked="" type="checkbox"/>		Projektname		Status	initial		
Sep. Stückliste gleicher Nr. <input type="checkbox"/>				Ursprung		Format	Blatt / Anz
Sep. Stückliste anderer Nr. <input type="checkbox"/>				Ersatz für		A4	1 / 1
		Bezeichnung		BME-Nr.		Index	
<b>BIOTRONIK</b> excellence for life		Aussenschaft Teil2					
1		2		3		Plotdatum: 04.03.2019	

# Inner mandrel



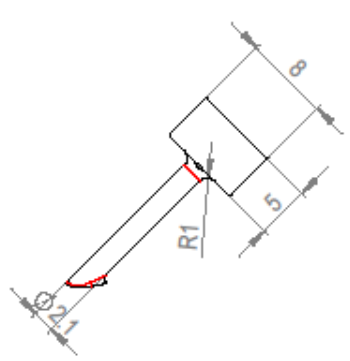
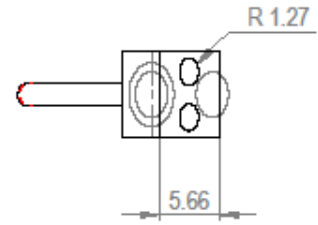
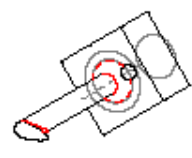
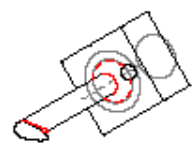




Wir reservieren alle Rechte in diesem Dokument und in dem dazugehörigen Material.  
 The recipient hereby acknowledges these rights and assumes the use of this document only for the purpose for which it was delivered. © Biotronik AG

Dieses Dokument ist unser geistiges Eigentum. Es darf ohne unsere ausdrückliche Genehmigung weder kopiert, vervielfältigt oder verwendet, noch an Dritte weitergegeben werden. Zuwiderhandlung ist strafbar und wird strafrechtlich verfolgt. Copyright reserved. © Biotronik AG

Änderungen <input type="checkbox"/>		Änderungen <input type="checkbox"/>		Erstellt 19.02.2019	pock_k1	Massstab 2:1
Ohne sep. Stückliste <input checked="" type="checkbox"/>		Projektname		Geprüft		<input type="checkbox"/>
Sep. Stückliste gleicher Nr. <input type="checkbox"/>				Freigegeben		
Sep. Stückliste anderer Nr. <input type="checkbox"/>				Auftrags-Nr.		
				Status initial	Format A4	Blatt / Anz. 1 / 1
				Ursprung		Index
				Ersatz für		
<b>BIOTRONIK</b> excellence for life		Benennung Innenschaft_3.50er_NEU			BME-Nr. 173100	

Plattendatum: 27.02.2019

# RD1 branch

1	2	3	4																																																												
A	Aussen- und Innenkanten ohne besondere Angaben gebrochen: 0.1-0.3 Allgemeine Toleranzen (ISO 2768-1 m)		A																																																												
B			B																																																												
C			C																																																												
D			D																																																												
E			E																																																												
F	<table border="1" style="width: 100%; border-collapse: collapse;"> <tr> <td style="width: 20%; font-size: 8px;">Andersungen</td> <td style="width: 20%; font-size: 8px;">Andersungen</td> <td style="width: 20%; font-size: 8px;">Erstellt</td> <td style="width: 20%; font-size: 8px;">04.03.2019</td> <td style="width: 20%; font-size: 8px;">pock_k1</td> <td style="width: 20%; font-size: 8px;">Massstab</td> </tr> <tr> <td></td> <td></td> <td style="font-size: 8px;">Geprüft</td> <td></td> <td></td> <td style="text-align: center; font-size: 12px;">2:1</td> </tr> <tr> <td></td> <td></td> <td style="font-size: 8px;">Freigegeben</td> <td></td> <td></td> <td></td> </tr> <tr> <td></td> <td></td> <td style="font-size: 8px;">Auftrags-Nr.</td> <td></td> <td></td> <td style="text-align: center;">  </td> </tr> <tr> <td colspan="2" style="font-size: 8px;">Ohne sep. Stückliste <input checked="" type="checkbox"/></td> <td colspan="2" style="font-size: 8px;">Projektname</td> <td style="font-size: 8px;">Status</td> <td style="font-size: 8px;">initial</td> </tr> <tr> <td colspan="2" style="font-size: 8px;">Sep. Stückliste gleicher Nr. <input type="checkbox"/></td> <td colspan="2" style="font-size: 8px;"></td> <td style="font-size: 8px;">Ursprung</td> <td style="font-size: 8px;">Format</td> </tr> <tr> <td colspan="2" style="font-size: 8px;">Sep. Stückliste anderer Nr. <input type="checkbox"/></td> <td colspan="2" style="font-size: 8px;"></td> <td style="font-size: 8px;">Ersatz für</td> <td style="font-size: 8px;">A4</td> </tr> <tr> <td colspan="2" style="font-size: 8px;"></td> <td colspan="2" style="font-size: 8px;"></td> <td style="font-size: 8px;">BME-Nr.</td> <td style="font-size: 8px;">Blatt / Anz</td> </tr> <tr> <td colspan="2" style="font-size: 8px;"></td> <td colspan="2" style="font-size: 8px;"></td> <td style="font-size: 8px;"></td> <td style="font-size: 8px;">1 / 1</td> </tr> <tr> <td colspan="2" style="font-size: 8px;"></td> <td colspan="2" style="font-size: 8px;"></td> <td style="font-size: 8px;"></td> <td style="font-size: 8px;">Index</td> </tr> </table>		Andersungen	Andersungen	Erstellt	04.03.2019	pock_k1	Massstab			Geprüft			2:1			Freigegeben						Auftrags-Nr.				Ohne sep. Stückliste <input checked="" type="checkbox"/>		Projektname		Status	initial	Sep. Stückliste gleicher Nr. <input type="checkbox"/>				Ursprung	Format	Sep. Stückliste anderer Nr. <input type="checkbox"/>				Ersatz für	A4					BME-Nr.	Blatt / Anz						1 / 1						Index	F
Andersungen	Andersungen	Erstellt	04.03.2019	pock_k1	Massstab																																																										
		Geprüft			2:1																																																										
		Freigegeben																																																													
		Auftrags-Nr.																																																													
Ohne sep. Stückliste <input checked="" type="checkbox"/>		Projektname		Status	initial																																																										
Sep. Stückliste gleicher Nr. <input type="checkbox"/>				Ursprung	Format																																																										
Sep. Stückliste anderer Nr. <input type="checkbox"/>				Ersatz für	A4																																																										
				BME-Nr.	Blatt / Anz																																																										
					1 / 1																																																										
					Index																																																										
		<table border="1" style="width: 100%; border-collapse: collapse;"> <tr> <td style="width: 50%; padding: 5px;">RD1</td> <td style="width: 50%;"></td> </tr> </table>		RD1		E																																																									
RD1																																																															
1	2	3	4																																																												

Dieses Dokument ist unser geistiges Eigentum. Es darf ohne unsere ausdrückliche Genehmigung weder kopiert, vervielfältigt oder verwendet, noch an Dritte weitergegeben werden. Zuwiderhandlung ist strafbar und wird strafrechtlich verfolgt. Copyright reserved © Biotronik AG

Plotdatum: 04.03.2019

# Cover

1
2
3
4

Außen- und Innenkanten ohne besondere Angaben gebrochen: 0.1-0.3  
 Allgemeine Toleranzen (ISO 2768-1 m)

A
B
C
D
E

Änderungen	

Änderungen	

Erstellt	27.02.2019	pock_k1
Geprüft		
Freigegeben		
Auftrags-Nr.		
Status	initial	
Ursprung		
Ersatz für		

Massstab	2:1

Ohne sep. Stückliste	<input checked="" type="checkbox"/>	Projektname
Sep. Stückliste gleicher Nr.	<input type="checkbox"/>	
Sep. Stückliste anderer Nr.	<input type="checkbox"/>	

Benennung	Deckel_distal_NEU
-----------	-------------------

BME-Nr.	173074
---------	--------

Format	A4
Blatt / Anz	1 / 1
Index	

1
2
3
Fließdatum: 04.03.2019

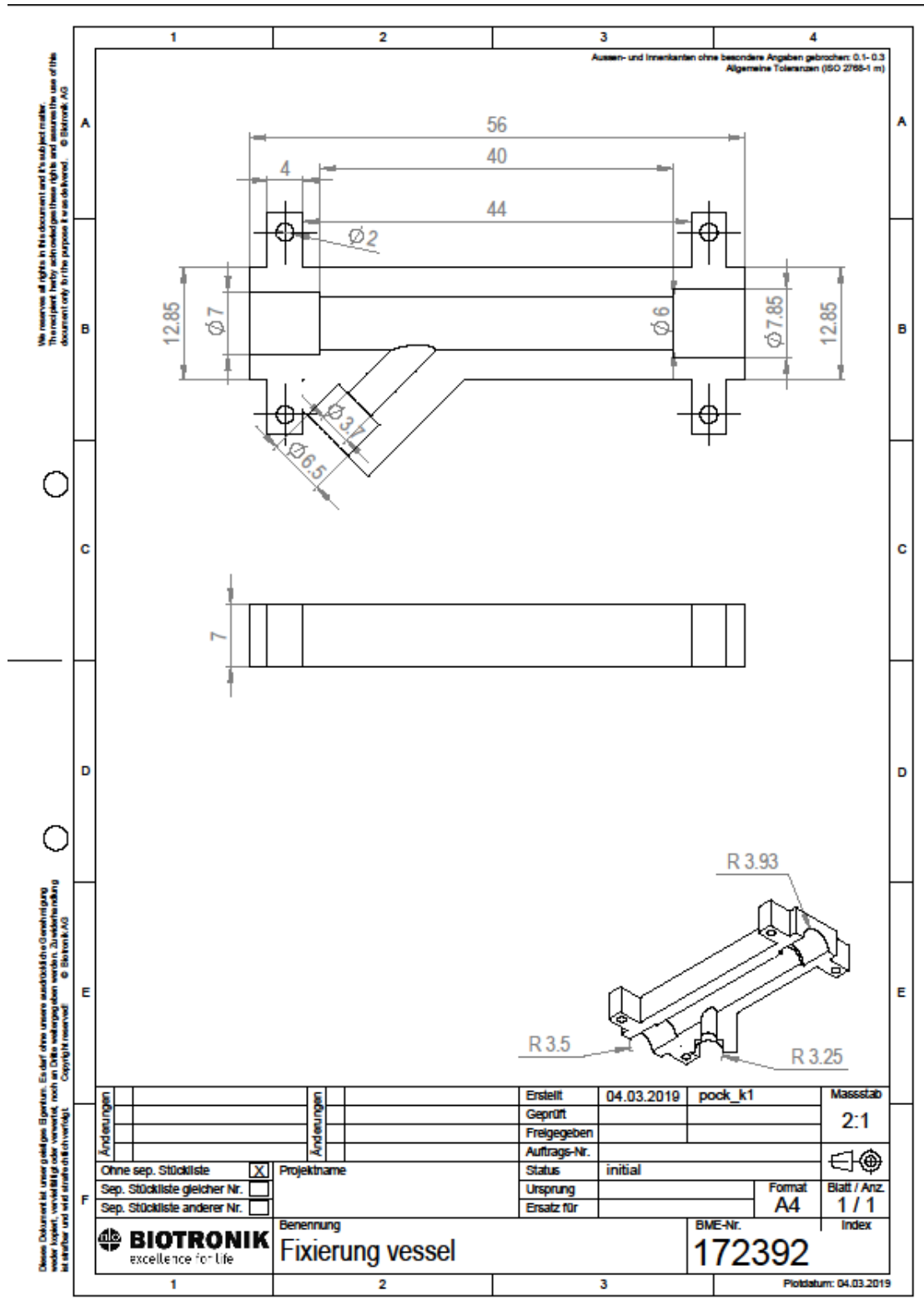
Dieses Dokument ist unser geistiges Eigentum. Es darf ohne unsere ausdrückliche Genehmigung weder kopiert, vervielfältigt oder verwendet, noch an Dritte weitergegeben werden. Zuwiderhandlungen sind strafbar und werden strafrechtlich verfolgt. Copyright reserved © Biotronik AG

Wir reservieren alle Rechte in diesem Dokument und es ist subject matter. The recipient hereby acknowledges these rights and assumes the use of this document only for the purpose it was delivered. © Biotronik AG

# Stenosis

	1	2	3	4								
<p style="font-size: small;">Wir reservieren alle Rechte in diesem Dokument und in dem zugehörigen Material. The recipient hereby acknowledges these rights and assumes the use of this document only for the purpose for which it was delivered. © Biotronik AG</p> <p style="font-size: x-small;">Dieses Dokument ist unser geistiges Eigentum. Es darf ohne unsere ausdrückliche Genehmigung weder kopiert, vervielfältigt oder verwendet, noch an Dritte weitergegeben werden. Zu jeder Handlung ist unserer und schriftlich vorliegt. Copyright reserved. © Biotronik AG</p>	Außen- und Innenkanten ohne besondere Angaben gebrochen: 0.1-0.3 Allgemeine Toleranzen (ISO 2768-1 m)											
A				A								
B				B								
C				C								
D				D								
E				E								
F	<table border="1" style="width: 100%; border-collapse: collapse;"> <tr> <td style="width: 20%;">                 Änderungen  <input type="checkbox"/>  <input type="checkbox"/>  <input type="checkbox"/> </td> <td style="width: 20%;">                 Änderungen  <input type="checkbox"/>  <input type="checkbox"/>  <input type="checkbox"/> </td> <td style="width: 20%;">                 Erstellt 27.02.2019                  Geprüft                  Freigegeben                  Auftrags-Nr.                  Status initial                  Ursprung                  Ersatz für             </td> <td style="width: 20%;">                 pock_k1                  10:1                  Blatt / Anz 1 / 1                  Index             </td> </tr> <tr> <td colspan="2">                 Ohne sep. Stückliste <input checked="" type="checkbox"/> Projektname                  Sep. Stückliste gleicher Nr. <input type="checkbox"/>                  Sep. Stückliste anderer Nr. <input type="checkbox"/> </td> <td colspan="2">                 Benennung  <b>stenosis_3.50er</b>                  BME-Nr.  <b>173102</b> </td> </tr> </table>			Änderungen <input type="checkbox"/> <input type="checkbox"/> <input type="checkbox"/>	Änderungen <input type="checkbox"/> <input type="checkbox"/> <input type="checkbox"/>	Erstellt 27.02.2019 Geprüft Freigegeben Auftrags-Nr. Status initial Ursprung Ersatz für	pock_k1 10:1 Blatt / Anz 1 / 1 Index	Ohne sep. Stückliste <input checked="" type="checkbox"/> Projektname Sep. Stückliste gleicher Nr. <input type="checkbox"/> Sep. Stückliste anderer Nr. <input type="checkbox"/>		Benennung <b>stenosis_3.50er</b> BME-Nr. <b>173102</b>		
Änderungen <input type="checkbox"/> <input type="checkbox"/> <input type="checkbox"/>	Änderungen <input type="checkbox"/> <input type="checkbox"/> <input type="checkbox"/>	Erstellt 27.02.2019 Geprüft Freigegeben Auftrags-Nr. Status initial Ursprung Ersatz für	pock_k1 10:1 Blatt / Anz 1 / 1 Index									
Ohne sep. Stückliste <input checked="" type="checkbox"/> Projektname Sep. Stückliste gleicher Nr. <input type="checkbox"/> Sep. Stückliste anderer Nr. <input type="checkbox"/>		Benennung <b>stenosis_3.50er</b> BME-Nr. <b>173102</b>										
1	2	3	Plattendatum: 27.02.2019									

# Fixation device for implantation

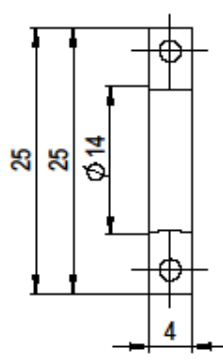
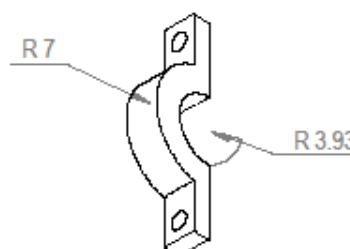
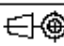



Wir reservieren alle Rechte in diesem Dokument und in dem zugehörigen Material. Der Empfänger behält sich alle Rechte vor und übernimmt die Verantwortung für die Verwendung dieses Dokuments nur zu dem Zweck, für den es bestimmt ist. © Biotronik AG

Dieses Dokument ist unser geistiges Eigentum. Es darf ohne unsere ausdrückliche Genehmigung weder kopiert, vervielfältigt oder verwendet, noch an Dritte weitergegeben werden. Zuwiderhandlung ist strafbar und wird strafrechtlich verfolgt. Copyright reserved! © Biotronik AG

Andereungen		Andereungen		Erstellt	04.03.2019	pock_k1	Massstab
				Geprüft			2:1
				Freigegeben			
				Auftrags-Nr.			
Ohne sep. Stückliste <input checked="" type="checkbox"/>		Projektname		Status	initial		
Sep. Stückliste gleicher Nr. <input type="checkbox"/>				Ursprung		Format	Blatt / Anz.
Sep. Stückliste anderer Nr. <input type="checkbox"/>				Ersatz für		A4	1 / 1
<b>BIOTRONIK</b> excellence for life		Benennung		BME-Nr.		Index	
		Fixierung vessel		172392			
1	2	3	Plattdatum: 04.03.2019				

# Mock vessel holder

1	2	3	4
A	Außen- und Innenkanten ohne besondere Angaben gebrochen: 0.1-0.3 Allgemeine Toleranzen (ISO 2768-1 m)		A
B			B
C			C
D			D
E			E
Dieses Dokument ist unser geistiges Eigentum. Es darf ohne unsere ausdrückliche Genehmigung weder kopiert, vervielfältigt oder verwendet, noch an Dritte weitergegeben werden. Zu jeder Herstellung ist schriftlich und schriftlich zu verifizieren. Copyright reserved © Biotronik AG			
Änderungen Ohne sep. Stückliste <input checked="" type="checkbox"/> Sep. Stückliste gleicher Nr. <input type="checkbox"/> Sep. Stückliste anderer Nr. <input type="checkbox"/>	Änderungen Projektname	Erstellt 27.02.2019 pock_k1 Geprüft Freigegeben Auftrags-Nr. Status initial Ursprung Ersatz für	Massstab 2:1  Blatt / Anz 1 / 1 Index
 Benennung <b>Fixierung</b>		BME-Nr. <b>172288</b>	
1	2	3	Plattendatum: 27.02.2019



## 13.8 Test instruction – Implantation of stent in mock vessel

### Prüfanweisung



---

### Anweisung zur Durchführung der Dilatation an DES Systemen (auf RBP) mit anschliessender proximaler Post-dilatation

#### 1.1 OP 1 – Vorbereitung Messaufbau

Prüfmittel:	Modifiziertes ASTM Trackmodell Anschlagbolzen für Trackmodell Klemmblocke für Trackmodell Halterungen zum Stabilisieren des Führungskatheters Wasserbad ( $T = 37\text{ °C} \pm 2\text{ °C}$ ) Führungskatheter gemäss PP
Menge:	Siehe PP
Spezifikation:	Strecke in modifiziertem ASTM Trackmodell gemäss Vorgabe Design
Prüfablauf:	<ul style="list-style-type: none"><li>▶ Trackmodell in Wasserbad platzieren und fixieren gemäss Abb. 1</li><li>▶ Halterungen zum Stabilisieren des Führungskatheters gemäss Abb. 2 platzieren</li><li>▶ Führungskatheter durch Trackmodell schieben und im Modell gemäss Abb. 3 platzieren</li></ul>

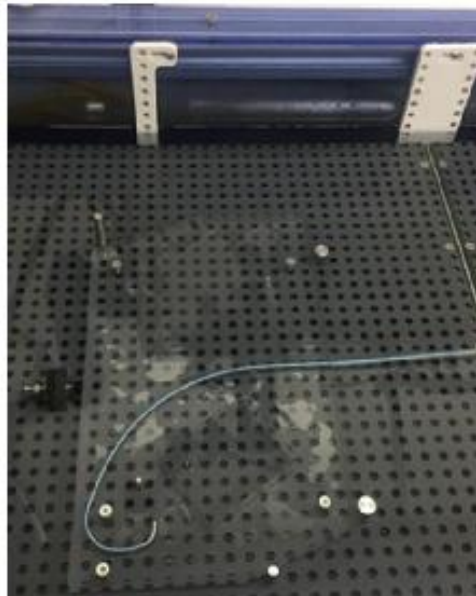


Abb. 1: Darstellung der Platzierung und Fixierung des Trackmodells im Wasserbad

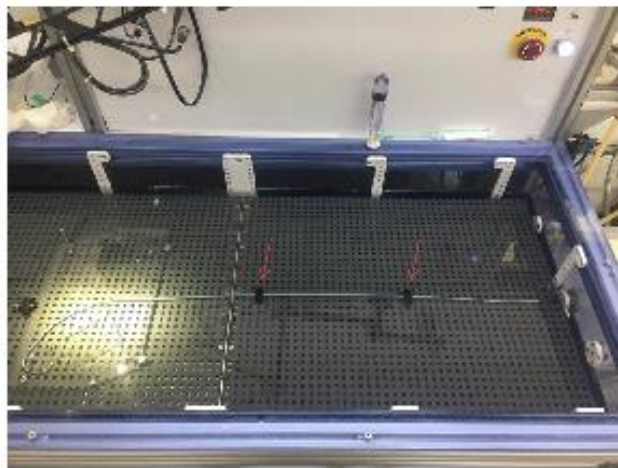


Abb. 2: Darstellung der Halter zum Fixieren des Führungskatheters

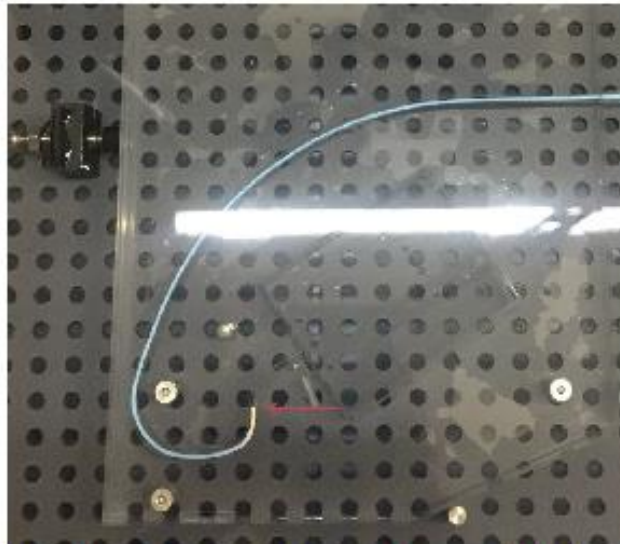


Abb. 3: Darstellung des Trackmodells mit Position des Führungskatheters

## 1.2 OP 2 – Durchführung Dilatationen

Prüfmittel:	Gefässmodelle gemäss PP Halterungen zur Fixierung der Gefässmodelle in Trackmodell Spritze zum Spülen des Führungskatheters und der Teststrecke (Entfernung der Luftblasen) Führungsdraht gemäss PP Delivery Systeme gemäss PP Manometer-Spritze Wasser (Prüfmedium) Non-compliant Ballon gemäss PP
Menge:	Siehe PP
Spezifikation:	Strecke in modifiziertem ASTM Trackmodell gemäss Vorgabe Design
Prüfablauf:	<ul style="list-style-type: none"> <li>▶ Platzierung des Gefässmodells sowie Fixierung dieses mit Halterungen im Trackmodell gemäss Abb. 4</li> <li>▶ Führungskatheter und Teststrecke mit Wasser spülen um Luftblasen zu entfernen</li> <li>▶ Führungsdraht durch Schleuse in vorgegebener Teststrecke einführen und gemäss Abb. 5 positionieren (~4-5 cm ausserhalb des Modells)</li> <li>▶ Delivery System einführen und Ballonmarker exakt unterhalb der distalen Markierung im Gefässmodell platzieren (siehe Abb. 6)</li> <li>▶ Manometer-Spritze mit Wasser füllen und diese an Luer des Katheters anschliessen</li> <li>▶ Vakuum anlegen (durch vollständigen Rückzug des Kolbens der Manometer-Spritze) und Katheter entlüften bis keine Luftblasen aus dem Prüfmedium mehr aufsteigen</li> <li>▶ Vakuum aufheben (durch Entlasten des Kolbens der Manometer-Spritze) bis Gegendruck spürbar ist</li> <li>▶ Ballon mit einer Geschwindigkeit von 2 Umdrehungen pro Sekunde bis Inflationsdruck von 14 atm (<math>\varnothing</math> 3.25 mm - RBP) erreicht ist inflatieren</li> <li>▶ Beim Erreichen des Inflationsdrucks diesen über manuelles Nachregeln konstant halten (~ 30 Sekunden)</li> <li>▶ Anschliessend Vakuum anlegen (vollständiger Rückzug des Kolbens der Manometer-Spritze)</li> <li>▶ Katheter entnehmen und Non-compliant Ballon durch Teststrecke bis zur Markierung im proximalen Bereich gemäss Abb. 7 platzieren</li> <li>▶ Manometer-Spritze mit Wasser füllen und diese an Luer des Ballonkatheters anschliessen</li> <li>▶ Vakuum anlegen (durch vollständigen Rückzug des Kolbens der Manometer-Spritze) und Katheter entlüften bis keine Luftblasen aus dem Prüfmedium mehr aufsteigen</li> <li>▶ Vakuum aufheben (durch Entlasten des Kolbens der Manometer-Spritze) bis Gegendruck spürbar ist</li> <li>▶ Ballon mit einer Geschwindigkeit von 2 Umdrehungen pro Sekunde bis Inflati-</li> </ul>

onsdruck von 18 atm ( $\varnothing$  3.85 mm – OexD+10%) erreicht ist inflatieren

- ▶ Beim Erreichen des Inflationsdrucks diesen über manuelles Nachregeln konstant halten (~ 30 Sekunden)
- ▶ Anschliessend Vakuum anlegen (vollständiger Rückzug des Kolbens der Manometer-Spritze)
- ▶ Wiederholung der letzten 3 Punkte um optimale Expansion zu gewährleisten
- ▶ Katheter entnehmen



Abb. 4: Darstellung der Platzierung des Gefässmodells im Trackmodell



Abb. 5: Darstellung der Platzierung des Führungsdrahts



Abb. 6: Darstellung der Platzierung des Delivery Systems im Gefäßmodell

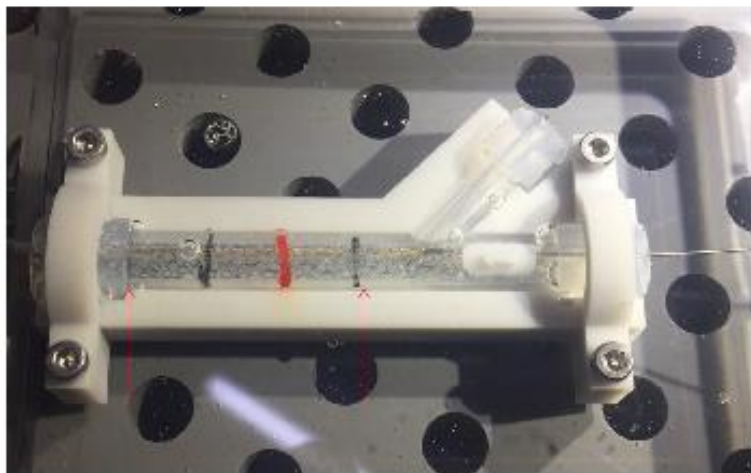


Abb. 7: Darstellung der Platzierung des Non-compliant Ballons im Gefäßmodell